UNIVERSIDADE FEDERAL DO AMAZONAS - UFAM
INSTITUTO DE CIÊNCIAS BIOLÓGICAS
PROGRAMA DE PÓS-GRADUAÇÃO EM IMUNOLOGIA BÁSICA E APLICADA

Infecção pelo vírus Zika em uma população da Amazônia Ocidental Brasileira: estudo da resposta imune, características clínicas e de diagnóstico

LIGIA FERNANDES ABDALLA

MANAUS - AMAZONAS
2018

UNIVERSIDADE FEDERAL DO AMAZONAS - UFAM
INSTITUTO DE CIÊNCIAS BIOLÓGICAS
PROGRAMA DE PÓS-GRADUAÇÃO EM IMUNOLOGIA BÁSICA E APLICADA

LIGIA FERNANDES ABDALLA

Infecção pelo vírus Zika em uma população da Amazônia Ocidental Brasileira: estudo da resposta imune, características clínicas e de diagnóstico

Tese apresentada ao Programa de Pós-Graduação em Imunologia Básica e Aplicada da Universidade Federal do Amazonas, como requisito para obtenção do título de Doutor em Imunologia Básica e Aplicada, na área de concentração "Biologia de agentes patogênicos".

Orientador: Dr. Felipe Gomes Naveca

Coorientador: Dr. Antônio Luiz Ribeiro Boechat Lopes

MANAUS - AMAZONAS
2018

Ficha Catalográfica

Ficha catalográfica elaborada automaticamente de acordo com os dados fornecidos pelo(a) autor(a).

A135i

Abdalla, Ligia Fernandes
Infecção pelo vírus Zika em uma população da Amazônia Ocidental Brasileira : Estudo da resposta imune, características clínicas e de diagnóstico / Ligia Fernandes Abdalla. 2018
LXXX f.: il. color; 31 cm.

Orientador: Felipe Gomes Naveca
Coorientador: Antônio Luiz Ribeiro Boechat Lopes
Tese (Doutorado em Imunologia Básica e Aplicada) - Universidade Federal do Amazonas.

1. zika. 2. RT-qPCR. 3. cxcl10. 4. saliva. 5. fibrilação atrial. I. Naveca, Felipe Gomes II. Universidade Federal do Amazonas III. Título

UNIVERSIDADE FEDERAL DO AMAZONAS - UFAM
INSTITUTO DE CIÊNCIAS BIOLÓGICAS
PROGRAMA DE PÓS-GRADUAÇÃO EM IMUNOLOGIA BÁSICA E APLICADA

FOLHA DE APROVAÇÃO

Infecção pelo vírus Zika em uma população da Amazônia Ocidental Brasileira: estudo da resposta imune, características clínicas e de diagnóstico

LIGIA FERNANDES ABDALLA

Tese defendida e aprovada pela Banca Examinadora constituída por:

Prof. Dr. Felipe Gomes Naveca (Presidente)
Instituto Leônidas e Maria Deane - Fundação Oswaldo Cruz

Prof. Dra. Aya sadahiro (Membro Interno)
Universidade Federal do Amazonas

Prof. Dr. Luís andré morais mariúba (Membro Interno)
Instituto Leônidas e Maria Deane - Fundação Oswaldo Cruz

Prof. Dr. Vanderson de souza sampaio (Membro Externo)
Fundação de Vigilância Sanitária do Amazonas

Prof. Dr. Gemilson Soares Pontes (Membro Externo)
Instituto Nacional de Pesquisas da Amazônia

Manaus, setembro de 2018

DEDICO ESTE TRABALHO

A DEUS,

Pelo Dom da Vida, pela faculdade da inteligência, pela presença constante e pela oportunidade de ser útil ao meu próximo.
Agradeço-te senhor por guiar meus passos, pelo amparo, proteção, saúde, família e por preencher de sentido minha existência,
Agradeço também pelas coisas que eu ainda não sou capaz de enxergar.

AOS MEUS PAIS EVENILDA E JORGE FERNANDES,

A quem devo o meu crescimento profissional e moral, me estimulando sempre com amor e carinho para que eu pudesse atingir esta conquista. Por me apoiarem nas minhas decisões e me ensinarem os verdadeiros valores da vida, sendo exemplos de perseverança, dignidade e honestidade.
Dedico este trabalho com toda minha devoção e agradecimentos.

AO MEU MARIDO JOÃO HUGO,

Pela alegria constante, pelo incansável incentivo, companheirismo, pelo conforto nas horas tristes e pela vibração nas minhas vitórias.
E simplesmente... por me amar e por acreditar em nós. Sem você nada disso seria possível! Te amo!

AOS MEUS IRMÃOS, DOUTORES, DAVID E HORÁCIO

Que me deram a oportunidade de conviver e crescer ao lado de pessoas maravilhosas e pelos seus exemplos na busca do meu sonho do doutorado.
Vocês são motivos de imenso orgulho pra mim!

AOS MEUS FILHOS ISABELLA E JOÃO HUGO,

Pela oportunidade de experimentar a mais pura forma de amar!
Por me fazerem ser menos egoísta e mais paciente!
Por me darem a cada dia mais e mais motivos para acordar sorrindo!
Por me fazer perceber que a vida pode ser mais leve e mostrar realmente o que importa nela!

AO MEU QUERIDO AMIGO E ORIENTADOR FELIPE,

Por ter acreditado desde o primeiro momento em meu potencial e ter me aceito como sua orientanda desde o mestrado. Pelo exemplo de seriedade, devoção e paciência. Por ter me ensinado desde a segurar a pipeta (apesar de eu ter padronizado meu próprio método!) até a me apaixonar pelas etapas laboratoriais. Por ter sido grande motivador na minha busca por respostas. Você é mais que merecedor da minha confiança e amizade! Jamais vou esquecer!

AGRADECIMENTOS

Graças a várias pessoas este projeto se concretizou. Não poderia deixar de agradecer cada uma delas.

À Direção do ILMD e a todos seus funcionários, que possibilitaram meu trabalho e minha convivência em um ambiente sempre muito agradável.

À Direção do HAM, por ter-nos aberto as portas da instituição e incentivar o desenvolvimento do trabalho científico.

À Secretaria do PPGIBA por manter as portas sempre abertas e por agilizar todas as nossas solicitações. Queria agradecer em especial ao Sr. **Edson** por sempre ter um sorriso no rosto e estar disposto à ajudar.

Ao Dr. **Antônio Luiz de Oliveira Boechat**, pelos conselhos, paciência e carinho.

Às companheiras de laboratório **Valdinete, Dana, Matty e Tati** pela colaboração na parte experimental deste trabalho. Sem vocês nada disso seria possível.

Ao **Dr. João Hugo Abdalla** pelo acompanhamento clínico de todos os pacientes e presença constante.

Aos amigos do curso: **Diana, Juliana, Mariana, Alysson, Márcia e Rosmery** pelo companheirismo, pela harmoniosa divisão de responsabilidades e pela oportunidade de grande crescimento científico através do trabalho em conjunto.

À querida e inesquecível **professora Aya**, por me fazer apaixonar a cada dia pela Imunologia e pelo exemplo de profissionalismo.

Aos **meus pacientes**, imprescindíveis na concepção deste trabalho. Agradeço-lhes e deixo meu carinho a todos a quem pude ter o prazer de conhecer. Que Deus os abençoe.

A todos os meus amigos de graduação e pós-graduação, que estiveram ao meu lado durante esta etapa, tornando nossa jornada muito mais agradável.

A todos aqueles que direta ou indiretamente colaboraram para a conclusão deste trabalho.

Meus sinceros agradecimentos

"Há pessoas que transformam o sol numa simples mancha amarela, mas há aquelas que fazem de uma simples mancha amarela o próprio sol."

Pablo Picasso

RESUMO

O *Zika virus* (ZIKV) é um arbovírus emergente da família Flaviviridae e do gênero *Flavivirus*, que até 2007 estava restrito a alguns casos de doença leve na África e na Ásia. No Brasil, suspeita-se que a entrada do vírus tenha se dado durante a Copa das Confederações de 2013 e no primeiro semestre de 2015, já havia casos confirmados em estados de todas as regiões do país. A epidemia brasileira revelou que a infecção geralmente leve e autolimitada poderia estar relacionada à distúrbios neurológicos. Os objetivos deste trabalho era esclarecer inúmeros questionamentos existentes em relação à infecção pelo ZIKV, visando contribuir com uma melhor compreensão dos mecanismos envolvidos na imunopatogênese e curso da doença. Como resultados, descreveu-se o primeiro relato de fibrilação atrial em pacientes com Zika, podendo ser considerado uma manifestação atípica durante a infecção pelo vírus; observou-se elevação de citocinas pró-inflamatórias durante a infecção ZIKV; identificou-se a quimiocina CXCL10 como um biomarcador potencial de infecção; caracterizou-se a saliva como fluído de escolha para o detecção do vírus Zika na fase aguda da doença e, montou-se um modelo de regressão logística para a classificação de casos de zika em relação à dengue, com base na avaliação clínica.

Palavras-chave: *Zika virus*, RT-qPCR, CXCL10, Saliva, Fibrilação Atrial, Clínica.

ABSTRACT

Zika virus (ZIKV) is an emergent arbovirus of the family Flaviviridae and the genus Flavivirus, which until 2007 was restricted to some cases of mild disease in Africa and Asia. In Brazil, it`s suspected that the entry of the virus occurred during the 2013 Confederations Cup and in the first half of 2015, there were already confirmed cases in states in all regions of the country. The Brazilian epidemic revealed that the usually mild and self-limiting infection could be related to neurological disorders. The objectives of this study were to clarify numerous questions regarding ZIKV infection, aiming to contribute to a better understanding of the mechanisms involved in the immunopathogenesis and course of the disease. As a result, the first report of atrial fibrillation in patients with Zika was described and could be considered an atypical manifestation during the virus infection; elevation of proinflammatory cytokines during ZIKV infection was observed; CXCL10 chemokine was identified as a potential biomarker for infection; saliva was characterized as the fluid of choice for the detection of Zika virus in the acute phase of the disease and a logistic regression model for the classification of cases of zika in relation to dengue was set up based on the clinical evaluation.

LISTA DE TABELAS

LISTA DE FIGURAS

LISTA DE ABREVIATURAS E SIGLAS

CDC	Centro para Controle de Doenças e Prevenção dos Estados Unidos da América
C	Capsídeo
CTLs	Células T citotóxicas
DENV	*Dengue virus*
E	Envelope
ECDC	Centro Europeu para Controle de Doenças
EDTA	Ácido Etilenodiamino Tetra-cético
ER	Retículo Endoplasmático
FIOCRUZ	Fundação Oswaldo Cruz
HAM	Hospital Adventista de Manaus
IGG	Imunoglobulina G
IGM	Imunoglobulina M
ILMD	Instituto Leônidas e Maria Deane
INF	Interferon
ISGs	Genes estimuladores de Interferon (*Interferon-stimulated genes*)
NK	Células *natural killer*
NS	Proteína Não-Estrutural
NAbs	Anticorpos Neutralizantes
OMS	Organização Mundial de Saúde
prM	Proteína pré-membrana
RNA	Ácido ribonucleico
RT-qPCR	Reação em Cadeia da Polimerase em Tempo Real conjugada a Transcrição Reversa
SE	Semana Epidemiológica
TCLE	Termo de Consentimento Livre e Esclarecido
ZIKV	*Zika virus*

SUMÁRIO

INTRODUÇÃO

O nome vírus Zika (em inglês, *Zika virus*; abreviatura: ZIKV) tem sua origem pela descoberta do vírus na floresta de Zika, perto de Entebbe, capital da República de Uganda. O vírus foi isolado pela primeira vez de um macaco sentinela em 1947, e após cinco anos, em 1952, foi descrito infectando humanos (SMITHBURN, 1952; SIMPSON, 1964). É considerada uma arbovirose emergente transmitida por mosquitos da família *Culicidae*, do gênero *Aedes.* Este gênero tem como um de seus principais representantes o *Aedes aegypti*, a espécie responsável pela propagação da dengue no Brasil (Figura 1). Existem ainda outras espécies de mosquitos no mundo capazes de transmissão do vírus como: *Aedes africanus*, *Aedes albopictus, Aedes polynesiensis e Aedes hensilli* (PETERSEN et al., 2016).

Figura 1: *Aedes aegypti*
Fonte: http://revistapesquisa.fapesp.br/2016/03/24/virus-zika-provavelmente-chegou-ao-brasil-em-2013/

Até o ano de 2007, o ZIKV estava restrito a poucos casos na África e Ásia, sendo depois associado a um surto de síndrome febril na Ilha Yap, Micronésia (Duffy et al. 2009). No dia 23 de fevereiro de 2016 foi publicado o primeiro artigo tratando sobre

a dispersão e origem filogenética do ZIKV no Brasil com sete isolados desse vírus (FARIA et al., 2016). Utilizando de ferramentas moleculares e de bioinformática, foi demonstrado que o ZIKV foi introduzido no Brasil entre maio e dezembro de 2013, possivelmente nos meses de julho e agosto, quando da realização da Copa das Confederações, um ano antes da Copa do Mundo de 2014. Nesse tempo o vírus, que apresenta 80% das infecções assintomáticas ou oligossintomáticas, passou despercebido sendo esse fato muito importante para a dispersão pelo Nordeste (FARIA et al., 2016; PINTO JUNIOR et al., 2015). No primeiro semestre de 2015, já havia casos confirmados em várias regiões do país (ZANLUCA et al., 2015; (CAMPOS; BANDEIRA; SARDI, 2015).

Em agosto de 2015, a epidemia brasileira revelou que a doença geralmente leve e autolimitada, poderia estar relacionada à distúrbios neurológicos graves, incluindo microcefalia e síndrome de Guillain-Barré (Leal, 2016; Krauer et al, 2017). O amplo espectro de manifestações clínicas fetais decorrentes da infecção pelo ZIKV levou a nova classificação denominada Síndrome Congênita do Zika. Em novembro de 2015, o Ministério da Saúde declarou a situação uma emergência nacional de saúde pública e, alguns meses depois, a Organização Mundial de Saúde (OMS) elevou esse alerta como uma emergência de saúde pública de preocupação internacional (AZEVEDO et al., 2016; DOS SANTOS et al., 2016; RATANACHAROENSIRI et al., 2017). Dessa forma, as arboviroses emergiram em locais antes indenes representando um potencial desafio para a Saúde Pública (LIMA-CAMARA, 2016)

Entre estes problemas está o fato de ainda não existir um exame sorológico confiável para o diagnóstico da Zika, o que implica na total dependência do diagnóstico através de exames moleculares, como a Reação em Cadeia da Polimerase em Tempo Real conjugada a Transcrição Reversa (RT-qPCR). A RT-

qPCR são realizadas normalmente em grandes centros de vigilância epidemiológica ou em hospitais de ensino sendo, portanto, um diagnóstico que demanda custo e tempo (CHARREL et al., 2016; CORMAN et al., 2016).

Não apenas o fato de existirem poucas opções de exames para o diagnóstico de Zika torna-se um obstáculo para o profissional de saúde, mas também o fato da manifestação clínica se assemelhar com pelo menos outras 10 doenças, entre elas estão: dengue, leptospirose, malária, rickettsiose, estreptococose do grupo A, rubéola, sarampo, e infecções por parvovírus, enterovírus, adenovírus, e alfavírus (por exemplo, chikungunya e outros) (CORMAN et al., 2016).

Mesmo com todos os avanços produzidos pela ciência mundial, ainda há muito o que ser estudado. O conhecimento imunofisiopatológico da infecção por ZIKV ainda é um campo muito obscuro e que necessita de maiores avanços. Sabe-se que a resposta immune desempenha um papel importante na evolução clínica das infecções virais sendo essencial na limitação da propagação dos vírus. Esses estudos são cruciais para a identificação de marcadores da infecção que podem ser utilizados no desenvolvimento de abordagens imunoterapêuticas e de prevenção por vacinas (KAM et al., 2017; ANDRADE; HARRIS, 2017; NAVECA et al., 2017).

.

1. REFERENCIAL TEÓRICO

1.1 Epidemiologia do ZIKV

Em março de 2017, a OMS publicou uma classificação de risco geográfico baseada nos vetores do ZIKV, desenvolvida em colaboração com o Centro Europeu para Controle de Doenças (ECDC) e o Centro para Controle de Doenças e Prevenção dos Estados Unidos (CDC). A estrutura de classificação da OMS inclui quatro categorias para classificar os territórios (Tabela 1, Figura 2):

Tabela 1

Classificação dos territórios de transmissão do vírus Zika

Classificação	**Definição**
Categoria 1	- Área com introdução **ou** - Reintrodução com transmissão em curso
Categoria 2	- Área com evidência da circulação do vírus antes de 2015 **ou** - Área anteriormente classificada na categoria 1 mas que já tem aproximadamente 2 anos da (re)introdução do vírus sem interrupção
Categoria 3	- Área com transmissão interrompida e com potencial para futuras transmissões
Categoria 4	- Área com vetor competente estabelecido, mas nenhuma transmissão documentada

Fonte:http://apps.who.int/iris/bitstream/handle/10665/254619/WHO-ZIKV-SUR-17.1-por.pdf;jsessionidjsessionid=5DEB4A84313C6A7078DF953219BB231B?sequence=5. Acesso: 01/06/2018.

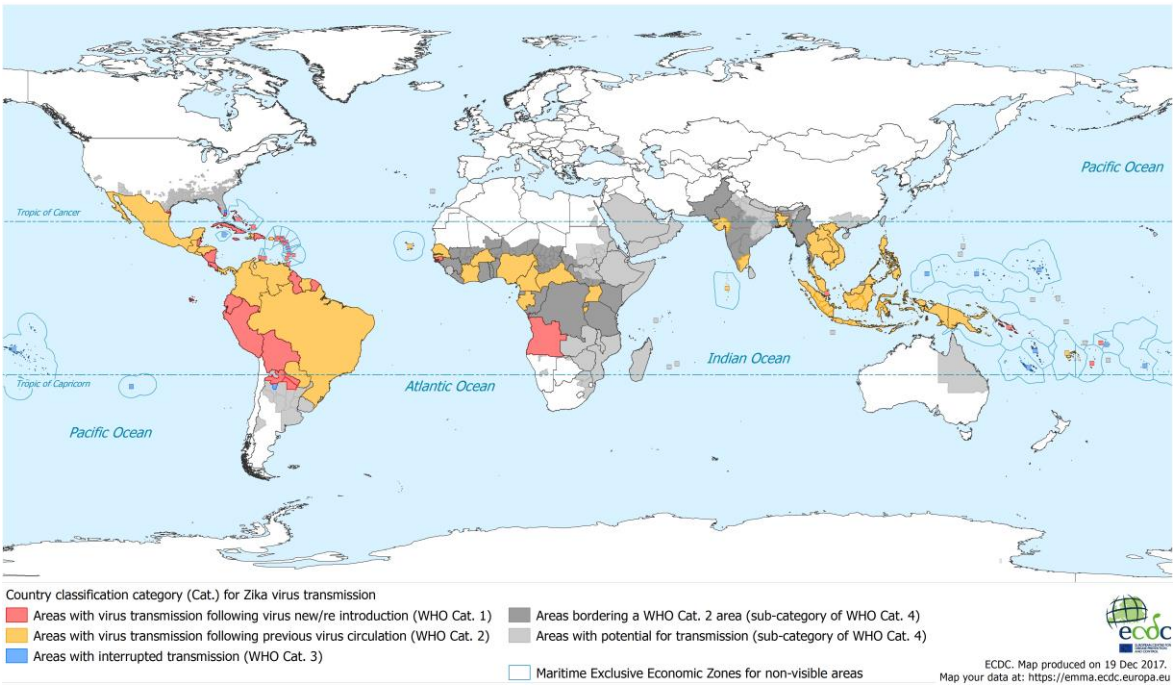

Figura 2: Classificação territorial de transmissão do vírus Zika.
Fonte: https://ecdc.europa.eu/en/publications-data/current-zika-transmission-worldwide

No Brasil, em 2016, foram registrados 216.207 casos prováveis infecção pelo vírus Zika no país e em 2017 foram identificados 17.594 casos suspeitos. Em 2018, até a SE 11, foram registrados 1.486 casos prováveis de doença pelo vírus Zika no país, com taxa de incidência de 0,7 casos/100 mil hab.; destes, 372 (25,0%) foram confirmados (Figura 3). Atualmente, a análise da taxa de incidência de casos prováveis de Zika (número de casos/100 mil hab.), segundo regiões geográficas, demonstra que as regiões Centro-Oeste e Norte apresentam as maiores taxas de incidência: 3,0 casos/100 mil hab. e 1,4 casos/100 mil hab., respectivamente. Entre as UFs, destacam-se Mato Grosso (5,9 casos/100 mil hab.), Tocantins (4,8 casos/100 mil hab.), e Goiás (3,9 casos/100 mil hab.) (MS, 2018).

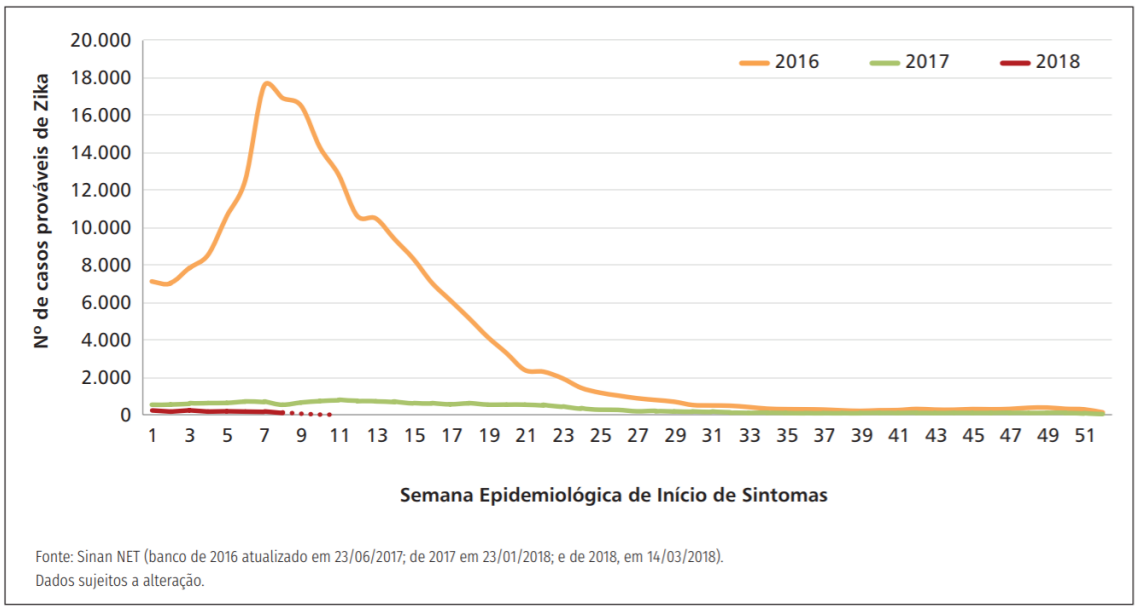

Figura 3: Casos prováveis de febre pelo vírus Zika no Brasil nos anos de 2016 à 2018 por semana epidemiológica.

Fonte:http://portalarquivos2.saude.gov.br/images/pdf/2018/abril/06/2018-012.pdf

1.2 Agente etiológico e ciclo replicativo

O ZIKV é um arbovírus emergente pertencente à família *Flaviviridae*, gênero *Flavivirus.* A família *Flaviviridae* corresponde a uma família de vírus que é composta pelos seguintes gêneros:

- Gênero *Flavivirus* com 67 espécies de vírus humanos e animais identificadas. Apresenta como principais representantes os vírus da febre amarela, o vírus do Nilo ocidental, da dengue (DENV), vírus da encefalite japonesa e o ZIKV.
- Gênero *Hepacivirus* com um representante, o vírus da hepatite C;
- Gênero *Pestivirus* com vírus que infectam animais mamíferos como o vírus da diarréia viral bovina e o da peste suína.

Como outros flavivírus, as partículas virais são envelopadas e esféricas, com cerca de 40 a 60 nanómetros de diâmetro, apresentando um genoma de ácido

ribonucleico (RNA) de cadeia simples (ssRNA) com 9,6 a 12,3 quilobases, linear e de polaridade positiva (Figura 4).

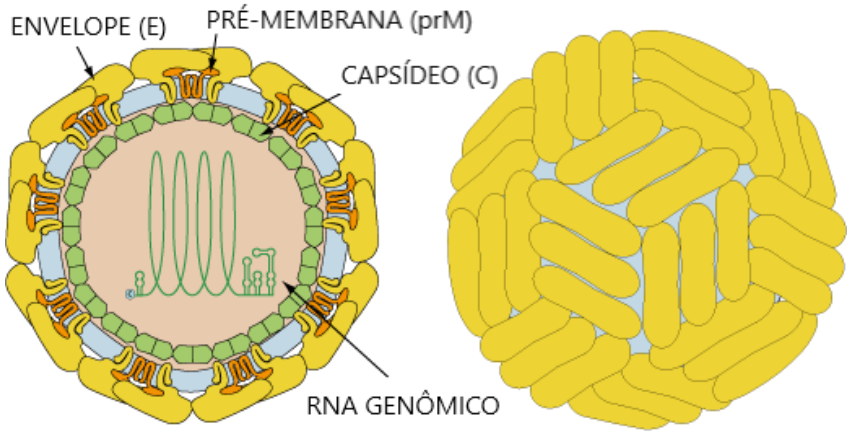

Figura 4: Estrutura do vírus Zika.
Fonte: adaptado de https://viralzone.expasy.org/6756. Acesso em: 04.06.2018

Os flavivírus se ligam às células por meio de interações entre as proteínas do envelope (E) do vírion e um grupo diversificado de receptores na célula-alvo, num processo denominado de adsorção. Os receptores celulares / fatores de ligação absolutamente necessários para a infecção ainda não foram identificados; moléculas implicadas na entrada de flavivírus nas células incluem várias lectinas (DC-SIGN, DC-SIGNR e receptor de manose), sulfato de heparina e moléculas da família TIM / TAM (LINDENBACH; RICE, 2003).

Uma vez ligados, os flavivírus são englobados pela membrana plasmática e internalizados nas células através de endocitose mediada por clatrina, ficando no interior de vesículas nas células. Posteriormente, o PH ácido ácido induz a fusão entre o envelope viral e a membrana do endossomo, liberando o RNA viral para o citoplasma. O RNA genômico sofre desnudamento, ou seja, é liberado no citoplasma sendo usado diretamente como RNA mensageiro na tradução, produzindo uma poliproteína, que contém proteínas estruturais e não estruturais. A poliproteína

codificada pelo genoma viral é posteriormente clivada por enzimas virais em três proteínas estruturais: capsídeo (C), pré-membrana (prM) e envelope (E) além de sete proteínas não estruturais (NS1, NS2A, NS2B, NS3, NS4A, NS4B e NS5) (Figura 5) (LINDENBACH; RICE, 2003).

Após o processamento proteolítico, as proteínas não-estruturais catalisam a replicação, através da síntese de RNA anti-genômico, que serve como molde para a produção de mais RNA genômico. Este pode ser usado para a tradução de mais proteínas virais ou juntamente com as proteínas estruturais, sofrer maturação dando origem a novo vírions.

Na etapa final, a montagem do vírion ocorre em membranas derivadas do retículo endoplasmático (ER), num processo denominado de maturação viral. Inicialmente ocorre a reunião do cápside e do ácido nucléico que, posteriormente é circundado pelo envelope durante a liberação. As proteínas virais específicas do envelope são sintetizadas durante a fase tardia da síntese protéica e são inseridas na membrana celular do hospedeiro. O nucleocápside associa-se com a superfície interior da membrana alterada, já contendo as proteínas virais. Durante a saída do nucleocápside da célula, a partícula viral é envelopada por esta membrana alterada sendo os lipídeos do envelope viral inteiramente derivados da célula hospedeira. Assim, uma partícula viral madura é liberada no espaço extracelular (Figura 6) (ZHAO et al., 2016; FERNANDEZ-GARCIA et al., 2009).

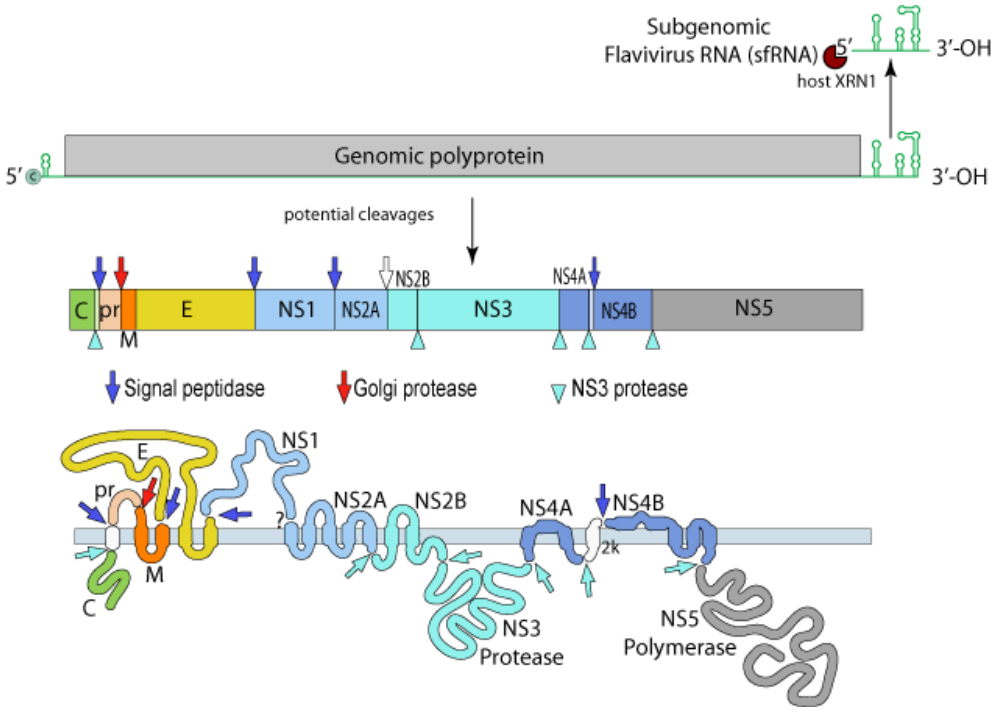

Figura 5: Estrutura do genoma do vírus Zika.
Fonte: https://viralzone.expasy.org/6756. Acesso em: 04.06.2018

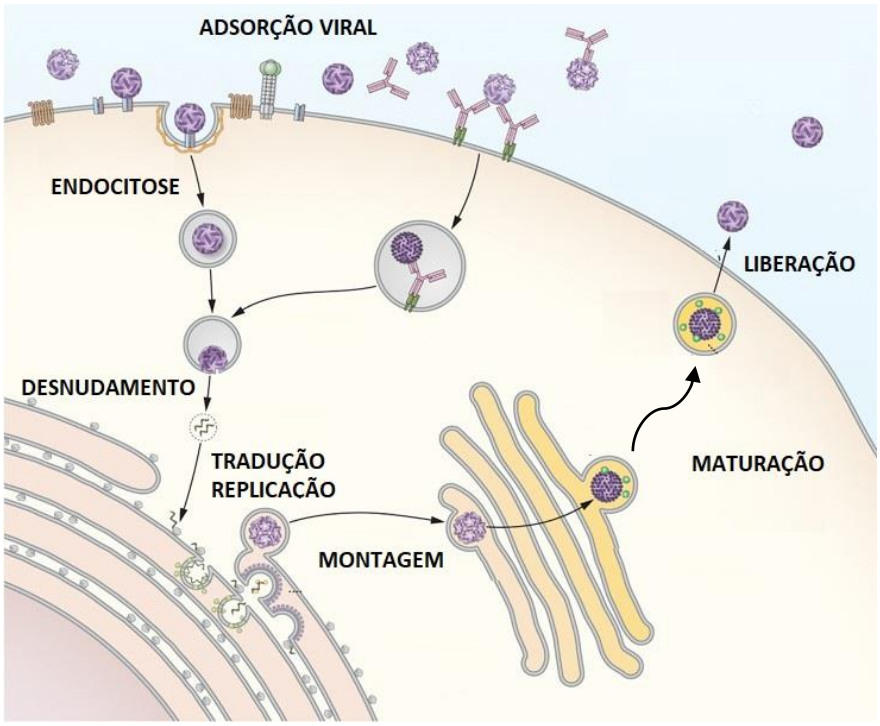

Figura 6: Ciclo replicativo do vírus Zika.
Fonte: Adaptado de https://microbewiki.kenyon.edu/index.php/Yellow_fever_virus Acesso em: 06.06.2018

1.3 Ciclo de transmissão e *fitness*

O ZIKV apesar de ser principalmente transmitido por mosquitos *Aedes*, também pode ser transmitido sexualmente, verticalmente e por outras vias (GRISCHOTT et al., 2016; PETERSEN et al., 2016; LEAL, 2016). Em humanos, há relatos da presença do virus em diferentes fluidos corporais como sangue, sêmen, urina e saliva. Essa detecção pode variar ao longo do tempo nos diferentes fluídos podendo afetar tanto a dinâmica de transmissão como o diagnóstico da infecção (PETERSEN et al., 2016; LUSTIG et al., 2016; FROESCHL et al., 2017; PRISANT et al., 2016; NICASTRI et al., 2016; MUSSO et al., 2015; ROZÉ et al., 2016; SUN et al., 2016; KODATI et al., 2017; FOY et al., 2011).

Por ser um vírus RNA, o ZIKV possui taxas elevadas de erro durante a replicação que podem levar ao acúmulo de mutações que contribuam para o aumento de seu *fitness*. Estudos realizados com outros arbovírus apontam a ocorrência de mutações no genoma viral como pontos importantes para: (i) a adaptação do vírus a novos vetores (ARIAS-GOETA et al., 2014); (ii) mudanças conformacionais em proteínas virais, impedindo ou diminuindo a eficiência de ligação dos anticorpos (DOWD; DEMASO; PIERSON, 2015); (iii) tornar a replicação e infecção mais eficientes (SILVEIRA et al., 2016).

1.4. Diagnóstico laboratorial da Zika

O diagnóstico laboratorial da Zika não é direto e apesar de testes sorológicos já terem sido desenvolvidos para detectar anticorpos anti-ZIKV, a reatividade cruzada com outros flavivírus complica a interpretação dos resultados em áreas onde outros arbovírus são endêmicos.

A detecção molecular do RNA do ZIKV por meio da RT-qPCR é o método de escolha para o diagnóstico do ZIKV. Mesmo com a alta sensibilidade e especificidade da RT-qPCR, o processo de detecção de RNA do ZIKV não é isento de dificuldades. Primeiro, a detecção depende da amostra ter uma concentração acima do limite de detecção do ensaio (geralmente muito pequeno) do RNA viral. Segundo, fatores como a integridade do RNA, variabilidade das sequências alvo, inibição da PCR e contaminação, podem resultar em resultados de RT-PCR incorretos (PETERSEN et al., 2016; CHARREL et al., 2016; CORMAN et al., 2016; WAGGONER; PINSKY, 2016).

Mais formalmente, o processo de detecção do ZIKV depende de uma hierarquia de três níveis de probabilidade: 1) a probabilidade de o paciente estar infectado; 2) a probabilidade de que a amostra coletada do paciente infectado contenha RNA do ZIKV; 3) a probabilidade da RT-qPCR em detectar o RNA do ZIKV em uma amostra que contém o vírus. Embora essa estrutura hierárquica esteja frequentemente implícita em estudos de testes diagnósticos, falta ainda um processo de detecção do ZIKV nos três níveis.

1.5 Manifestações clínicas da Zika

A apresentação clínica da infecção por ZIKV em seres humanos é muito parecida com a de outras arboviroses/viroses e estão frequentemente associadas a febre leve, cefaléia, exantema maculopapular, artralgia, linfoadenopatia e hiperemia conjuntival (DUFFY et al., 2009). Tais sintomas aparecem alguns dias (3-12 dias) após a picada do vetor infectado, sendo que infecções assintomáticas são comuns (PINTO JUNIOR et al., 2015). Em relação aos achados laboratoriais, bioquímicos e hematológicos, os dados na literatura ainda são ainda muito escassos e, por vezes, contraditórios (ELIAS COLOMBO et al., 2017; AZEREDO et al., 2018).

No entanto, manifestações clínicas atípicas já foram relatadas, incluindo complicações neurológicas (PINHEIRO et al., 2016), síndrome congênita (DE CARVALHO et al., 2017), problemas oculares (KODATI et al., 2017) e complicações cardiovasculares (ALETTI et al., 2016; ABDALLA et al., 2018). O grande número de casos atípicos, incluindo óbitos, podem indicar um perfil diferenciado das infecções pelo ZIKV no Brasil. Um estudo apontou que o ZIKV está mais eficiente para infectar humanos. Durante o caminho percorrido do continente africano até a América, o ZIKV acumulou mutações que o tornaram capaz de produzir uma replicação mais eficiente (FAYE et al., 2014).

1.6 Resposta Imunológica ao vírus Zika

A resposta imune do hospedeiro também desempenha um papel importante no curso clínico das infecções virais. Respostas imunes inatas e adaptativas contra os vírus têm como objetivo bloquear a infecção e eliminar as células infectadas. A

infecção é prevenida por interferons do tipo I como parte da imunidade inata e os anticorpos neutralizantes contribuem para a imunidade adaptativa. Uma vez que a infecção é estabelecida, as células infectadas são eliminadas pelas células *natural killer* (NK) na resposta inata e pelas células T citotóxicas ($CD8^+$) na resposta adaptativa (MEDZHITOV, 2007).

1.6.1 Imunidade Inata

Os componentes da imunidade natural, ou inata, são os primeiros a realizar o controle das infecções virais por meio do bloqueio da disseminação da particulas virais às células do hospedeiro, devido aos interferons do tipo I, assim como à morte das células infecadas, mediada pela ação de células NK ((MEDZHITOV, 2007).

A resposta mediada pelo interferon (IFN) desempenha um papel crítico no controle de flavivírus, como mostrado pelo aumento da susceptibilidade de infecção em camundongos com falta de componentes da via do IFN (LAZEAR et al., 2016; SHRESTA et al., 2004) e os numerosos mecanismos empregados pelos flavivírus para mediar este controle (MORRISON et al., 2013; QUICKE; SUTHAR, 2013).

Os flavivirus, por serem um vírus de RNA fita simples, vão ativar duas vias bioquímicas que desencadeiam a produção do interferon. A primeira via inclue o reconhecimento do RNA viral por receptores de reconhecimento de padrões (PRRs) nas famílias de receptores de RNA do tipo Toll (TLR7 e TLR8) endossomais e a segunda via compreende a ativação de receptores citoplasmáticos do tipo RIG-I (RLR) (LAZEAR; DIAMOND, 2014). Estas vias convergem para a ativação de proteínas quinases o que por sua vez ativam os fatores de transcrição de IRF e NF-

κB. Posteriormente, IRF e NF-κB estimulam a expressão de genes que atuam na transcrição do IFN I e que codificam as moléculas necessárias para a resposta inflamatória, respectivamente (SUTHAR; AGUIRRE; FERNANDEZ-SESMA, 2013).

Uma vez produzidas, as moléculas de IFN-I ligam-se ao receptor IFN-αβR ativando uma tirosina quinase citoplasmática que fosforila a proteína STAT2. Essa molécula transduz sinais e a tiva a transcrição de vários genes codificadores de citocinas, inclusive de IFN do tipo I. Entre esses genes, há o que codifica a 2' -5' oligoadenilato sintetase, que por sua vez ativa RNAse L, uma enzima que degrada os RNAs virais. Esse mecanismo leva á redução da síntese protéica e inibe a replicação viral (SUTHAR; AGUIRRE; FERNANDEZ-SESMA, 2013).

Vários estudos *in vitro* utilizando células humanas primárias e linhagens celulares derivadas de humanos foram realizadas para avaliar a resposta do IFN à infecção por ZIKV. Dependente do tipo de célula usada, a infecção pelo ZIKV resultou na produção do tipo I (α, β), tipo II (γ) e IFN tipo III (λ), bem como a ativação de vários genes estimulados por IFN (ISGs) (CHAUDHARY et al., 2017; HAMEL et al., 2015; BAYER et al., 2016).

Estudos também vêm demonstrando mecanismos empregados pelo ZIKV em evadir de resposta do tipo IFN. A proteína NS5 do ZIKV foi detectada degrando STAT2, levando à diminuição na sinalização do IFN tipo I e consequentemente o aumento da replicação viral. Outro estudo também sugere um outro mecanismo de inibição do IFN, onde a infecção pelo ZIKV atuaria como antagonista na fosforalização de STAT1 e STAT2 (BOWEN et al., 2017). Até o presente momento, não é claro o mecanismo utilizado pelo ZIKV para inibir a via do IFN e, ainda assim, se isso ocorre naturalmente durante uma infecção (CULSHAW et al., 2018). Novos estudos ainda precisam ser realizados para elucidar esse fato.

1.6.2 Imunidade Adaptativa

Outro componente importante da resposta antiviral é a resposta imune adaptativa que é mediada pelos anticorpos, que bloqueiam a ligação do vírus às células hospedeiras, e pelas células T $CD8^+$, que eliminam a infecção matando as células infectadas. Os anticorpos antivirais ligam-se ao envelope viral ou aos antígenos do capsídeo e funcionam principalmente como anticorpos neutralizantes (NAbs) para impedir a fixação e entrada do vírus na célula hospedeira. Assim, conseguem impedir tanto a infecção inicial quanto a disseminação célula a célula. Além da neutralização, os anticorpos podem opsonizar as partículas virais e promover a sua depuração por fagócitos. A ativação do sistema complemento também pode participar da imunidade viral mediada por anticorpos, principalmente através da promoção da fagocitose e lise direta do envelope ((MEDZHITOV, 2007).

Relativamente pouco se sabe sobre a resposta imune adaptativa à infecção pelo ZIKV ou seus efeitos na patogênese viral (PETERSON et al., 2017). Os principais alvos dos anticorpos específicos contra os flavivírus são as proteínas estruturais E e prM, juntamente com a proteína não-estrutural NS1 (HEINZ; STIASNY, 2012; MULLER; YOUNG, 2013). Vários anticorpos monoclonais humanos capazes de neutralizar o ZIKV *in vitro* e *in vivo* já foram isolados, porém, estes são estruturalmente semelhantes com os de outros flavivírus, especialmente o DENV (ROBBIANI et al., 2017). Além disso, dois anticorpos, que reconhecem múltiplos domínios da proteína E, foram encontrados causando proteção em camundongos infectados (WANG et al., 2016).

As células T $CD8^+$ medeiam a eliminação dos vírus que residem dentro das células. Estas reconhecem os peptídeos virais sintetizados endogenamente e são

apresentados por moléculas de classe I do Complexo Maior de Histocompatibilidade (MHC) da célula hospedeira (ABBAS, 2015). Um estudo em camundongos deficientes do receptor IFN tipo I (IFNR) mostrou que células T $CD8^+$ específicas para ZIKV tem como alvo predominantemente as proteínas prM, E e NS5, causando uma função protetora durante o curso da infecção (NGONO et al., 2017). Outro estudo, em modelos de camundongos transgênicos, verificou que células T CD8+ específicas para ZIKV reconhecem epítopos de todas as 10 proteínas virais e também observou o papel protetor dessas células durante a infecção. Neste último trabalho, quando os animais eram previamente imunizados ocorria uma redução da carga viral e, após depleção de células T CD8+, a carga viral voltava a aumentar (WEN et al., 2017b).

Até o momento, apenas três estudos descrevendo mediadores em pacientes infectados com Zika foram relatados (TAPPE et al., 2016; KAM et al., 2017; NAVECA et al., 2017). Em Tappe et al. (2016), um perfil confiável de biomarcadores imunológicos durante infecção não pôde ser estabelecida devido à pequena amostragem. Kam et al. (2017) descrevem vários mediadores pró-inflamatórios mais elevados em pacientes infectados pelo ZIKV, mais especificamente CXCL10, IL-10 e HGF observados entre pacientes com complicações neurológicas e, além disso, também encontraram níveis mais elevados de CXCL10, IL-22, MCP-1 e TNF-α em mulheres grávidas infectadas pelo ZIKV associados à malformações no desenvolvimento fetal. Naveca et al. (2018) também trouxeram novas perspectivas sobre a imunopatologia do ZIKV, identificando o CXCL10 como um potencial biomarcador de infecção aguda pelo ZIKV e, talvez, podendo este ser utilizado como um preditor de gravidade.

A literatura relata que as células T CD8 + desempenham um papel protetor contra o infecção pelo ZIKV. Além disso, descreve que alguns indivíduos montam respostas de células T CD8+ mais fracas do que outras; estas respostas de células T mais fracas, em combinação com uma baixa resposta de anticorpos, podem levar a manifestações graves da doença, enquanto células T eficientes ou resposta de anticorpo pode ser suficiente para proteção (WEN et al., 2017; NGONO et al., 2017).

A imunidade protetora adaptativa ao ZIKV tem sido atribuída principalmente à Células T CD8+ e anticorpos neutralizantes, enquanto a participação das células T CD4+ na resistência permaneceu amplamente descaracterizada. Estudos recentes têm relacionado uma resposta de anticorpos neutralizantes e sinalização do IFNγ dependentes de células T CD4+ que ocorre durante a primeira semana de infecção, caracterizando a participação desses componentes na resistência ao ZIKV durante a infecção primária (LUCAS et al., 2018).

2. JUSTIFICATIVA

Diante do exposto e considerando os inúmeros questionamentos existentes em relação à infecção pelo ZIKV, torna-se imprescindível o desenvolvimento de estudos que contribuam para o rápido e correto diagnóstico, conhecimento das características clínicas, da resposta imune e das manifestações atípicas relacionadas à infecção pelo mesmo, visando contribuir com uma melhor compreensão dos mecanismos envolvidos na imunopatogênese e curso da doença.

3. OBJETIVOS

Objetivo geral

Avaliar clínico e laboratorialmente a fase aguda de infecção pelo ZIKV identificando as possíveis associações que possam contribuir para o diagnóstico da zika.

Objetivos específicos

1. Detectar os níveis séricos de citocinas, quimiocinas e fatores de crescimento dos pacientes infectados;
2. Verificar por meio de parâmetros moleculares (RT-qPCR) a presença do vírus na saliva, urina e plasma dos pacientes e avaliar o melhor fluído para diagnóstico da Zika;
3. Analisar os achados clínicos e laboratoriais a fim de identificar pontos potencialmente úteis para o diagnóstico da doença;
4. Descrever possíveis manifestações atípicas durante a fase aguda da infecção pelo vírus.

4. MATERIAL E MÉTODOS

4.1 Tipo de estudo

Trata-se de um estudo transversal observacional do tipo caso-controle para avaliar clínico e laboratorialmente a fase aguda de infecção pelo ZIKV e identificar possíveis marcadores para o diagnóstico.

4.2 Área de estudo

Os pacientes foram atendidos e as coletas das amostras realizadas no Hospital Adventista de Manaus (HAM) localizado na cidade de Manaus, Amazonas. O HAM foi escolhido por ser instituição sentinela referência da rede privada no tratamento e acompanhamento dos casos de adultos com suspeita de Zika. As análises laboratoriais foram feitas no Instituto Leônidas e Maria Diane (ILMD) – Fiocruz, Manaus, Amazonas e no Instituto René Rachou – Fiocruz, Minas Gerais.

4.3 População de estudo

Participaram deste estudo 353 pacientes atendidos no Hospital Adventista em Manaus, Amazonas (HAM), entre 11 de fevereiro e 17 de maio de 2016, com suspeita de infecção pelo ZIKV**,** além de um grupo controle composto por 100 indivíduos saudáveis residentes em Manaus – AM.

O Hospital Adventista foi a instituição eleita por ter sido sentinela na rede privada no atendimento dos adultos suspeitos de ZIKV durante o surto epidemiológico ocorrido no ano de 2016.

4.4 Critérios de inclusão e exclusão

4.4.1 Critérios de inclusão

Foram incluídos na pesquisa indivíduos de ambos os sexos, entre 18 e 65 anos, de demanda espontânea, com suspeita clínica de infecção por ZIKV que aceitaram assinar o Termo de Consentimento Livre e Esclarecido (TCLE).

Os critérios clínicos de inclusão basearam-se no que o OMS definiu como casos suspeitos de infecção por ZIKV: exantema maculopapular acompanhada por pelo menos um dos seguintes sinais ou sintomas: febre máxima de 38,5ºC, conjuntivite sem secreção, artralgia ou edema articular (BRASIL, 2016). Todos os pacientes incluídos estavam na fase aguda da doença, de um a seis dias (mediana de 3 dias), após o início dos sintomas.

O grupo controle foi composto de indivíduos saudáveis, com idade entre 18 e 65 anos residentes em Manaus – AM.

4.4.2 Critérios de não inclusão

Não foram elegíveis para o estudo gestantes, indígenas e pacientes apresentando alguma imunodeficiência conhecida ou com alguma doença infecciosa diagnosticada. Foram também excluídos os indivíduos que apresentaram diagnóstico laboratorial positivo para outras arboviroses ou doenças infecto-contagiosas.

4.5 Aspectos éticos

O protocolo do estudo foi aprovado pelo Comitê de Ética da Universidade do Estado Amazonas (CAAE: 56745116.6.0000.5016) e com a Declaração de Helsinque de 1975, revisada em 1983. Todos os sujeitos forneceram consentimento informado por escrito.

4.6 Fluxograma

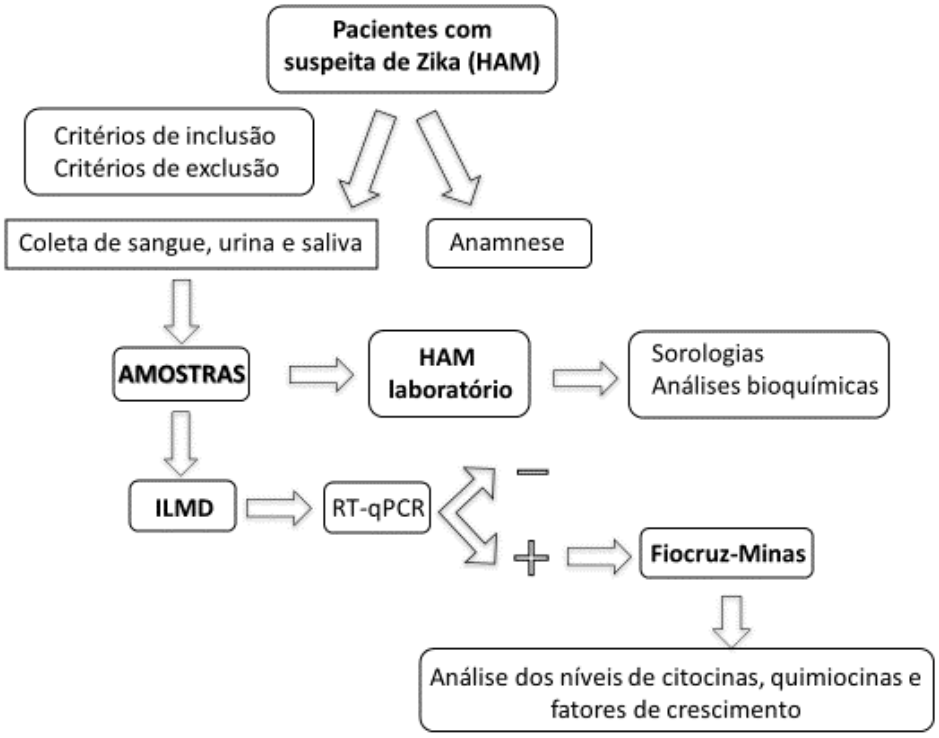

4.7 Ficha Clínica e anamnese

De cada paciente foram coletados dados demográficos referentes a nome, endereço, telefone, idade, data de nascimento, etnia, escolaridade, sexo e estado civil. Os sinais e sintomas de relevância clínica como presença de exantema, prurido, febre, artralgia, edema articular, cefaleia, conjuntivite, mialgia, linfadenopatia, diarreia, náusea, vômito, presença de doenças sistêmicas e gestação

foram colhidos através de um questionário de forma objetiva. Os dados foram anotados em uma ficha padronizada **(APÊNDICE A)** para facilitar a análise de dados e digitados em um banco de dados do Excel.

4.8 Coleta das amostras

Três amostras biológicas foram coletadas de cada paciente sendo essas: soro, urina e saliva. As amostras de sangue periférico foram coletadas por punção venosa em tubos com sistema a vácuo contendo o anticoagulante ácido etilenodiamino tetra-cético (EDTA) *(BD Vacutainer® EDTA K2)*. A coleta da urina foi realizada em coletores do tipo universal. Para coleta da saliva os voluntários mastigaram um pedaço de aproximadamente 1 cm de um tubo de látex, número 203 (Auriflex, São Roque, SP), previamente esterilizado, para estimular a produção da mesma. A saliva produzida durante os primeiros 30 segundos foi deglutida, sendo subseqüentemente coletada por 5 minutos em coletores universais (ABDALLA et al., 2010).

As amostras de sangue foram enviadas ao laboratório de rotina do HAM onde eram realizadas a centrifugação e separação do soro. Além disso, eram feitos os testes rápido para Dengue (NS1 - CTK Biotech OnSite) e testes sorológicos. Os testes sorológicos (IGM e IGG) utilizaram a tecnologia de imunoensaio enzimático para dengue (Serion Elisa classic Dengue), rubéola (Abbott AxSYM), sarampo (Bio-Rad Laboratories, Hercules, CA) e Parvovírus B19 (Serion Elisa), como recomendado pelos fabricantes.

4.9 Processamento das amostras

4.9.1 RT-PCR em Tempo Real

As amostras de soro, urina e saliva eram posteriormente enviadas ao Instituto Leônidas e Maria Deane - Fiocruz Amazônia - para realização de Reação em Cadeia da Polimerase da Transcriptase Reversa em Tempo Real (RT-qPCR) para ZIKV (LANCIOTTI et al., 2008); Chikungunya (LANCIOTTI et al., 2007) e DENV (GURUKUMAR et al., 2009). Um protocolo multiplex também avaliou amostras de soro para infecção pelo vírus Mayaro e pelo vírus Oropouche (GOMES NAVECA et al., 2017c).

As extrações do RNA foram realizadas com o kit comercial QIAmp® *RNA kit* (*QIAGEN, Chatsworth, CA, USA*), sendo utilizado 140 µl de cada espécime, eluído em 60 µl de tampão AVE, de acordo com as recomendações descritas pelo fabricante **(APÊNDICE B)**. Em seguida, as amostras de RNA foram congeladas a -80°C para realização dos testes moleculares.

Dois protocolos de Reação em Cadeia da Polimerase da Transcriptase Reversa em Tempo Real (RT-qPCR) foram utilizados. O primeiro foi previamente descrito por Lanciotti (LANCIOTTI et al., 2008), tendo como alvo o gene do envelope do ZIKV (ENV), enquanto o segundo protocolo foi delineado pelo nosso grupo, baseado nas sequências nucleotídicas disponíveis do gene da proteína não estrutural 5 (NS5) genótipo asiático do ZIKV. Ambos os protocolos foram realizados como reações individuais usando 2,5µL de cada RNA, com o kit TaqMan® Fast Virus 1-Step em um sistema de PCR em tempo real StepOnePlus ™ (Applied Biosystems, EUA), sob as seguintes condições: 50°C para cinco minutos

(transcrição reversa), 95°C por 20 segundos, seguidos por 45 ciclos de 95°C por três segundos e 60°C por 60 segundos **(APÊNDICE C)**. Todas as amostras foram relatadas como positivas se apresentassem um valor de limiar de ciclo (Ct) <38.

4.9.2 Análise dos níveis de citocinas, quimiocinas e fatores de crescimento

Os soros dos pacientes também foram enviados para o Instituto René Rachou (Fiocruz Minas Gerais) para análise dos níveis de citocinas, quimiocinas e fatores de crescimento.

Ensaio com 27 analitos-microesferas de alta performance (Bio-Rad, Hercules, CA, EUA) foi empregado para detecção e quantificação de múltiplos alvos, incluindo: CXCL8 (IL-8); CXCL10 (IP-10); CCL11 (Eotaxina); CCL3 (MIP-1α); CCL4 (MIP-1β); CCL2 (MCP-1); CCL-5 (RANTES); IL-1, IL-6, TNF-a, IL-12; IFN-y, IL-17; IL-1Ra (antagonista do receptor de IL-1); IL-2; IL-4; IL-5; IL-7; IL-9; IL-10; IL-13; IL-15; FGF-básico; PDGF; VEGF; G-CSF e GM-CSF. As amostras foram testadas de acordo com as instruções do fabricante no instrumento Bio-Plex 200 (Bio-Rad).

4.10 Análise estatística

4.10.1 Análise estatística referente aos artigos 1 e 2

As análises estatísticas foram inicialmente realizadas utilizando o GraphPad Prism (GraphPad Software 6.0, San Diego, CA, EUA). A análise comparativa dos registros clínicos foi realizada utilizando-se Teste exato de Fisher. A análise dos níveis de biomarcadores foi realizada utilizando testes U de Mann-Whitney. As

correlações multivariadas foram analisadas com o teste não paramétrico de Spearman. teste (alfa .05) em execução no software JMP, v13.1.0 (Instituto SAS, Cary, NC, EUA). Correlações (Spearman r) foram representados por uma matriz de mapa de cores. A dinâmica da viremia, quimiocinas, citocinas, e fatores de crescimento foram avaliados usando a mediana do valor de cada analito. Análise comparativa dos biomarcadores foi realizada pelo teste de Kruskal-Wallis seguido pelo teste de Dunn. Para todos os testes, as diferenças foram consideradas significativo quando p <0,05 usando testes bicaudais. As estratégias de gerenciamento de dados foram aplicadas para identificar perfis gerais e específicos do tempo. Para a assinatura de biomarcador a análise foi realizada conforme descrito anteriormente (LUIZA-SILVA et al., 2011). Gráficos de radar foram usados para compilar assinaturas de biomarcadores de controles e infectados pelo ZIKV, aplicando o percentil de 75% como limite. Diagramas de Venn foram criados para identificar atributos compartilhados e exclusivos, juntamente com a linha do tempo do início dos sintomas (http://bioinformatics.psb.ugent.be/webtools/Venn/). Software Cytoscape v3.2.0 (http://www.cytoscape.org/) foi empregado para visualizar e integrar múltiplos atributos em redes nodais circulares. Conectando bordas foram desenhados para ressaltar cada associação como (linha contínua) ou negativa (linha tracejada). O biomarcador padrão de cluster foi definido por heatmaps montados usando Software R (função heatmap.2; v3.0.1). Árvores de decisão de algoritmos foram gerados com o software WEKA v3.6.11 (Universidade de Waikato, Nova Zelândia) para identificar atributos de raiz e ramo e segregar pacientes dos controles. Curvas ROC foram construídas para definir o corte e identificar biomarcadores com melhor desempenho discriminando pacientes infectados pelo ZIKV de controles. Índices de desempenho (co-positividade, co-negatividade,

positivo e razões de verossimilhança negativas) foram calculados usando MedCalc software v7.3 (Ostend, Bélgica).

4.10.2 Análise estatística referente aos artigos 3

Para analisar o processo de detecção foi utilizado o modelo de ocupação multinível desenvolvido por Nichols et al, (2009). As probabilidades e covariáveis foram avaliadas utilizando modelos descritos anteriormente (McClintock et al, 2010; MacKenzie & Bailey, 2004). Ajustamos os modelos por meio de máxima verossimilhança e avaliamos o desempenho relativo usando a versão de Akaike (AICc) e métricas relacionadas (Burnham & Anderson, 2002). As análises foram feitas em PRESENCE v. 11.8.

4.10.3 Análise estatística referente aos artigos 4

Foi utilizada a Razões de chances (*odds ratios* – OR) de diagnóstico de zika em relação à dengue. A presença de sinais e sintomas (exantema maculopapular, febre, prurido, artralgia, edema articular, cefaleia, conjuntivite, mialgia, linfadenopatia, diarreia, náuseas e vômitos) foram estimadas por meio de modelo de regressão logística múltipla. Para a entrada e retenção (*stepwise backward*) das variáveis explicativas no modelo considerou-se a significância estatística da associação de ZIKV com a presença de sinais e sintomas nos níveis de 20% e 5%, respectivamente. A significância estatística foi determinada pelo teste de *Wald* e a qualidade do ajuste do modelo final pela análise de medidas de *deviance*, utilizando-se o programa Stata 12.

5. RESULTADOS PARCIAIS

Como resultados parciais, foram publicados dois artigos:

Artigo 1 - Atrial fibrillation in a patient with Zika vírus infection – relato de caso referente ao objetivo específico número 4 - Descrever possíveis manifestações atípicas durante o curso da infecção pelo vírus **(ANEXO 1)**;

Artigo 2 - Analysis of the immunological biomarker profile during acute Zika virus infection reveals the overexpression of CXCL10, a chemokine linked to neuronal damage – artigo completo referente ao objetivo específico número 1 - Detectar os níveis séricos de citocinas, quimiocinas e fatores de crescimento dos pacientes infectados e comparar com o grupo controle **(ANEXO 2)**;

Além disso, dois artigos estão sendo desenvolvidos:

Artigo 3 - Molecular detection of Zika virus in serum, urine and saliva from acute-phase patients: effects of differential RNA shedding and RT-PCR sensitivity - artigo completo, em fase de correções de texto, referente ao objetivo específico número 2 - Verificar por meio de parâmetros moleculares (RT-qPCR) a presença do vírus na saliva, urina e plasma dos pacientes e avaliar o melhor fluído para diagnóstico da Zika **(ANEXO 3)**;

Artigo 4 - Clinical and laboratory profile of patients infected by Zika vírus - artigo completo, em fase de análise de dados, referente ao objetivo específico número 3 - Analisar os achados clínicos e laboratoriais a fim de identificar pontos potencialmente úteis para o diagnóstico da doença.

Referente a esse artigo foi apresentado um trabalho intitulado “Desenvolvimento de modelo de regressão logística múltipla para apoio ao diagnóstico diferencial das infecções sintomáticas pelo vírus Zika e Dengue” no MEDTROP 2018.

REFERÊNCIAS

ABDALLA, L. F. et al. Mycobacterium leprae in the periodontium, saliva and skin smears of leprosy patients. **Rev. odonto ciênc. Rev. odonto ciênc**, v. 2525, n. 22, 2010.

ABDALLA, L. F. et al. Atrial fibrillation in a patient with Zika virus infection. **Virology Journal**, v. 15, n. 1, 2018.

ALETTI, M. et al. Transient myocarditis associated with acute Zika virus infection. **Clinical Infectious Diseases**, p. ciw802, 2016.

ANDRADE, D. V; HARRIS, E. Recent advances in understanding the adaptive immune response to Zika virus and the effect of previous flavivirus exposure. **Virus Research**, p. 1–7, 2017.

ARIAS-GOETA, C. et al. Chikungunya virus adaptation to a mosquito vector correlates with only few point mutations in the viral envelope glycoprotein. **Infection, Genetics and Evolution**, v. 24, p. 116–126, jun. 2014.

AZEREDO, E. L. et al. Clinical and Laboratory Profile of Zika and Dengue Infected Patients: Lessons Learned From the Co-circulation of Dengue, Zika and Chikungunya in Brazil. **PLoS Currents**, 2018.

AZEVEDO, R. S. S. et al. Zika virus epidemic in Brazil. I. Fatal disease in adults: Clinical and laboratorial aspects. **Journal of Clinical Virology**, v. 85, p. 56–64, dez. 2016.

BAYER, A. et al. Type III Interferons Produced by Human Placental Trophoblasts Confer Protection Against Zika Virus Infection HHS Public Access. **Cell Host Microbe**, v. 19, n. 5, p. 705–712, 2016.

BOWEN, J. R. et al. Zika Virus Antagonizes Type I Interferon Responses during Infection of Human Dendritic Cells. **PLoS Pathogens**, v. 13, n. 2, 2017.

BRASIL. Protocolo para implantação de unidades sentinelas para Zika vírus. p. 7, 2016.

CAMPOS, G. S.; BANDEIRA, A. C.; SARDI, S. I. Zika Virus Outbreak, Bahia, Brazil. **Emerging Infectious Diseases**, v. 21, n. 10, p. 1885–1886, out. 2015.

CHARREL, R. N. et al. Background review for diagnostic test development for Zika virus infection. **Bulletin of the World Health Organization**, v. 94, n. 8, p. 574–584D, 2016.

CHAUDHARY, V. ET AL. Selective Activation of Type II Interferon Signaling by Zika Virus NS5 Protein. **J Virol**, v. 91, n. 20, 2017.

CORMAN, V. M. et al. Clinical comparison, standardization and optimization of Zika virus molecular detection. **Bulletin of the World Health Organization**, n. April, 2016.

CULSHAW, A. et al. Open Peer Review The immunology of Zika Virus [version 1; referees: 2 approved]. **F1000 Faculty Rev**, v. 11, n. 7, p. 203203–7, 2018.

DE CARVALHO, N. S. et al. Zika virus and pregnancy: An overview. **American Journal of Reproductive Immunology**, v. 77, n. 2, p. 1–8, 2017.

DOS SANTOS, T. et al. Zika Virus and the Guillain–Barré Syndrome — Case Series from Seven Countries. **New England Journal of Medicine**, v. 375, n. 16, p. 1598–1601, 20 out. 2016.

DOWD, K. A.; DEMASO, C. R.; PIERSON, T. C. Genotypic Differences in Dengue Virus Neutralization Are Explained by a Single Amino Acid Mutation That Modulates Virus Breathing. **mBio**, v. 6, n. 6, p. e01559-15, 3 nov. 2015.

DUFFY, M. R. et al. Zika Virus Outbreak on Yap Island, Federated States of Micronesia. **The New England Journal of Medicine**, v. 360, p. 2536–2543, 2009.

ELIAS COLOMBO, T. et al. Clinical, laboratory and virological data from suspected ZIKV patients in an endemic arbovirus area. 2017.

FARIA, N. R. et al. Zika virus in the Americas: Early epidemiological and genetic findings. **Science**, v. 352, n. 6283, p. 345–349, 2016.

FAYE, O. et al. Molecular Evolution of Zika Virus during Its Emergence in the 20th Century. **PLoS Neglected Tropical Diseases**, v. 8, n. 1, p. e2636, 9 jan. 2014.

FERNANDEZ-GARCIA, M.-D. et al. Pathogenesis of Flavivirus Infections: Using and Abusing the Host Cell. **Cell Host & Microbe**, v. 5, n. 4, p. 318–328, 23 abr. 2009.

FOY, B. D. et al. Probable Non-Vector-borne Transmission of Zika Virus, Colorado, USA. **Emerging Infectious Diseases**, v. 17, n. 5, p. 880–882, 2011.

FROESCHL, G. et al. Long-term kinetics of Zika virus RNA and antibodies in body fluids of a vasectomized traveller returning from Martinique: A case report. **BMC Infectious Diseases**, v. 17, n. 1, p. 1–9, 2017.

GOMES NAVECA, F. et al. Analysis of the immunological biomarker profile during acute Zika virus infection reveals the overexpression of CXCL10, a chemokine already linked to neuronal damage Short Title: CXCL10 overexpression in Acute Zika Virus Infection. 2017a.

GOMES NAVECA, F. et al. Analysis of the immunological biomarker profile during acute Zika virus infection reveals the overexpression of CXCL10, a chemokine already linked to neuronal damage Short Title: CXCL10 overexpression in Acute Zika Virus Infection. 2017b.

GOMES NAVECA, F. et al. Multiplexed reverse transcription real-time polymerase chain reaction for simultaneous detection of Mayaro, Oropouche, and Oropouche-like viruses. **Mem Inst Oswaldo Cruz Rio de Janeiro**, v. 112, n. 7, p. 510–513, 2017c.

GRISCHOTT, F. et al. Non-vector-borne transmission of Zika virus: A systematic review. **Travel Medicine and Infectious Disease**, v. 14, n. 4, p. 313–330, 2016.

GURUKUMAR, K. et al. Development of real time PCR for detection and quantitation of Dengue Viruses. **Virology Journal**, v. 6, n. 610, 2009.

HAMEL, R. et al. Biology of Zika Virus Infection in Human Skin Cells. **Journal of Virology**, v. 89, n. 17, p. 8880–8896, 2015.

HEINZ, F. X.; STIASNY, K. Flaviviruses and their antigenic structure. **Journal of clinical virology : the official publication of the Pan American Society for Clinical Virology**, v. 55, n. 4, p. 289–95, 1 dez. 2012.

KAM, Y.-W. et al. Specific Biomarkers Associated With Neurological Complications and Congenital Central Nervous System Abnormalities From Zika Virus–Infected

Patients in Brazil. **The Journal of Infectious Diseases JID The Journal of Infectious Diseases ®**, v. 172216, n. 2017, p. 216172–81, 2017.

KODATI, S. et al. Bilateral posterior uveitis associated with Zika virus infection. **www.thelancet.com**, v. 389, 2017.

LANCIOTTI, R. S. et al. Chikungunya Virus in US Travelers Returning from. v. 13, n. 5, p. 764–767, 2007.

LANCIOTTI, R. S. et al. Genetic and serologic properties of Zika virus associated with an epidemic, Yap State, Micronesia, 2007. **Emerging Infectious Diseases**, v. 14, n. 8, p. 1232–1239, 2008.

LAZEAR, H. M. et al. A Mouse Model of Zika Virus Pathogenesis. **Cell Host and Microbe**, v. 19, n. 5, p. 720–730, 2016.

LAZEAR, H. M.; DIAMOND, M. S. New Insights into Innate Immune Restriction of West Nile Virus Infection. 2014.

LEAL, W. S. Zika mosquito vectors: the jury is still out. **F1000Research**, v. 5, n. 0, p. 2546, 2016.

LIMA-CAMARA, T. N. Emerging arboviruses and public health challenges in Brazil. **Revista de Saúde Pública**, v. 50, n. 0, 2016.

LINDENBACH, B. D.; RICE, C. M. Molecular biology of flaviviruses. **Advances in Virus Research**, v. 59, p. 23–61, 1 jan. 2003.

LUCAS, C. G. O. et al. Critical role of CD4+ T cells and IFNγ signaling in antibody-mediated resistance to Zika virus infection. **Nature Communications**, v. 9, n. 1, p. 3136, 2018.

LUIZA-SILVA, M. et al. Cytokine Signatures of Innate and Adaptive Immunity in 17DD Yellow Fever Vaccinated Children and Its Association With the Level of Neutralizing Antibody. **Journal of Infectious Diseases**, v. 204, n. 6, p. 873–883, 15 set. 2011.

LUSTIG, Y. et al. Detection of Zika virus RNA in whole blood of imported Zika virus disease cases up to 2 months after symptom onset, Israel, December 2015 to April 2016. **Eurosurveillance**, v. 21, n. 26, p. 1–4, 2016.

MULLER, D. A.; YOUNG, P. R. The flavivirus NS1 protein: Molecular and structural biology, immunology, role in pathogenesis and application as a diagnostic biomarker. **Antiviral Research**, v. 98, n. 2, p. 192–208, 1 maio 2013.

MUSSO, D. et al. Detection of Zika virus in saliva. **Journal of Clinical Virology**, v. 68, p. 53–55, 2015.

NGONO, A. E. et al. Mapping and Role of the CD8 + T Cell Response During Primary Zika Virus Infection in Mice HHS Public Access. **Cell Host Microbe January**, v. 11, n. 211, p. 35–46, 2017.

NICASTRI, E. et al. Zika Virus Infection in the Central Nervous System and Female Genital Tract. **Emerg Infect Dis**, v. 22, n. 12, p. 2228–2230, 2016.

PETERSEN, L. R. et al. Zika Virus. **New England Journal of Medicine**, v. 374, n. 16, p. 1552–1563, 2016.

PETERSON, E. et al. Infection and Preventing Infection in Brain Are Important for

Controlling Virus Adaptive Immune Responses to Zika Virus Adaptive Immune Responses to Zika Virus Are Important for Controlling Virus Infection and Preventing Infection in Brain and Testes. **DCSupplemental The Journal of Immunology by guest on April The Journal of Immunology**, v. 198, n. 25, p. 3526–3535, 2017.

PINHEIRO, T. J. et al. Manifestações neurológicas das infecções pelos vírus zika e chikungunya. **Arquivos de Neuro-Psiquiatria**, v. 74, n. 11, p. 937–943, 2016.

PINTO JUNIOR, V. L. et al. Vírus Zika: Revisão para Clínicos. **Acta Médica Portuguesa**, v. 28, n. 6, p. 760, 3 dez. 2015.

PRISANT, N. et al. Zika virus in the female genital tract. **The Lancet Infectious Diseases**, v. 16, n. 9, p. 1000–1001, 2016.

QUICKE, K. M.; SUTHAR, M. S. The Innate Immune Playbook for Restricting West Nile Virus Infection. **Viruses**, v. 5, p. 2643–2658, 2013.

RATANACHAROENSIRI, A. et al. Zika Virus: An Emerging Epidemic. **Journal of research in pharmacy practice**, v. 6, n. 1, p. 1–2, 2017.

ROBBIANI, D. F. et al. Recurrent Potent Human Neutralizing Antibodies to Zika Virus in Brazil and Mexico. **Cell**, v. 169, n. 4, p. 597–609.e11, 4 maio 2017.

ROZÉ, B. et al. Zika virus detection in cerebrospinal fluid from two patients with encephalopathy, Martinique, February 2016. **Euro surveillance : bulletin Européen sur les maladies transmissibles = European communicable disease bulletin**, v. 21, n. 16, p. 1–4, 2016.

SECRETARIA DE VIGILÂNCIA EM SAÚDE - MINISTÉRIO DA SAÚDE. Boletim Epidemiológico. v. 49, n. 14, 2018.

SHRESTA, S. et al. Interferon-Dependent Immunity Is Essential for Resistance to Primary Dengue Virus Infection in Mice, Whereas T-and B-Cell-Dependent Immunity Are Less Critical. **JOURNAL OF VIROLOGY**, v. 78, n. 6, p. 2701–2710, 2004.

SILVEIRA, G. F. et al. Single point mutations in the helicase domain of the NS3 protein enhance dengue virus replicative capacity in human monocyte-derived dendritic cells and circumvent the type I interferon response. **Clinical & Experimental Immunology**, v. 183, n. 1, p. 114–128, jan. 2016.

SIMPSON, D. I. ZIKA VIRUS INFECTION IN MAN. **Transactions of the Royal Society of Tropical Medicine and Hygiene**, v. 58, p. 335–8, jul. 1964.

SMITHBURN, K. C. Neutralizing Antibodies Against Certain Recently Isolated Viruses in the Sera of Human Beings Residing in East Africa. **The Journal of Immunology**, v. 69, n. 2, 1952.

SUN, J. et al. Presence of Zika virus in conjunctival fluid. **JAMA Ophthalmology**, v. 134, n. 11, p. 1330–1332, 2016.

SUTHAR, M. S.; AGUIRRE, S.; FERNANDEZ-SESMA, A. Innate Immune Sensing of Flaviviruses. **PLoS Pathog**, v. 9, n. 9, p. 1003541, 2013.

TAPPE, D. et al. Cytokine kinetics of Zika virus-infected patients from acute to reconvalescent phase. **Medical Microbiology and Immunology**, v. 205, p. 269–273, 2016.

WAGGONER, J. J.; PINSKY, B. A. Zika virus: Diagnostics for an emerging pandemic threat. **Journal of Clinical Microbiology**, v. 54, n. 4, p. 860–867, 2016.

WANG, Q. et al. Molecular determinants of human neutralizing antibodies isolated from a patient infected with Zika virus. **Science translational medicine**, v. 8, n. 369, p. 369ra179, 14 dez. 2016.

WEN, J. et al. Dengue virus-reactive CD8+T cells mediate cross-protection against subsequent Zika virus challenge. **Nature Communications**, v. 8, n. 1, 2017a.

WEN, J. et al. Identification of Zika virus epitopes reveals immunodominant and protective roles for dengue virus cross-reactive CD8+ T cells. **Nature Microbiology**, v. 2, n. 6, p. 17036, 13 mar. 2017b.

ZANLUCA, C. et al. First report of autochthonous transmission of Zika virus in Brazil. **Mem Inst Oswaldo Cruz Rio de Janeiro**, v. 110, n. 4, p. 569–572, 2015.

ZHAO, H. et al. Structural Basis of Zika Virus-Specific Antibody Protection. **Cell**, v. 166, p. 1016–1027, 2016.

ANEXO 1

Abdalla et al. Virology Journal (2018) 15:23
DOI 10.1186/s12985-018-0938-2

Virology Journal

CASE REPORT Open Access

Atrial fibrillation in a patient with Zika virus infection

Ligia Fernandes Abdalla[1,2†], João Hugo Abdalla Santos[3,4†], Renata Teodora Jales Barreto[4], Erick Martins e Souza[3], Fabrício Fonseca D'Assunção[2], Márcio Aurélio Borges[4], Valdinete Alves Nascimento[5,6], George Allan Villarouco da Silva[1,7], Victor Costa de Souza[5,6], Rajendranath Ramasawmy[1,7,8], Ana Carolina Campi-Azevedo[9], Jordana Graziela Coelho-dos-Reis[9], Lis Ribeiro do Vale Antonelli[9], Andréa Teixeira-Carvalho[9], Olindo Assis Martins-Filho[9] and Felipe Gomes Naveca[1,5,6,10*]

Abstract

Background: Zika virus is an emerging arbovirus of the family *Flaviviridae* and genus *Flavivirus* that until 2007 was restricted to a few cases of mild illness in Africa and Asia.

Case presentation: We report a case of atrial fibrillation disclosed during an acute Zika virus infection in a 49-year-old man. Different biological samples were analyzed for the molecular diagnosis of Zika by real-time PCR, however only the saliva specimen was positive. The patient's wife tested positive in the serum sample, although she was an asymptomatic carrier. Moreover, a complete overview of patient's biomarkers, including cytokines, chemokines, and growth-factors levels, was analyzed and compared to gender and age matching non-infected controls, as well as other Zika infected patients, considering the 95%CI of the mean values. Elevated levels of CXCL8, CCL11, CCL2, CXCL10, IL-1β, IL-6, TNF-α, IFN-γ, IL-17, IL-1Ra, IL-4, IL-9, FGF-basic, PDGF, G-CSF, and GM-CSF were observed in the Atrial fibrillation patient, in contrast to uninfected controls. Furthermore, increased levels of CCL5, IL-1β, TNF-α, IFN-γ, IL-9, G-CSF, and GM-CSF were observed only in the atrial fibrillation patient, when compared to other Zika patients.

Conclusions: To our knowledge, this is the first description of this type of cardiac disorder in Zika patients which may be considered another atypical manifestation during Zika virus infection.

Keywords: Zika virus, Arboviruses, Atrial fibrillation, Cardiac disorders

Background

Zika disease is an emerging illness caused by an arbovirus of the family *Flaviviridae* and genus *Flavivirus* [1]. In 1947, Zika virus (ZIKV) was isolated from a rhesus monkey in the Zika forest in Uganda, and 5 years later, in 1952, it was described infecting humans [2, 3]. Until 2007, ZIKV was restricted to a few cases of mild illness in Africa and Asia, and then it was associated with an outbreak of acute febrile illness in the Yap Island, Micronesia [4]. In Brazil, the virus was identified in autochthonous cases in the first months of 2015 [5, 6]. In August of the same year, an increase in the number of neonates with microcephaly was detected in Brazil and the hypothesis that ZIKV infection caused the microcephaly epidemic was formulated [7]. In November 2015, the Ministry of Health declared the situation a national public health emergency and a few months after this, WHO elevates this alert as a Public Health Emergency of International Concern [8–10].

ZIKV infections are often associated with slight fever, headache, maculopapular rash, arthralgia and conjunctivitis [4]. However, atypical clinical manifestations have been previously reported including neurological complications [11], congenital syndrome [12], ocular problems [13] and cardiovascular complications [14]. Here, we report a case of atrial fibrillation during a confirmed case of acute ZIKV infection.

* Correspondence: felipe.naveca@fiocruz.br
†Equal contributors
[1]Programa de Pós-Graduação em Imunologia Básica e Aplicada, Universidade Federal do Amazonas, Manaus, Amazonas, Brazil
[5]Laboratório de Ecologia de Doenças Transmissíveis na Amazônia, Instituto Leônidas e Maria Diane – Fiocruz Amazônia, Manaus, Amazonas, Brazil
Full list of author information is available at the end of the article

Case presentation

JLLP, a 49-year-old man, industrial worker, resident in Manaus, Amazonas, Brazil, was admitted to the emergency at Hospital Adventista de Manaus (HAM). The patient showed skin rash, pruritus, arthralgia, headache, myalgia, bilateral conjunctivitis, fever (38.5 °C) and hypertensive crisis with blood pressure (BP) of 240/120 mmHg, but heart rate and cardiac auscultation were normal. The patient had no travel history and described the appearance of symptoms 3 days before seeking medical attention. Besides, the patient reported the absence of hypertensive episodes or any other cardiac disorder in the past.

Immediately, the treatment for the hypertensive crisis was initiated with sodium nitroprusside (250 ml glycated serum 5% + Nipride − 1 ampoule = 2 ml) administered 5 ml/h by continuous infusion. In the following two, three and 4 hours it was administered 7 ml, 10 ml and 15 ml of sodium nitroprusside, respectively, but the blood pressure was still elevated. No abnormalities in electrocardiogram (ECG) and chest radiography (CR) were observed.

The patient was still refractory to blood pressure control (BP 238/120 mmHg) 4 hours after starting treatment, and showed elevated blood glucose levels (250 mg/dL), therefore, he was transferred to the Intensive Care Unit (ICU). Suddenly, the patient suffered a cardiac arrhythmia (atrial fibrillation - AF) which was chemically reversed with an attack dose of two ampoules (6 ml) of intravenous amiodarone hydrochloride (50 mg/ml). For the maintenance dose, six ampoules of amiodarone (8 ml/h) were administered in 5% glycated serum (250 ml) by continuous infusion for 12 h.

Due to the symptoms presented at the time of attendance, and the ongoing Zika outbreak in course, the patient and his wife, an asymptomatic contact, were inserted into the protocol for ZIKV surveillance. Both had samples of blood, urine, and saliva collected for arboviral testing by the reverse transcription real-time polymerase chain reaction (RT-qPCR).

On the sixth day of hospitalization, the patient underwent magnetic resonance imaging (MRI); echocardiographic doppler (DE) and coronary angiography (CA). Only the MRI was altered with bilateral supratentorial microangiopathic gliosis. A second ECG was performed on the eighth day of hospitalization, which presented no alterations and the patient was discharged. Serological tests for other infectious diseases were negative and the RT-qPCR results showed positivity for ZIKV in the saliva sample. Although still asymptomatic, his wife also tested positive for ZIKV in the serum sample.

Materials and methods

The patient's blood sample was collected for Dengue virus NS1 testing (CTK Biotech OnSite rapid test) and IgM/IgG serologic testing using enzyme immunoassay technology for dengue (Serion Elisa classic Dengue). The sample was also tested for rubella (Abbott AxSYM); measles (Bio-Rad Laboratories, Hercules, CA) and Parvovirus B19 (Serion Elisa), as recommended by the manufacturers'.

The serum, urine and saliva samples of the patient and his wife were sent to Instituto Leônidas e Maria Deane - Fiocruz Amazônia - to test for ZIKV [15]; Chikungunya virus (CHIKV) [16]; DENV [17]. A multiplex protocol also evaluated serum samples for Mayaro virus (MAYV) and Oropouche virus (OROV) infection [18].

The patient's serum was also sent to Instituto René Rachou (Fiocruz Minas Gerais) for the analysis of cytokines, chemokines, and growth-factors levels. High-performance microbeads 27-plex assay (Bio-Rad, Hercules, CA, USA) was employed for detection and quantification of multiple targets, including: CXCL8 (IL-8); CXCL10 (IP-10); CCL11 (Eotaxin); CCL3 (MIP-1α); CCL4 (MIP-1β); CCL2 (MCP-1); CCL-5 (RANTES); IL1- β, IL-6, TNF- α, IL-12; IFN- γ, IL-17; IL-1Ra (IL-1 receptor antagonist); IL-2; IL-4; IL-5; IL-7; IL-9; IL-10; IL-13; IL-15; FGF-basic; PDGF; VEGF; G-CSF and GM-CSF. The sample was tested according to the manufacturer's instructions on a Bio-Plex 200 instrument (Bio-Rad). The patient's results were compared to two reference groups: I) a control group consisting of 54 healthy male subjects, age ranging from 18 to 40 years (median = 30 years), all living in Manaus – AM and II) a group consisting of 24 ZIKV-infected male patients, with classical zika illness presentation, age ranging from 20 to 59 years (median = 37 years), all living in Manaus – AM. The mean values for each biomarker were compared with the 95%CI values of each reference groups.

Supplementary exams included: hematological and biochemical tests; electrocardiogram (ECG); chest radiography (CR); abdominal ultrasonography (AU); coronary angiography (CA); doppler echocardiographic (DE) and magnetic resonance imaging (MRI).

Results

Serology and molecular tests

The DENV NS1 testing was negative, as well as the serological tests for rubella, parvovirus B19, and measles IgM, whereas positive serological results were observed for rubella and measles IgG.

The RT-qPCR showed positivity to ZIKV in the patient's saliva (mean Ct value: 32.3) and in the serum of his wife (mean Ct value: 31.1). No positivity was found for DENV, CHIKV, MAYV or OROV.

Cytokine, chemokine and growth factors levels

The serum levels of chemokines, cytokines and growth factor were evaluated and the data presented in Fig. 1. The results demonstrated that there was an increase in

the levels of chemokines (CXCL8, CCL11, CCL2 and CXCL10); pro-inflammatory cytokines (IL-1β, IL-6, TNF-α, IFN-γ and IL-17); regulatory cytokines (IL-1Ra, IL-4 and IL-9) and growth factors (FGF-basic, PDGF, G-CSF and GM-CSF) in the ZIKV-infected patient with atrial fibrillation, considering the 95%CI of the mean values observed for a control group of gender-matching healthy individuals. No difference was observed for the CCL4 and CCL5 (chemokines) and VEGF (growth factor). Conversely, lower levels of CCL3, IL-12, IL-5, IL-10, IL-13 were observed in the ZIKV-infected patient with atrial fibrillation as compared to the healthy controls (Fig. 1a).

The overall biomarker profile observed in the ZIKV-infected patient with atrial fibrillation was also compared with a group of gender-matching ZIKV-infected patient. Data analysis revealed that the case reported here displayed increased the levels of CCL5, IL-1β, TNF-α, IFN-γ, IL-9, G-CSF and GM-CSF and decreased levels of CCL4, IL-12, IL-13 and VEGF as compared with the 95%CI of the mean values found in the group patients infected with the ZIKV. No differences were observed for the CXCL8, CCL11, CCL3, CCL2, CXCL10, IL-6, IL-17, IL-1Ra, IL-4, IL-5, IL-10, FGF-basic and PDGF (Fig. 1b).

Supplementary exams

The blood samples for hematological and biochemical tests were collected during the acute phase of the disease, 4 days after the onset of symptoms, and showed: hematocrit: 46%; hemoglobin: 15 g/dl, leukocytes: $16{,}900 \times 10^3$ mm^3, platelets: $143{,}000 \times 10^3$ mm^3; lymphocytes: 26%; eosinophils: 2%; neutrophils: 88%; monocytes:

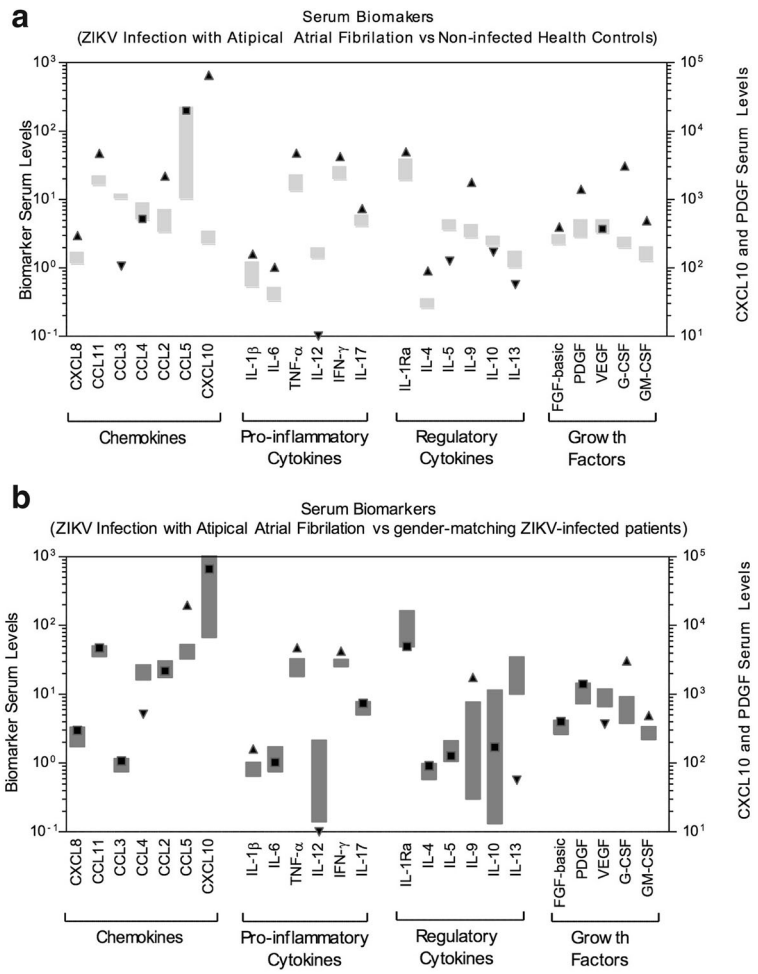

Fig. 1 Overview of serum chemokines, cytokines and growth factors of the atrial fibrillation patient compared to control groups. Serum biomarkers: CXCL8 (IL-8); CXCL10 (IP-10); CCL11 (Eotaxin); CCL3 (MIP-1α); CCL4 (MIP-1β); CCL2 (MCP-1); CCL-5 (RANTES); IL1-β, IL-6, TNF-α, IL-12; IFN-γ, IL-17; IL-1Ra (IL-1 receptor antagonist); IL-2; IL-4; IL-5; IL-7; IL-9; IL-10; IL-13; IL-15; FGF-basic; PDGF; VEGF; G-CSF and GM-CSF were measured by high performance microbeads 27-plex assay, as described in materials and methods, with the 95%CI represented by gray boxes. Black arrows represent an increase (up) or decrease (down) in the patient's biomarkers level in comparison to control groups; a black square represents biomarkers levels at the 95%CI. **a** Biomarkers' levels: case vs. gender matching non-infected heath controls; (**b**) Biomarkers' levels: case vs. gender matching ZIKV-infected patients

4%; ALT: 26 U/L; AST: 24 U/L; GGT: 32 U/L; creatinine: 0,78 mg/dL; urea: 25 mg/dL; alkaline phosphatase: 56 mg/dL; total bilirubin: 0,5 mg/dL; direct bilirubin: 0,2 mg/dL; indirect bilirubin: 0,3 mg/dL; creatine phosphokinase: 62 U/L; prothrombin time (PT):14,5 s; prothrombin activity: 84,5%; albumin: 3,2 g/dL and C protein: 21 mg/L.

The patient underwent two ECG, one performed during the hospitalization period and other 8 days after, without abnormalities. Among the image exams, only the MRI results showed an alteration, a bilateral supratentorial microangiopathic gliosis, which may be related to acute myocardial infarction.

Discussion

In the present study, we described a case of AF in a patient with ZIKV infection, 4 days after the onset of symptoms. Until the present time, there is no similar reports relating cardiac arrhythmias and ZIKV virus infection. However, a case of myocarditis associated with to ZIKV infection during the acute phase of illness [14]. Considering that the patient of this study had no prior history of cardiovascular disease and no other heart abnormality was observed in the image exams, we may hypothesize the association of FA with the acute ZIKV infection.

Some studies have reported the relation of a cardiac disorder and arbovirus infection. In a survey carried out in a cardiovascular reference center during a dengue epidemic in Colombia (2010), 24 patients with dengue were related to cardiovascular symptoms, and 42.8% of these individuals had heart rhythm disturbances [19]. Another case report described West Nile virus causing myocarditis with an arrhythmia that led to patient death [20]. In 1972, a study described cases of Chikungunya related to cardiac manifestations such as myocarditis and cardiomyopathy [21].

Studies in rodents reinforce this theory, once changes in the ventricular repolarization were observed in ECG after ZIKV infection. Authors also found abnormalities in the synaptic conduction of motor neurons in the heart and cardiac muscles, and such changes could trigger arrhythmic processes [22]. Furthermore, myocarditis during ZIKV infections was also demonstrated in a mouse model [23], where multiple necrosis loci and myocarditis, possibly associated with pulmonary edema, were observed.

Different studies have reported the detection of viral RNA in various body fluids such as blood [24], saliva [25] and urine [26]. Indeed, Musso (2015) found that the ability to detect ZIKV RNA in saliva was higher compared to blood and recommend using different biological fluids to increase the sensitivity of the molecular detection of ZIKV. Based on these studies, and on our results where the ZIKV detection was higher in saliva samples (unpublished data), we chose to collect serum, urine and saliva samples. Interesting, only the patient's saliva sample was positive in the RT-qPCR.

As some studies have pointed to asymptomatic cases of ZIKV infection through sexual contact [27] or blood transfusion [28], we decided to collect samples from the patient's wife, an asymptomatic contact, and positivity was confirmed in the plasma sample. This result is fascinating since the literature is still very scarce regarding the asymptomatic cases of ZIKV infection.

Concerning the results found in hematological and biochemical tests, the patient presented mild thrombocytopenia ($143{,}000 \times 10^3$ mm^3), leukocytosis ($16{,}900 \times 10^3$ mm^3) and neutrophilia (88%). Comparing these findings with other flaviviruses, the frequent alterations observed in dengue infection are thrombocytopenia, hemoconcentration (with increased hematocrit) and leukopenia; leukocytosis is also described, but in elderly patients [29]. In Yellow fever, at the beginning of the disease, the blood count shows leukocytosis with neutrophilia and then evolves to leucopenia, lymphocytosis, and thrombocytopenia at later stages [30]. About 50% of the patients infected with West Nile virus present leukocytosis and other 15% shows leukopenia [31].

We observed alterations in the immune response with elevated levels of some cytokines, chemokines and growth factors in contrast to healthy controls. Other studies also found an increase of several pro-inflammatory cytokines including IL-18, TNF-α, IFN-γ, IL-8, IL-6, GRO-α and IL-17 [32, 33]. When compared to other individuals who are also in the acute phase of ZIKV infection, the patient also had elevated levels in different biomarkers. Other studies have observed a direct link between inflammation and atrial remodeling and, consequently, AF maintenance [34]. In general, the results revealed that the ZIKV-infected patient with atrial fibrillation presented a typical serum biomarker storm already reported for ZIKV-infected patients [33], with a more prominent pro-inflammatory status mediated by CCL5, IL-1β, TNF-α, and IFN-γ. This result links the inflammatory cytokines to the atrial fibrillation onset and prognostic implications, as previously reported [35]. Therefore, it is possible that the elevation of pro-inflammatory cytokines during ZIKV infection may increase the risk of AF.

Conclusion

Our findings support the cardiac involvement as one of the atypical manifestations during ZIKV infections. The present results also strengthen the importance of collecting other body fluids in addition to serum, to improve the diagnostic of Zika. Besides, we describe several biomarkers levels altered in comparison to healthy controls and other Zika patients.

Abbreviations
AF: Atrial fibrillation; BP: Blood pressure; CA: Coronary angiography; CHIKV: Chikungunya virus; CR: Chest radiography; DE: Echocardiographic doppler; DENV: Dengue virus; ECG: Electrocardiogram; HAM: Hospital Adventista de Manaus; ICU: Intensive Care Unit; MAYV: Mayaro virus; MRI: Magnetic resonance imaging; OROV: Oropouche virus; RT-qPCR: Reverse transcription real-time polymerase chain reaction; WHO: World Health Organization; ZIKV: Zika virus

Acknowledgements
The authors are thankful to the Programa de Desenvolvimento Tecnológico em Insumos e Saúde - PDTIS-FIOCRUZ for the use the flow cytometry (IRR) and Real-Time (ILMD) facilities. We are also grateful to the Hospital Adventista de Manaus (HAM) for the patient follow-up, hematological, biochemical, serological and complementary examinations.

Funding
FGN is funded by Conselho Nacional de Desenvolvimento Científico e Tecnológico (http://www.cnpq.br, grant 440856/2016–7) and Coordenação de Aperfeiçoamento de Pessoal de Nível Superior (http://www.capes.gov.br, grants 88881.130825/2016–00 and 88887.130823/2016–00). OAMF is funded by the Conselho Nacional de Desenvolvimento Científico e Tecnológico (http://www.cnpq.br, grant 440682/2016–9); Coordenação de Aperfeiçoamento de Pessoal de Nível Superior (http://www.capes.gov.br, grant 88881.130829/2016–01) and Financiadora de Estudos e Projetos (http://www.finep.gov.br, grant TED264/16). The funders had no role in study design, data collection and analysis, decision to publish or preparation of the manuscript.

Availability of data and materials
Luminex data is available upon request.

Authors' contributions
All authors were involved in writing the article or reviewing it critically for important intellectual content, and all authors approved the final version to be submitted for publication. Patient follow-up, interpretation of clinical exams and sample collection - JHAS, RTJB, MAB, LFA. Design of the study - JHAS, RTJB, LFA, FGN. Data acquisition - JHAS, MAB, EMS, FFD, VAN, GAVS; VCS; FGN. Laboratory analysis and interpretation of data - VAN; GAVS; VCS; RR; OAMF; ATC; ACCA; JGCR; LRVA; FGN. Preparation of the manuscript and submission - JHAS, LFA; RTJB; EMS; FFD; OAMF; ACCA; JGCR; LRVA; ATC; FGN.

Ethics approval and consent to participate
All the procedures performed were according to the Ethics Committee of the State University of Amazonas (CAAE: 56,745,116.6.0000.5016) and with the Declaration of Helsinki of 1975, revised in 1983.

Consent for publication
Written informed consent was obtained from the patient for publication of this report.

Competing interests
The authors declare that they have no competing interests.

Publisher's Note

Author details
[1]Programa de Pós-Graduação em Imunologia Básica e Aplicada, Universidade Federal do Amazonas, Manaus, Amazonas, Brazil. [2]Universidade do Estado do Amazonas, Manaus, Amazonas, Brazil. [3]Universidade Federal do Amazonas, Manaus, Amazonas, Brazil. [4]Hospital Adventista de Manaus, Manaus, Amazonas, Brazil. [5]Laboratório de Ecologia de Doenças Transmissíveis na Amazônia, Instituto Leônidas e Maria Diane – Fiocruz Amazônia, Manaus, Amazonas, Brazil. [6]Programa de Pós-Graduação em Biologia Celular e Molecular, Instituto Oswaldo Cruz, Fiocruz, Rio de Janeiro, Brazil. [7]Fundação de Medicina Tropical – Dr Heitor Vieira Dourado, Manaus, Amazonas, Brazil. [8]Universidade Nilton Lins, Manaus, Amazonas, Brazil. [9]Instituto René Rachou – Fiocruz Minas, Minas Gerais, Brazil. [10]Programa de Pós-Graduação em Biologia da Interação Patógeno-Hospedeiro, Instituto Leônidas e Maria Diane – Fiocruz Amazônia, Manaus, Amazonas, Brazil.

Received: 2 November 2017 Accepted: 19 January 2018
Published online: 25 January 2018

References
1. Kuno G, Chang GJ, Tsuchiya KR, Karabatsos N, Cropp CB. Phylogeny of the genus Flavivirus. J Virol. 1998;72:73–83.
2. Smithburn KC. Neutralizing antibodies against certain recently isolated viruses in the sera of human beings residing in East Africa. J Immunol. 1952; 69:223–34.
3. Simpson DI. Zika virus infection in man. Trans R Soc Trop Med Hyg. 1964;58: 335–8.
4. Duffy MR, Chen TH, Hancock WT, Powers AM, Kool JL, Lanciotti RS, et al. Zika virus outbreak on Yap Island, Federated States of Micronesia. N Engl J Med. 2009;360:2536–43.
5. Campos GS, Bandeira AC, Sardi SI. Zika Virus Outbreak, Bahia. Brazil Emerg Infect Dis. 2015;21:1885–6.
6. Zanluca C, de Melo VCA, Mosimann ALP, Santos Dos GIV, Santos Dos CND, Luz K. First report of autochthonous transmission of Zika virus in Brazil. Mem Inst Oswaldo Cruz. 2015;110:569–72.
7. PAHO. Increase of microcephaly in the northeast of Brazil. 2015 Nov pp. 1–2. Report No.: 17 November 2015. Epidemiological Alert available at: http://www.paho.org/hq/index.php?option=com_docman&task=doc_view&Itemid=270&gid=32285&lang=en.
8. Azevedo RSS, Araujo MT, Martins Filho AJ, Oliveira CS, Nunes BTD, Cruz ACR, et al. Zika virus epidemic in Brazil. I. Fatal disease in adults: clinical and laboratorial aspects. J Clin Virol. 2016;85:56–64.
9. Santos Dos T, Rodriguez A, Almiron M, Sanhueza A, Ramon P, de Oliveira WK, et al. Zika virus and the Guillain-Barré syndrome - case series from seven countries. N Engl J Med. 2016;375:1598–601.
10. Ratanacharoensiri A, Huggins L, Johnson M, Patel I. Zika Virus: An Emerging Epidemic. J Res Pharm Pract. 2017;6:1–2.
11. Pinheiro TJ, Guimarães LF, Silva MTT, Soares CN. Neurological manifestations of Chikungunya and Zika infections. Arq Neuropsiquiatr. 2016;74:937–43.
12. de Carvalho NS, de Carvalho BF, Dóris B, Silverio Biscaia E, Arias Fugaça C, de Noronha L. Zika virus and pregnancy: an overview. Am J Reprod Immunol. 2017;77:e12616.
13. Kodati S, Palmore TN, Spellman FA, Cunningham D, Weistrop B, Sen HN. Bilateral posterior uveitis associated with Zika virus infection. Lancet. 2017; 389:125–6.
14. Aletti M, Lecoules S, Kanczuga V, Soler C, Maquart M, Simon F, et al. Transient myocarditis associated with acute Zika virus infection. Clin Infect Dis. 2017;64:678–9.
15. Lanciotti RS, Kosoy OL, Laven JJ, Velez JO, Lambert AJ, Johnson AJ, et al. Genetic and serologic properties of Zika virus associated with an epidemic, yap state, Micronesia, 2007. Emerg Infect Dis. 2008;14:1232–9.
16. Lanciotti RS, Kosoy OL, Laven JJ, Panella AJ, Velez JO, Lambert AJ, et al. Chikungunya virus in US travelers returning from India, 2006. Emerg Infect Dis. 2007;13:764–7.
17. Gurukumar KR, Priyadarshini D, Patil JA, Bhagat A, Singh A, Shah PS, et al. Development of real time PCR for detection and quantitation of dengue viruses. Virol J. 2009;6:10.
18. Naveca FG, Nascimento VAD, de Souza VC, Nunes BTD, Rodrigues DSG, Vasconcelos PFDC. Multiplexed reverse transcription real-time polymerase chain reaction for simultaneous detection of Mayaro, Oropouche, and Oropouche-like viruses. Mem Inst Oswaldo Cruz. 2017;112:510–3.
19. Saldarriaga C, Roncancio G, González N, Fortich F. Manifestaciones cardiacas del dengue. Reporte de una serie de casos durante la epidemia colombiana de 2010. Revista Colombiana de Cardiología. 2013;20:366–9.
20. Kushawaha A, Jadonath S, Mobarakai N. West nile virus myocarditis causing a fatal arrhythmia: a case report. Cases J. 2009;2:7147.
21. Obeyesekere I, Hermon Y. Myocarditis and cardiomyopathy after arbovirus infections (dengue and chikungunya fever). Br Heart J. 1972;34:821–7.
22. Chan JFW, Choi GKY, Yip CCY, Cheng VCC, Yuen K-Y. Zika fever and congenital Zika syndrome: an unexpected emerging arboviral disease. J Inf Secur. 2016;72:507–24.
23. Weinbren MP, Williams MC. Zika virus: further isolations in the Zika area, and some studies on the strains isolated. Trans R Soc Trop Med Hyg. 1958;52:263–8.
24. Barzon L, Pacenti M, Berto A, Sinigaglia A, Franchin E, Lavezzo E, et al. Isolation of infectious Zika virus from saliva and prolonged viral RNA shedding in a traveller returning from the Dominican Republic to Italy, January 2016. Euro Surveill. 2016;21:30159.

25. Musso D, Roche C, Nhan TX, Robin E, Teissier A, Cao-Lormeau V-M. Detection of Zika virus in saliva. J Clin Virol. 2015;68:53–5.
26. Gourinat AC, O'Connor O, Calvez E, Goarant C, Dupont-Rouzeyrol M. Detection of Zika virus in urine. Emerg Infect Dis. 2015;21:84–6.
27. Deckard DT, Chung WM, Brooks JT, Smith JC, Woldai S, Hennessey M, et al. Male-to-male sexual transmission of Zika virus - Texas, January 2016. MMWR Morb Mortal Wkly Rep. 2016;65:372–4.
28. Williamson PC, Linnen JM, Kessler DA, Shaz BH, Kamel H, Vassallo RR, et al. First cases of Zika virus-infected US blood donors outside states with areas of active transmission. Transfusion. 2017;57:770–8.
29. Kuo HJ, Lee IK, Liu JW. Analyses of clinical and laboratory characteristics of dengue adults at their hospital presentations based on the World Health Organization clinical-phase framework: Emphasizing risk of severe dengue in the elderly. J Microbiol Immunol Infect. 2017;S1684-1182(17):30067-1. https://www.sciencedirect.com/science/article/pii/S1684118217300671.
30. Monath TP. Yellow fever: an update. Lancet Infect Dis. 2001;1:11–20.
31. Petersen LR, Marfin AA, Gubler DJ. West Nile virus. JAMA. 2003;290:524–8.
32. Kam YW, Leite JA, Lum F-M, Tan JJL, Lee B, Judice CC, et al. Specific biomarkers associated with neurological complications and congenital central nervous system abnormalities from Zika virus–infected patients in Brazil. J Infect Dis. 2017;16:172.
33. Naveca FG, Pontes G, Chang A, da Silva GAV, do Nascimento VA, Monteiro DCDS, et al. Analysis of the immunological biomarker profile during acute Zika virus infection reveals the overexpression of CXCL10, a chemokine already linked to neuronal damage. bioRxiv. 2017. https://doi.org/10.1101/185041.
34. Frustaci A, Chimenti C, Bellocci F, Morgante E, Russo MA, Maseri A. Histological substrate of atrial biopsies in patients with lone atrial fibrillation. Circulation. 1997;96:1180–4.
35. Hadi HA, Alsheikh-Ali AA, Mahmeed WA, Suwaidi JMA. Inflammatory cytokines and atrial fibrillation: current and prospective views. J Inflamm Res. 2010;3:75–97.

ANEXO 2

Analysis of the immunological biomarker profile during acute Zika virus infection reveals the overexpression of CXCL10, a chemokine linked to neuronal damage

Felipe Gomes Naveca[1,2]/+, Gemilson Soares Pontes[3], Aileen Yu-hen Chang[4], George Allan Villarouco da Silva[2,7], Valdinete Alves do Nascimento[1], Dana Cristina da Silva Monteiro[2], Marineide Souza da Silva[2], Lígia Fernandes Abdalla[2,5], João Hugo Abdalla Santos[6], Tatiana Amaral Pires de Almeida[1], Matilde del Carmen Contreras Mejía[1], Tirza Gabrielle Ramos de Mesquita[7], Helia Valeria de Souza Encarnação[7], Matheus de Souza Gomes[8], Laurence Rodrigues Amaral[8], Ana Carolina Campi-Azevedo[9], Jordana Graziela Coelho-dos-Reis[9], Lis Ribeiro do Vale Antonelli[9], Andréa Teixeira-Carvalho[9], Olindo Assis Martins-Filho[9], Rajendranath Ramasawmy[7,10]

[1]Fundação Oswaldo Cruz-Fiocruz, Instituto Leônidas e Maria Deane, Programa de Pós-Graduação em Biologia da Interação Patógeno-Hospedeiro, Manaus, AM, Brasil
[2]Universidade Federal do Amazonas, Programa de Pós-Graduação em Imunologia Básica e Aplicada, Manaus, AM, Brasil
[3]Instituto Nacional de Pesquisas da Amazônia, Manaus, AM, Brasil
[4]George Washington University, Washington DC, United States of America
[5]Universidade do Estado do Amazonas, Manaus, AM, Brasil
[6]Hospital Adventista de Manaus, Manaus, AM, Brasil
[7]Fundação de Medicina Tropical Dr Heitor Vieira Dourado, Manaus, AM, Brasil
[8]Universidade Federal de Uberlândia, Patos de Minas, MG, Brasil
[9]Fundação Oswaldo Cruz-Fiocruz, Centro de Pesquisas René Rachou, Belo Horizonte, MG, Brasil
[10]Universidade Nilton Lins, Manaus, AM, Brasil

BACKGROUND Infection with Zika virus (ZIKV) manifests in a broad spectrum of disease ranging from mild illness to severe neurological complications and little is known about Zika immunopathogenesis.

OBJECTIVES To define the immunologic biomarkers that correlate with acute ZIKV infection.

METHODS We characterized the levels of circulating cytokines, chemokines, and growth factors in 54 infected patients of both genders at five different time points after symptom onset using microbeads multiplex immunoassay; comparison to 100 age-matched controls was performed for statistical analysis and data mining.

FINDINGS ZIKV-infected patients present a striking systemic inflammatory response with high levels of pro-inflammatory mediators. Despite the strong inflammatory pattern, IL-1Ra and IL-4 are also induced during the acute infection. Interestingly, the inflammatory cytokines IL-1β, IL-13, IL-17, TNF-α, and IFN-γ; chemokines CXCL8, CCL2, CCL5; and the growth factor G-CSF, displayed a bimodal distribution accompanying viremia. While this is the first manuscript to document bimodal distributions of viremia in ZIKV infection, this has been documented in other viral infections, with a primary viremia peak during mild systemic disease and a secondary peak associated with distribution of the virus to organs and tissues.

MAIN CONCLUSIONS Biomarker network analysis demonstrated distinct dynamics in concurrence with the bimodal viremia profiles at different time points during ZIKV infection. Such a robust cytokine and chemokine response has been associated with blood-brain barrier permeability and neuroinvasiveness in other flaviviral infections. High-dimensional data analysis further identified CXCL10, a chemokine involved in foetal neuron apoptosis and Guillain-Barré syndrome, as the most promising biomarker of acute ZIKV infection for potential clinical application.

Key words: Zika virus - CXCL10 - biomarkers - chemokines - cytokines

The Zika virus (ZIKV) is an arthropod-borne *Flavivirus*, transmitted mainly by female *Aedes* mosquitos and it that usually causes a mild illness characterized by conjunctivitis, pruritus, muscle and joint pain, rash, and slight fever. Outbreaks of ZIKV infection were first recorded in Micronesia and later in French Polynesia, where atypical manifestations were initially documented, including Guillain-Barré syndrome (Oehler et al. 2014). In Brazil, ZIKV infection during pregnancy has been linked to an unusual increase in the number of microcephaly cases (de Oliveira et al. 2016). Following the Brazilian report of congenital malformations, the number of microcephaly cases in French Polynesia was reanalysed, and a connection with ZIKV was further es-

doi: 10.1590/0074-02760170542
Financial support: CNPq, CAPES, FINEP.
FGN and OAMF were supported by CNPq (Grants 440856/2016-7, 440682/2016-9) and CAPES (Grants 88881.130825/2016-00, 88887.130823/2016-00, 88881.130829/2016-01); OAMF is also funded by FINEP (Grant TED264/16).
+ Corresponding author: felipe.naveca@fiocruz.br
FGN, OAM-F, RR, GSP, AY-hC and AT-C contributed equally to this work.
Received 14 December 2017
Accepted 14 February 2018

tablished. The broad spectrum of foetal clinical manifestations resulting from ZIKV infection led to a new classification termed congenital Zika syndrome.

The host immune response plays an important role in the clinical course of patients with viral infection. Particularly, cellular immunity and key components of the innate immune response, such as interferons and other cytokines/chemokines, play an essential role in limiting viral spread. To date, only two studies describing immune mediators in Zika-infected patients have been reported (Tappe et al. 2016, Kam et al. 2017). In Tappe et al. (2016), a reliable immunological biomarker profile during acute infection could not be established due to the small sample size. Kam et al. (2017) describes immune markers from a cohort from Campinas, Brazil, showing an inflammatory immune response and several immune mediators specifically higher in ZIKV-infected patients, with a statistically significant difference was observed in the levels of CXCL10, IL-10, and HGF observed between patients with and without neurological complications. Kam et al. (2017) also found higher levels of CXCL10, IL-22, MCP-1, and TNF-α in ZIKV-infected pregnant women carrying babies with foetal growth associated malformations.

In this study, we evaluated the immune response during acute ZIKV infection by analysing the serum levels of cytokines, chemokines, and growth factors from an adult cohort of 54 ZIKV-infected cases and 100 controls from Manaus, Brazil over five time points during symptomatic ZIKV infection. We present the time course of cytokine response in relation to viremia and identify a chemokine that may serve as a biomarker of acute ZIKV infection, thus providing new insights into ZIKV neuropathogenesis.

MATERIALS AND METHODS

Study population and design - We used non-probabilistic convenience sampling and a cross-sectional experimental design, together with robust statistical analysis and data mining, for the evaluation of the immunological biomarker profile during acute ZIKV infection. In the first half of 2016, a total of 54 suspected ZIKV-infected cases (29 non-pregnant females and 25 males, all adults) were recruited at Hospital Adventista de Manaus, Amazonas state, Brazil. All patients presented a maculopapular rash, with or without fever, and at least one of the following symptoms: pruritus, arthralgia, joint swelling, or conjunctival hyperemia within five days after symptom onset. Age-matched non-infected (NI) controls, 46 females and 54 males, were enrolled for comparison and basic characteristics, including data from physical examination and virological findings, were obtained. Comprehensive laboratory records, including routine laboratory tests, were available for 21 patients (15 male and six female).

Ethics statement - The study protocol was approved by the Ethics Committee of the Universidade do Estado do Amazonas (CAAE: 56745116.6.0000.5016), and all subjects provided written informed consent.

Differential molecular diagnosis of Zika and viral load estimative - Serum samples were sent to Fiocruz Amazônia and tested for ZIKV (envelope coding region) (Lanciotti et al. 2008), chikungunya virus (CHIKV) (Lanciotti et al. 2007), dengue virus (DENV) (Gurukumar et al. 2009), Mayaro virus (MAYV) and Oropouche virus (OROV) (Naveca et al. 2017) by real-time quantitative polymerase chain reaction (RT-qPCR). Samples positive for CHIKV, DENV, MAYV, or OROV were excluded from further analysis. Sample inclusion criteria also required the internal control (spiked MS2 bacteriophage) to display a Ct value between 30-32. The viremia was estimated by RT-qPCR using absolute quantification by the standard curve method and reported as viral RNA copies /mL.

Dengue virus serology - Serum samples were tested for previous exposure to DENV using Serion ELISA classic Dengue Virus IgG (Institut Virion/Serion GmbH, Germany).

Microbeads assay for serum biomarkers - A high-performance microbeads 27-plex assay (Bio-Rad, Hercules, CA, USA) was employed for detection and quantification of multiple targets, including: CXCL8 (IL-8), CXCL10 (IP-10), CCL11 (Eotaxin), CCL3 (MIP-1α), CCL4 (MIP-1β), CCL2 (MCP-1), CCL5 (RANTES), IL-1β, IL-6, TNF-α, IL-12, IFN-γ, IL-17, IL-1Ra (IL-1 receptor antagonist), IL-2, IL-4, IL-5, IL-7, IL-9, IL-10, IL-13, IL-15, FGF-basic, PDGF, VEGF, G-CSF, and GM-CSF. Samples were tested on a Bio-Plex 200 instrument (Bio-Rad) according to the manufacturer's instructions. The serum levels of IL-2, IL-7, and IL-15 were below the detection limits in several samples and were excluded from further analysis. The results were expressed as pg/mL.

Statistical analysis and data mining - Statistical analyses were initially performed using GraphPad Prism (GraphPad Software 6.0, San Diego, CA, USA). Comparative analysis of the clinical records was carried out using Fisher's exact test. The analysis of biomarker levels in NI controls vs. ZIKV-infected cases and between genders was performed using Mann-Whitney U tests. Multivariate correlations for biomarker levels and routine laboratory tests were analysed with the nonparametric Spearman's test (alpha .05) running on the JMP Software, v13.1.0 (SAS Institute, Cary, NC, USA). Correlations (Spearman r) were represented by a colour map matrix.

The dynamics of viremia, chemokines, cytokines, and growth factors were evaluated using the median value of each analyte. Comparative analysis of the biomarkers was carried out by Kruskal-Wallis test followed by Dunn's test. For all tests, differences were considered significant when $p < .05$ using two-tailed tests.

Data management strategies were applied to identify general and time-specific profiles. Biomarker signature analysis was carried out as previously described (Luiza-Silva et al. 2011). Radar charts were used to compile the biomarker signatures of NI controls and ZIKV-infected cases, applying the 75th percentile as the threshold. Venn diagrams were created to identify shared and unique attributes, along with the timeline of the symptoms onset (http://bioinformatics.psb.ugent.be/webtools/Venn/). Cytoscape software v3.2.0 (http://www.cytoscape.org/) was employed for visualizing and integrating multiple attributes into circular nodal networks. Connecting edges were drawn to underscore each association as posi-

tive (solid line) or negative (dashed line). The biomarker cluster pattern was defined by heatmaps assembled using R software (heatmap.2 function; v3.0.1). Decision tree algorithms were generated with WEKA software v3.6.11 (University of Waikato, New Zealand) to identify root and branch attributes and segregate patients from controls. ROC curves were built to define the cut-off and identify biomarkers with better performance in discriminating ZIKV-infected patients from NI controls. Performance indices (co-positivity, co-negativity, positive and negative likelihood ratios) were calculated using MedCalc software v7.3 (Ostend, Belgium).

RESULTS

Demographics, clinical records and virological data - The 54 Brazilian Zika cases, 29 non-pregnant females (median age 38 years, interquartile range (IQR) 27.5 - 46.5) and 25 males (median age 37 years, IQR 30 - 50), were enrolled between the first and fifth day after symptom onset. A group of 100 non-infected control subjects who were residents of Manaus, Amazonas, Brazil were also included (46 females (median age 28 years, IQR 23 - 36) and 54 males (median age 29.5 years, IQR 23 - 36). The median viremia level, expressed as copies/mL, was 2,031 (minimum = 133, maximum = 2.4 x 10^6, IQR: 881 - 5,268). The frequency of specific ZIKV symptoms was similar between men and women, with the exception that men had an increased frequency of fever compared to women (100% versus 67%, p = 0.005) (Table I). DENV IgG testing showed that 94.4% (51/54) of the patients were positive, two had an undetermined result, and one male subject was negative.

Correlation of immunological biomarkers with routine laboratory tests during acute ZIKV infection - The data on 45 continuous variables including immunological biomarkers, routine laboratory tests, age, viremia, and symptoms onset were analysed (Fig. 1A). Overall, moderate correlations were observed for several variables, and the strongest correlations were observed between TNF-a and CCL5 (Spearman r = 0.8245), and lymphocytes (%) and neutrophils (%) (Spearman r = 0.8084). All results were represented in a colour map matrix, where statistically supported associations (p <.05) between routine laboratorial tests and immunological biomarkers were highlighted (Fig. 1B).

ZIKV-infected patients display high levels of circulating biomarkers - Elevated levels of pro-inflammatory cytokines (IL-1β, IL-6, TNF-α, IFN-g and IL-17, except IL-12, which was higher in controls), chemokines (CXCL8, CCL11, CCL3, CCL4, CCL2, CCL5, and CXCL10) and growth factors (FGF-basic, PDGF, VEGF, G-CSF, and GM-CSF) were found in ZIKV-infected cases (Fig. 2, pink panels), whereas higher levels of IL-5 and IL-13 were seen in controls (Fig. 2, blue panels). Interestingly, the levels of IL-4 and IL-1Ra were also higher among patients as compared to controls. No differences were observed for IL-9 and IL-10 (Fig. 2, grey panels). A similar pat-

TABLE I

Demographical aspects, clinical records and virological status of Zika virus (ZIKV)-infected patients

Parameters	All	Females	Males	p
Non-infected controls				
n	100	46	54	NA
Age (years)	29.0 (23-36)	28.0 (23-36)	29.5 (23-36)	0.58
ZIKV-infected patients				
n	54	29	25	n.a.
Age (years)	37.5 (29-48)	38.0 (27.5-46.5)	37.0 (30-50)	0.79
Days of symptoms onset	2.5 (2-4)	2.0 (1-4)	3.0 (2-4)	0.32
Rash	95.0%	94.4%	95.5%	1.00
Fever	85.0%	66.7%	100.0%	**0.005**
Myalgia	82.5%	83.3%	81.8%	1.00
Conjunctival hyperemia	75.0%	66.7%	81.8%	0.30
Pruritus	70.0%	66.7%	72.7%	0.73
Headache	65.0%	66.7%	63.6%	1.00
Arthralgia	60.0%	72.2%	50.0%	0.20
Joint swelling	25.0%	33.3%	18.2%	0.30
Vomiting or nausea	25.0%	33.3%	18.2%	0.30
Diarrhea	17.5%	27.8%	9.1%	0.21
Lymphadenopathy	12.5%	11.1%	13.6%	1.00
Viremia (ZIKV RNA copies/mL)	2,031 (881-5,268)	2,130 (1,078-5,268)	1,786 (802-8,720)	0.77

Data are reported as median and interquartile range (IQR) for age, days of symptoms onset and viremia. Statistical differences were assessed by Mann-Whitney test. Comparative analysis of clinical records observed in females and males was carried out by Fisher's exact test. Significant differences were considered at $p < 0.05$ for comparisons between females *vs.* males and are underscored by **bold/underlined** format. Viremia is expressed as copies /mL as described in material and methods. NA: not applicable.

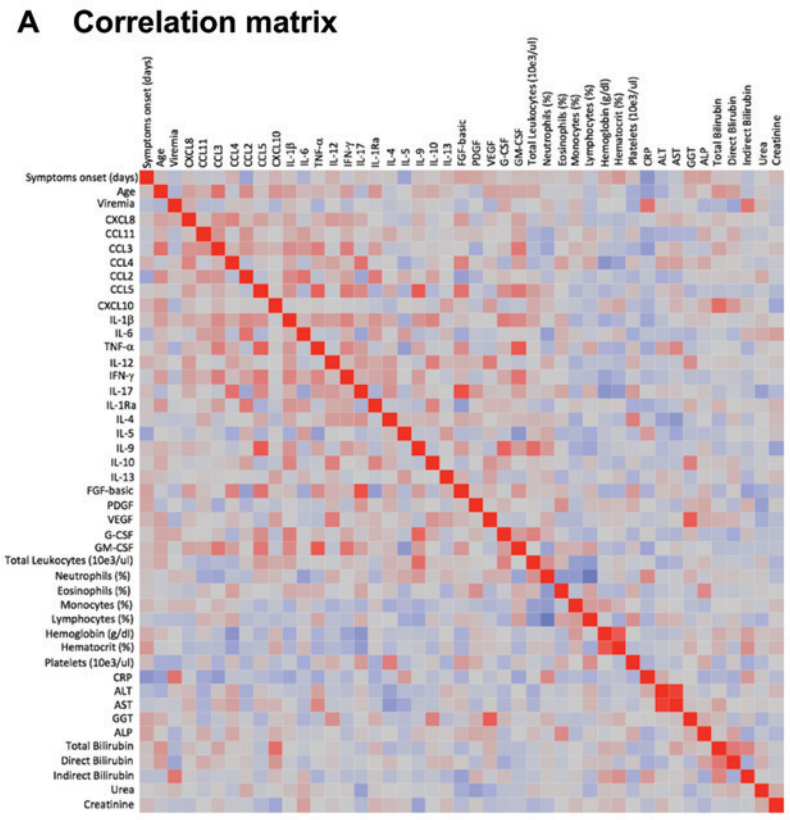

B Correlation indexes

Source atributes	Target atributes	Spearman ρ	p values
ALP	Viremia	-0,5613	0,01
ALT	CCL4	0,4492	0,04
AST	IL-4	-0,5532	0,01
AST	CXCL10	0,457	0,04
AST	CCL4	0,4764	0,03
AST	CCL5	0,4554	0,04
C-reactive protein (CRP)	Symptons onset (days)	-0,4886	0,03
C-reactive protein (CRP)	Viremia	0,5449	0,01
C-reactive protein (CRP)	CXCL10	-0,4976	0,03
C-reactive protein (CRP)	CCL3	-0,4645	0,04
Creatinine	IL-9	-0,6443	0,001
Direct Bilirubin	G-CSF	-0,5576	0,01
GGT	IL-10	0,4671	0,04
GGT	VEGF	0,5969	0,007
Hematocrit (%)	IL-17	-0,5144	0,01
Hematocrit (%)	CCL4	-0,4756	0,02
Hemoglobin (g/dL)	IL-1β	-0,437	0,04
Hemoglobin (g/dL)	IL-9	-0,4476	0,04
Hemoglobin (g/dL)	IL-17	-0,6159	0,003
Hemoglobin (g/dL)	IFN-γ	-0,4946	0,02
Hemoglobin (g/dL)	CCL4	-0,4678	0,03
Indirect Bilirubin	FGF basic	-0,4542	0,04
Lymphocytes (%)	CCL8	-0,4811	0,03
Monocytes (%)	IL-9	-0,4497	0,04
Neutrophils (%)	IL-13	0,509	0,02
Platelets (10^3/ µL)	Viremia	-0,4333	0,04
Total Leukocytes (10^3/ µL)	IL-9	0,6071	0,003
Total Leukocytes (10^3/ µL)	IL-10	0,4709	0,03
Urea	IL-17	-0,4564	0,04
Urea	PDGF-bb	-0,4928	0,02

Fig. 1: immunological biomarker correlations with the results of routine laboratory tests, age, viremia, and symptoms. The nonparametric Spearman's test was applied to evaluate multiple correlations between immunological biomarkers and the results of routine laboratory tests. A colour map matrix was plotted showing the strength and direction of these correlations (-1 blue, to +1 red), panel A. Statistically significant correlations ($p < .05$) between immunological biomarkers and routine tests are highlighted in the inserted table, panel B.

tern was observed when results were stratified by gender, although infected males presented significant lower levels of CCL3, CCL4, CCL5, IL-17, FGF-basic, and GM-CSF than females. No significant differences were observed between female and male controls (Table II).

Bimodal viremia is accompanied by increased levels of a defined group of biomarkers - Viremia and biomarker levels were assessed at different time points (day 1 upon symptoms onset was denoted as D1, etc.), with D1 (n = 11), D2 (n = 13), D3 (n = 10), D4 (n = 09), and D5 (n = 05). A bimodal distribution was observed, with two viremia peaks at D2 and D4, with the lowest viremia levels at D5 (Fig. 3, grey panel). Dynamics of CCL5, TNF-α, IFN-γ, IL-17, and G-CSF were closely related to viremia (Fig. 3A). A similar bimodal distribution was observed for IL-1b and IL-13 (Fig. 3B). The highest levels of CXCL8 and CCL2 were observed at D1 and D2 (Fig. 3C). An inverse correlation was observed for IL-12, IL-10, and VEGF (Fig. 3D), where the highest levels were observed at the lowest levels of viremia. The levels of CCL3, CXCL10, IL-6, and FGF-basic displayed a distinct pattern, with the lowest levels observed at D3, coinciding with the first drop in viremia (Fig. 3E). A valley at D4 followed by an increase at D5 was observed for CCL11, CCL4, IL-1Ra, and IL-4 (Fig. 3F), and unique patterns were observed for IL-5, IL-9, PDGF, and GM-CSF (Fig. 3G).

Biomarkers were also evaluated in controls, and the IQR are represented by dashed lines (Fig. 4). Most biomarker levels differed between patients and controls at all time points, except for IL-10 at D1 and D2, and IL-1b at D3. No differences were observed for IL-9.

ZIKV infection elicited a set of general and timeline-specific biomarkers - The biomarker levels were used to build a signature (Fig. 5A-B) as described in the Methods section. A significant difference in the overall profile was observed in ZIKV-infected cases as compared to controls. Furthermore, the radar chart revealed that 19/24 (79%) biomarkers were highly induced by ZIKV infection. Almost all biomarkers analysed were found at levels above the global median in more than 75% of the infected patients (Fig. 5, B panel).

Venn diagram analysis showed that four chemokines (CCL4, CCL2, CCL5, CXCL10), two cytokines (IL-6, IL-4), and two growth factors (PDGF, G-CSF) were significantly induced at all time points (Fig. 5C). Of note, TNF-α appears as the only biomarker at the intersection of the viremia peaks (D2 and D4). In contrast, IL-10 is the only unregulated biomarker at viremia valleys (D3 and D5), while increased levels of IL-12 appear at D5 (Fig. 5D).

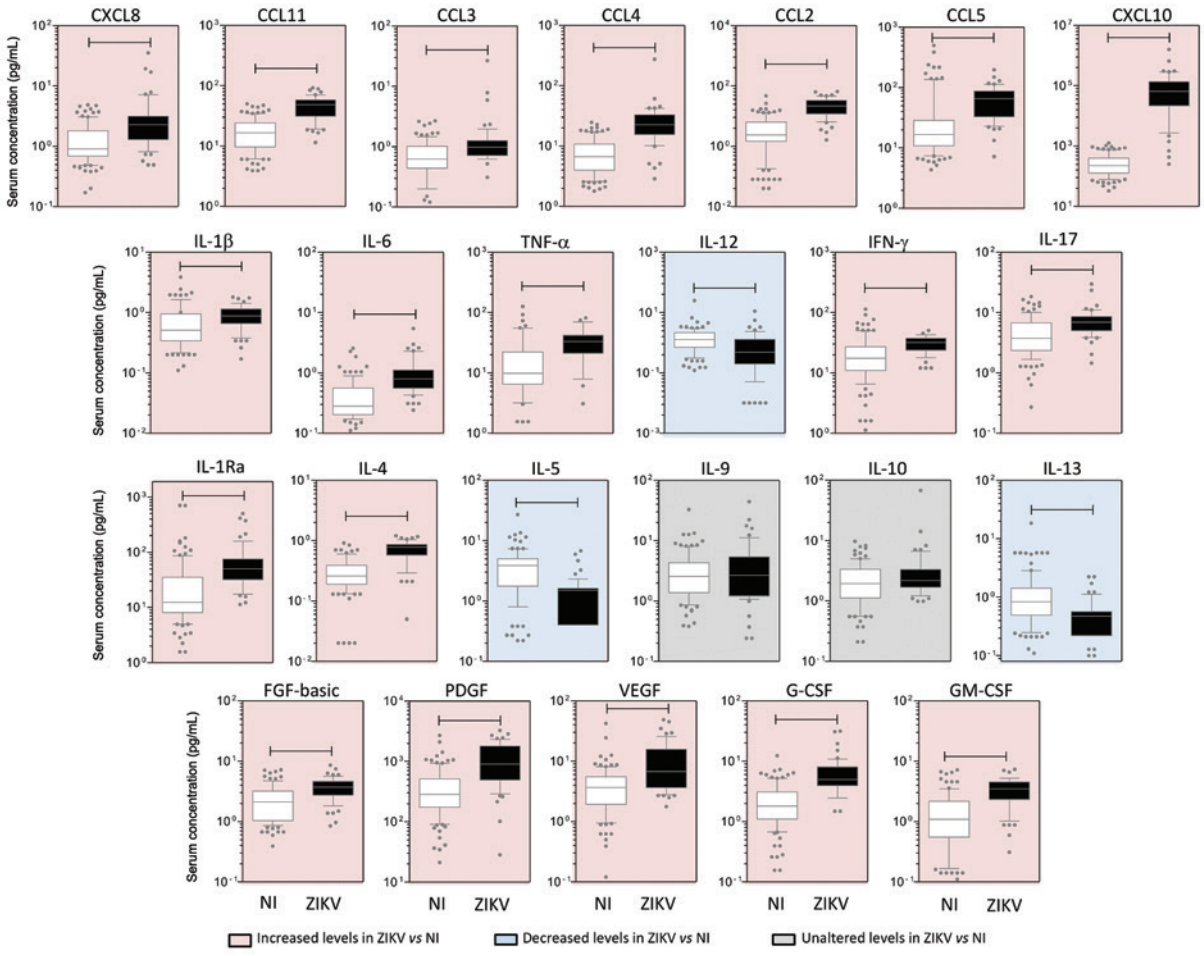

Fig. 2: panoramic overview of serum chemokines, cytokines, and growth factors during early stages of Zika virus (ZIKV) infection in adults. Serum biomarkers (CXCL8, CCL11, CCL3, CCL4, CCL2, CCL5, CXCL10, IL-1β, IL-6, TNF-α, IL-12, IFN-γ, IL-17, IL-1Ra, IL-4, IL-5, IL-9, IL-10, IL-13, FGF-basic, PDGF, VEGF, G-CSF, and GM-CSF) were measured in ZIKV-infected patients (D1 to D5, ZIKV = ■, n = 54) and non-infected subjects [non-infected (NI) = □, n = 100] by high performance Luminex 27-plex assay as described in Methods. Data are expressed as pg/mL and are displayed in box and whisker (10-90 percentile) plots. Comparative analysis between NI vs. ZIKV was performed by Mann-Whitney test and significant differences at $p < .05$ are underscored by connecting lines. Coloured backgrounds highlight increased (pink), decreased (blue), and unaltered (grey) levels of serum biomarkers in ZIKV as compared to NI.

Distinct biomarker networks are observed at different time points - Cytoscape software was used to conduct a correlative analysis of immunological biomarkers. The exploratory analysis demonstrated that earlier infection was associated with more complex biomarker networks. Most correlations at D1 and all correlations at D2 were positive (solid lines). The level of complexity decreased from D1 to D5 (Fig. 6).

High-dimensional data analysis identified CXCL10 as the most promising biomarker for a putative clinical application - A heatmap matrix was constructed to evaluate the profile of biomarkers associated with ZIKV infection. CXCL10 clustered with one clade separately from the other attributes (Fig. 7A). In addition, a decision tree was built to identify the biomarker most able to segregate patients. This approach confirmed the heatmap observations indicating CXCL10 as the most specific biomarker, followed by IL-4 and VEGF. The analysis showed a very high global accuracy (99.4%) with a leave-one-out cross-validation of 96.8% (Fig. 7B). The significance of these attributes (CXCL10, IL-4, and VEGF) was assessed by 3D-plots, and the performance of the root attribute (CXCL10) was evaluated by scatterplot distribution and ROC curve analysis (Fig. 7C-D). CXCL10 alone showed a very high global accuracy ranging from 0.952-0.998. Together, the results demonstrated that CXCL10 measurement identified 94% of the patients, with no false positive identification and outstanding indices (co-positivity, co-negativity, and likelihood ratio).

DISCUSSION

The pathogenesis of ZIKV infection is still largely unknown, and the main determinants of disease manifestations are not yet well established. Understanding serum immunomodulators during acute infection may be a first step in elucidating the mechanisms underlying ZIKV-induced immunopathology.

TABLE II

Serum chemokines, cytokines and growth factors early after Zika virus (ZIKV) infection (D1 to D5) in adult females and males

	Females (F) n = 29			Males (M) n = 25				Score ZIKV/NI	
Analytes	NI	ZIKV	p (1)	NI	ZIKV	p (2)	p (3)	(F)	(M)
CXCL8	0.87 (0.54-1.67)	2.26 (1.57-3.26)	**0.0001**	0.98 (0.70-1.93)	2.30 (1.19-3.11)	**0.0018**	0.5669	2.6	2.3
CCL11	16.44 (9.29-22.22)	48.94 (30.12-61.91)	**0.0001**	16.65 (10.62-25.20)	43.82 (29.11-56.95)	**0.0001**	0.3488	3.0	2.6
CCL3	0.59 (0.41-0.86)	1.15 (0.80-1.32)	**0.0001**	0.65 (0.45-1.13)	0.89 (0.67-1.07)	**0.0469**	**0.0205**	1.9	1.4
CCL4	7.28 (4.56-12.20)	28.76 (18.76-35.67)	**0.0001**	5.94 (3.75-9.79)	20.18 (12.63-26.64)	**0.0001**	**0.0162**	4.0	3.4
CCL2	2.08 (1.00-4.97)	20.73 (13.45-34.70)	**0.0001**	2.46 (1.94-7.15)	21.98 (11.86-32.34)	**0.0001**	0.9862	10.0	8.9
CCL5	15.17 (11.36-34.98)	82.77 (64.75-108.00)	**0.0001**	17.00 (9.83-25.70)	34.06 (23.66-65.81)	**0.0001**	**0.0001**	5.5	2.0
CXCL10	232 (128-434)	71,219 (32,899-148,407)	**0.0001**	218 (109-392)	44,645 (10,423-69,757)	**0.0001**	0.1030	307	205
IL-1β	0.52 (0.24-0.96)	0.93 (0.56-1.19)	**0.0176**	0.52 (0.29-1.00)	0.77 (0.61-1.14)	0.1511	0.5374	1.8	1.5
IL-6	0.29 (0.20-0.57)	0.79 (0.63-1.00)	**0.0001**	0.28 (0.21-0.55)	0.81 (0.52-1.73)	**0.0001**	0.1944	2.7	2.9
TNF-α	9.76 (6.10-20.20)	35.87 (25.45-44.08)	**0.0001**	10.08 (6.45-22.62)	26.93 (15.02-41.84)	**0.0015**	0.1101	3.7	2.7
IL-12	1.26 (0.51-2.30)	0.63 (0.22-1.66)	0.0554	1.39 (0.96-2.17)	0.34 (0.09-1.08)	0.0001	0.1895	0.5	0.2
IFN-γ	14.97 (9.63-24.54)	31.91 (26.39-38.65)	**0.0001**	19.79 (14.14-27.31)	26.41 (23.61-35.97)	**0.0035**	0.4283	2.1	1.3
IL-17	3.84 (2.21-7.53)	7.88 (6.28-9.02)	**0.0001**	3.57 (2.50-6.76)	5.96 (4.41-7.15)	**0.0114**	**0.0092**	2.1	1.7
IL-1Ra	11.81 (7.81-28.66)	47.00 (34.03-65.59)	**0.0001**	12.33 (8.95-36.13)	54.94 (30.77-115.10)	**0.0001**	0.3623	4.0	4.5
IL-4	0.27 (0.20-0.39)	0.81 (0.59-0.86)	**0.0001**	0.26 (0.17-0.41)	0.73 (0.53-0.90)	**0.0001**	0.6890	3.0	2.8
IL-5	3.16 (1.67-5.02)	1.50 (0.40-1.61)	**0.0001**	4.70 (2.00-5.35)	1.38 (1.07-1.61)	**0.0001**	0.5792	0.5	0.3
IL-9	2.21 (1.19-4.11)	3.10 (1.69-5.72)	0.0783	2.62 (1.59-4.69)	1.42 (1.18-3.83)	0.0837	0.0518	1.4	0.5
IL-10	1.73 (0.75-3.39)	2.11 (1.65-3.22)	0.1046	1.95 (1.51-3.02)	2.25 (1.52-3.41)	0.5478	0.9571	1.2	1.2
IL-13	0.75 (0.37-1.34)	0.48 (0.22-0.57)	**0.0135**	0.98 (0.80-1.57)	0.57 (0.37-0.57)	**0.0001**	0.3634	0.6	0.6
FGF-basic	1.84 (1.01-3.14)	4.34 (3.71-5.27)	**0.0001**	2.24 (1.28-3.73)	3.24 (2.13-4.24)	**0.0468**	**0.0014**	2.4	1.4
PDGF	359 (125-585)	1,012 (616-1,933)	**0.0001**	258 (196-403)	823 (416-1,578)	**0.0001**	0.3670	2.8	3.2
VEGF	2.87 (1.78-6.29)	6.72 (4.18-16.33)	**0.0001**	3.70 (2.17-4.97)	6.26 (3.66-15.21)	**0.0005**	0.5668	2.3	1.7
G-CSF	1.86 (1.04-2.86)	5.96 (4.43-8.05)	**0.0001**	1.83 (1.19-3.29)	4.94 (3.42-7.66)	**0.0001**	0.2400	3.2	2.7
GM-CSF	0.87 (0.52-2.00)	3.76 (3.03-4.64)	**0.0001**	1.35 (0.54-2.16)	2.88 (1.73-3.91)	**0.0003**	**0.0256**	4.4	2.1

Data are reported as median levels (IQR) in pg/mL. Statistical analysis was performed by Mann-Whitney test and significance reported as p-values: p(1), p(2), and p(3) for comparisons between non-infected (NI) *vs.* ZIKV females, NI *vs.* ZIKV males and ZIKV females *vs.* ZIKV males, respectively. Significant differences between NI *vs.* ZIKV are underscored in **bold** format. Differences between ZIKV females *vs.* ZIKV males are highlighted by **bold-underlined** format. No significant differences were observed between NI females *vs.* NI males. Score represents the fold change (analyte median value in infected patient divided by analyte median value in controls) segregated by gender.

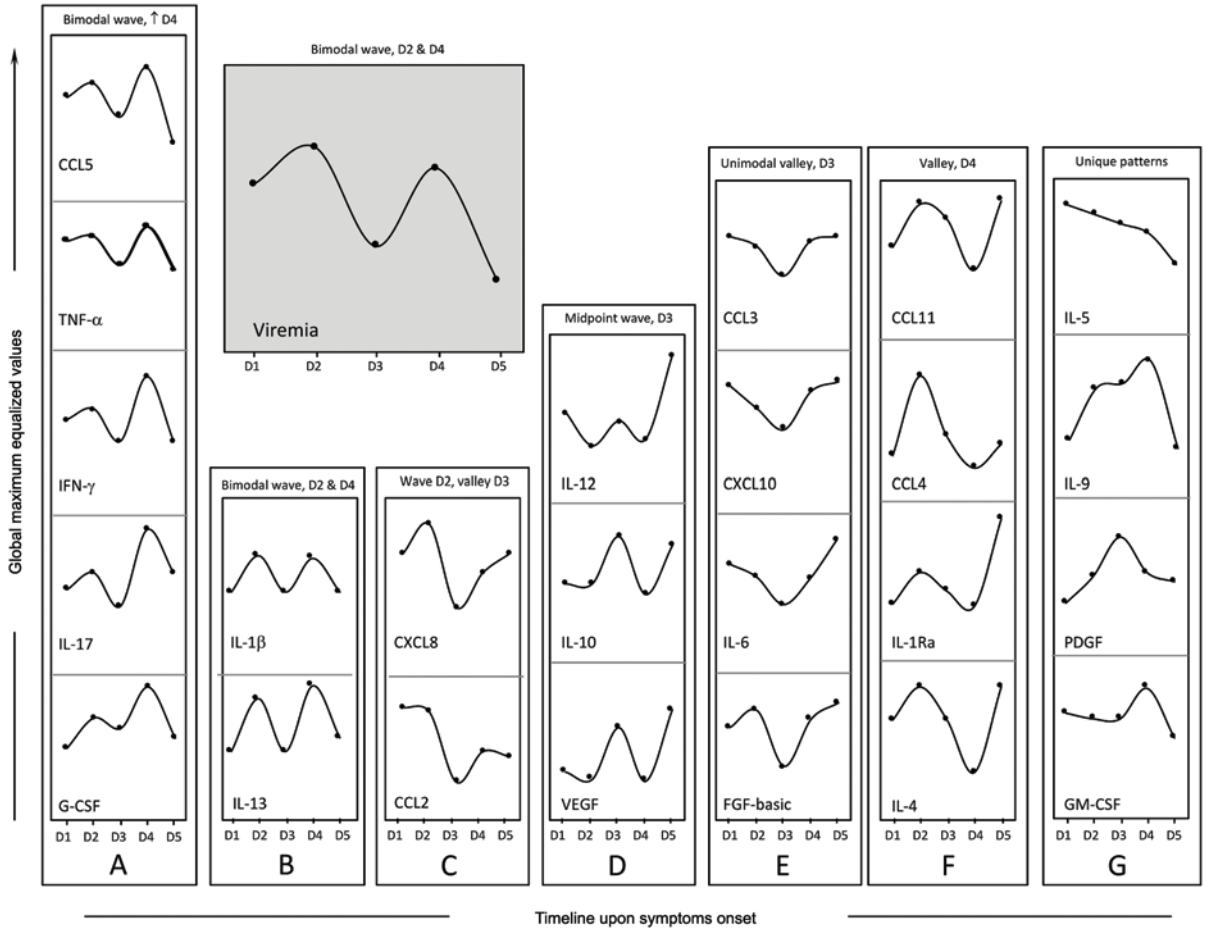

Fig. 3: rhythms of viremia, chemokines, cytokines, and growth factors during early stages of Zika virus (ZIKV) infection in adults. Cross-sectional follow-up of viremia and serum biomarkers was carried out in ZIKV-infected patients categorized according to the time (days) of symptom onset (D1, n = 11; D2, n = 13; D3, n = 10; D4 n = 9 and D5 n = 5). Viremia displayed a bimodal profile with similar waves at D2 and D4 (grey panel). Distinct patterns were identified for clusters of biomarkers, as they displayed kinetic curves shaping a bimodal wave at D2 and a higher wave [↑] at D4 (panel A: CCL5, TNF-α, IFN-γ, IL-17, and G-CSF); a bimodal profile with similar waves at D2 and D4 (panel B: IL-1β and IL-13); a wave at D2 and a valley at D3 (panel C: CXCL8 and CCL2); a midpoint wave at D3 (panel D: IL-12, IL-10, and VEGF); a unimodal valley at D3 (panel E: CCL3, CXCL10, IL-6, and FGF-basic); a valley at D4 (panel F: CCL11, CCL4, IL-1Ra, and IL-4) or a unique pattern (panel G: IL-5, IL-9, PDGF, and GM-CSF). Data are displayed as global maximum equalized median values of the serum concentrations (pg/mL) for each biomarker.

We show that the immune response during the acute phase of ZIKV infection is polyfunctional and broadly inflammatory, as evidenced by significantly elevated levels of IL-4, IL-17, IFN-γ, IL-1β, IL-1Ra, TNF-α, and IL-6 in patients as compared to controls. This is consistent with findings from Kam et al. (2017) that a robust pro-inflammatory cytokine response occurs during acute ZIKV infection, with elevations of IL-18, TNF-α, IFN-γ, IL-8, IL-6, GRO-α, and IL-7. A polyfunctional immune activation associated with increased CCL2, CXCL10, IL-6, IL-8, VEGF, and G-CSF levels but decreased levels of IL-13 was also described in the amniotic fluid of ZIKV-positive pregnant women whose infants had microcephaly (Ornelas et al. 2017). Additionally, other studies found higher serum levels of IL-5 and IL-13 amongst healthy controls as compared to infected individuals (Galliez et al. 2016, Kam et al. 2017). Both IL-5 and IL-13 are effector molecules essential to type 2-inflammation, especially in atopic asthma and viral respiratory tract infections (Edwards et al. 2017). However, the role of these cytokines in the ZIKV-host response is still unclear.

When we stratified the results by gender, ZIKV-infected males presented lower levels of CCL3, CCL4, CCL5, IL-17, FGF-basic, and GM-CSF. The reason for this difference is unknown in the context of ZIKV infection; however, this finding is consistent with the literature demonstrating that females tend to mount a higher innate and adaptive immune system response to viruses as compared to men (Klein 2012). In addition, this discrepancy could be due to females being sampled on average one day earlier than men, with a median time from onset to diagnostic sampling of two days for females and three days for males.

It is possible that previous exposure to flavivirus antigens may affect the immune response to ZIKV infection. In the present study, almost all patients (51/54) tested positive for DENV IgG antibodies. Manaus has had several dengue epidemics, including co-circulation of different serotypes (Figueiredo et al. 2008). Moreover, the Ama-

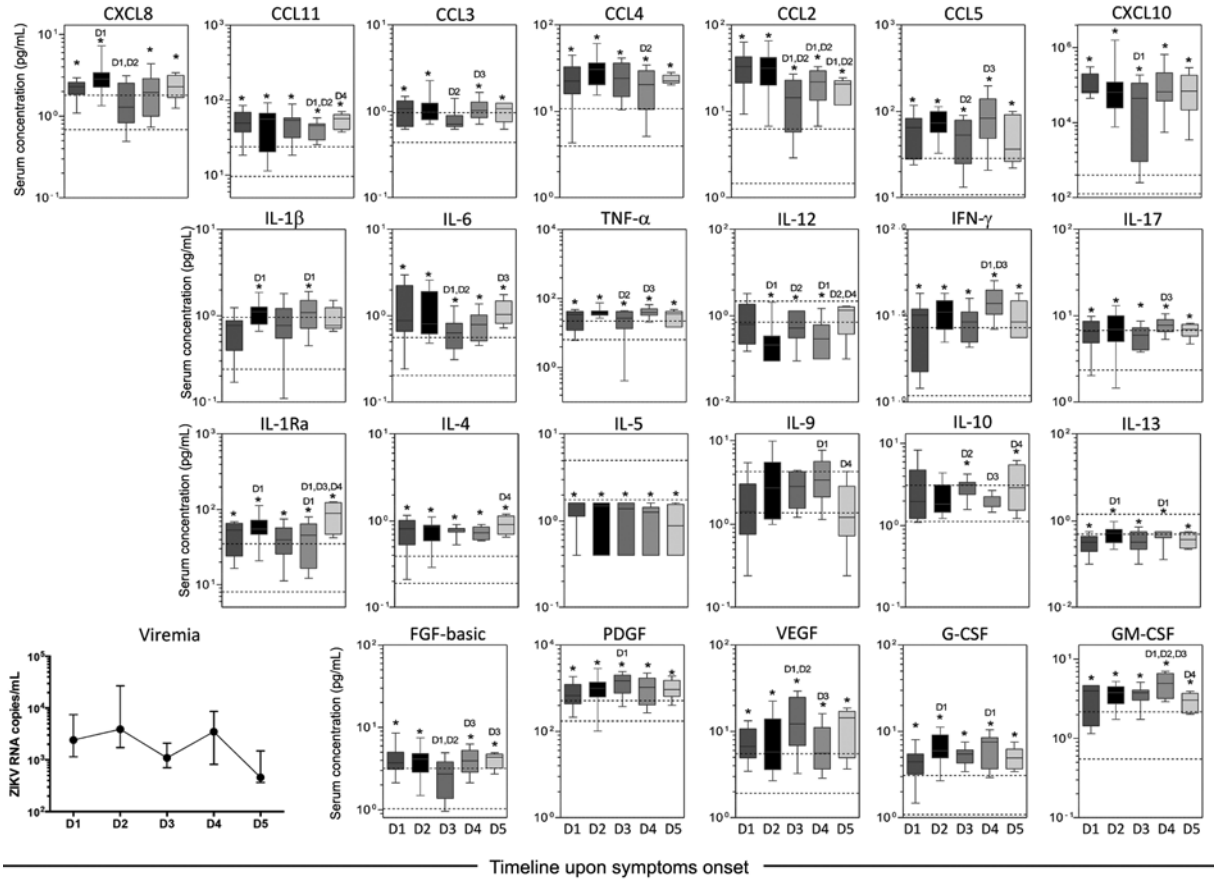

Fig. 4: kinetics of viremia, serum chemokines, cytokines, and growth factors during early stages of Zika virus (ZIKV) infection in adults. Cross-sectional analysis of viremia and serum biomarkers was performed in ZIKV-infected patients categorized according to the time (days) of symptom onset (D1, n = 11; D2, n = 13; D3, n = 10; D4, n = 09 and D5, n = 05). ZIKV RNA copies/mL are displayed as the median and interquartile range (IQR). Biomarker data are expressed in pg/mL and are displayed in box and whisker (10-90 percentile) plots. Multiple comparisons amongst distinct time points of symptom onset were performed by Kruskal-Wallis test followed by Dunn's post-test. Significant differences at $p < .05$ were identified at D1, D2, D3, and D4 as compared to day 1, day 2, day 3, and day 4, respectively. Analysis was also carried out by Mann-Whitney test to compare each time point from ZIKV-infected patients with those from a single group of non-infected controls (NI). Significant differences at $p < .05$ are marked by asterisks (*). Reference ranges for each biomarker were established as interquartile ranges (25th-75th percentiles) observed in NI (dashed lines). Distinct patterns were identified for clusters of biomarkers, as they displayed kinetic curves shaping a bimodal wave at D2 and a higher wave [↑] at D4 (CCL-5, TNF-α, IFN-γ, IL-17, and G-CSF), a bimodal profile with similar waves at D2 and D4 (IL-1β and IL-13), a wave at D2 and a valley at D3 (CXCL8 and CCL2), a midpoint wave at D3 (IL-12, IL-10, and VEGF), a unimodal valley at D3 (CCL3, CXCL10, IL-6, and FGF-basic), a valley at D4 (CCL11, CCL4, IL-1Ra, and IL-4) or a unique pattern (IL-5, IL-9, PDGF, and GM-CSF).

zonas state is endemic for the yellow fever virus (YFV) and has very high YFV-vaccination coverage. Thus, most individuals enrolled in this study experienced previous flavivirus exposure potentially modulating the cytokine and chemokine responses. These differences in prior flavivirus exposure may account for some differences in the cytokine and chemokine profiles shown in the study by Kam et al. (2017), which examined a Brazilian cohort of patients from Campinas, Brazil, where yellow fever vaccination was not required by the government at the time of their study as it is in Manaus, Brazil.

Consistent with our results, an immune response induced during the acute phase has previously been described in infections caused by ZIKV and other flaviviruses, including YFV and West Nile virus (ter Meulen et al. 2004, Klein et al. 2005, Tappe et al. 2016). In the case of ZIKV infection, the mechanism of the inflammatory immune response has not been clearly delineated. The immune response may be triggered by viral upregulation of the expression of pattern recognition receptors (PRRs) engaged in downstream pathways and the inflammatory antiviral response, such as IRF7, IFN-α, IFN-β, and CCL5 (Hamel et al. 2015). Interestingly, we showed a strong positive correlation between IFN-α and CCL5, suggesting that the synergistic effect of these cytokines might be crucial for the outcome of acute inflammation caused by ZIKV.

Our findings also revealed higher levels of growth factors and chemokines among patients as compared to controls. Similarly, prior research showed increased levels of CXCL10, CCL5, CCL3, and VEGF in patients acutely infected with ZIKV, while elevated levels of GM-CSF, CCL4, and FGF-basic biomarkers were observed only in the recovery phase (Tappe et al. 2016). Our study

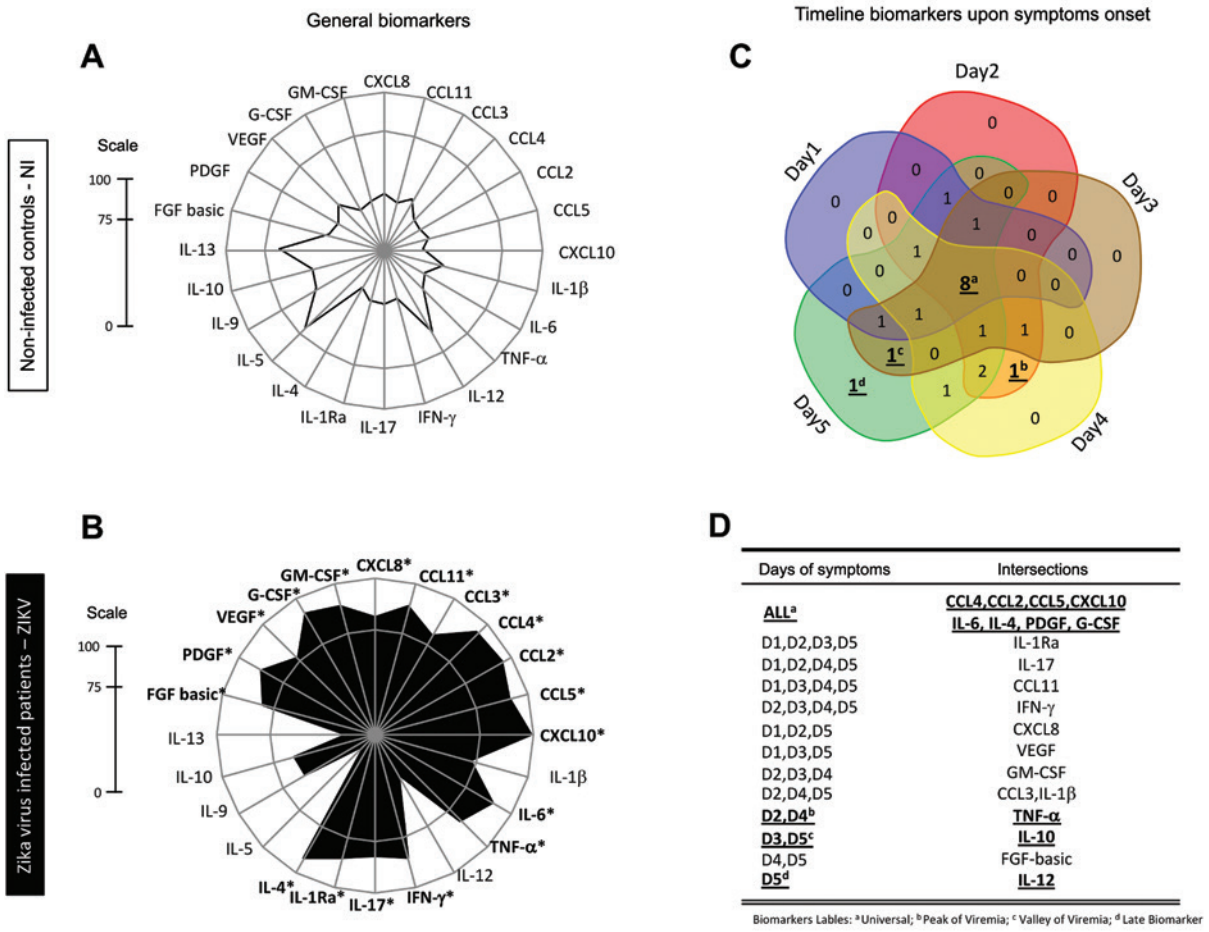

D

Days of symptoms	Intersections
ALL[a]	**CCL4,CCL2,CCL5,CXCL10 IL-6, IL-4, PDGF, G-CSF**
D1,D2,D3,D5	IL-1Ra
D1,D2,D4,D5	IL-17
D1,D3,D4,D5	CCL11
D2,D3,D4,D5	IFN-γ
D1,D2,D5	CXCL8
D1,D3,D5	VEGF
D2,D3,D4	GM-CSF
D2,D4,D5	CCL3,IL-1β
D2,D4[b]	**TNF-α**
D3,D5[c]	**IL-10**
D4,D5	FGF-basic
D5[d]	**IL-12**

Biomarkers Lables: [a]Universal; [b]Peak of Viremia; [c] Valley of Viremia; [d] Late Biomarker

Fig. 5: biomarker levels upon symptom onset and along a time course during early stage Zika virus (ZIKV) infection in adults. Biomarker signatures of non-infected (NI) (□) and ZIKV (■) were constructed as described in Methods. Data are presented in radar charts as the proportion of subjects with serum biomarker levels above the global population median values in (A) NI subjects, and (B) ZIKV-infected patients. Biomarkers with levels above the global median in more than 75% of subjects were highlighted by asterisks (*). (C) A Venn diagram showing the intersections of common attributes and well as selected biomarkers along the timeline of symptom onset: day 1 (blue), day 2 (red), day 3 (brown), day 4 (yellow), and day 5 (green). (D) Venn diagram report summarizing selected attributes with patterns labelled as (a) universal, (b) peak of viremia, (c) valley of viremia, or (d) late biomarkers (inserted table).

demonstrated that all chemokines and growth factors analysed were significantly increased in the acute phase when compared with non-infected controls. In fact, the role of growth factors in the pathogenesis of arboviral infections remains a matter of debate. We demonstrate that a remarkable increase of FGF-basic, PDGF, VEGF, G-CSF, and GM-CSF identifies the acute phase of ZIKV infection, which suggests the importance of chemokines and growth factors in the initiation and regulation of the acute phase immune response.

Increased serum concentrations of both CXCL (CXCL8 and CXCL10) and CCL chemokines (CCL2, CCL3, CCL4, CCL5, and CCL11) were found in acute ZIKV infection. The role of CCL5 in arbovirus-induced immunopathology remains a controversial issue, but levels of this chemokine, along with CCL2 and CCL3, were previously linked to the severity of dengue virus infections, including neurological disease and impairment of neuronal survival (Sathupan et al. 2007, Zlotnik and Yoshie 2012).

Furthermore, we found strong correlations between TNF-a and CCL5 concentrations and the percentages of circulating neutrophils and lymphocytes in acute ZIKV infection. This finding is likely due to the role of TNF-a and CCL5 in leukocyte chemoattraction and demonstrates the important role of this cytokine and chemokine in the stimulation of the innate and adaptive immune system in response to ZIKV infection.

This manuscript is the first to describe the bimodal nature of viremia in acute Zika infection and the corresponding peaks in inflammatory cytokine production. A biological model explaining bimodal viremia was first described in a classical study of using mousepox virus (Fenner 1948). Similarly, flaviviruses are initially replicated in Langerhans cells at the site of inoculation and in draining regional lymph nodes. Despite a robust antiviral innate immune response that eliminates viral infected cells, some virus particles are disseminated by the blood (primary viremia). Therefore, several organs and tissues may be-

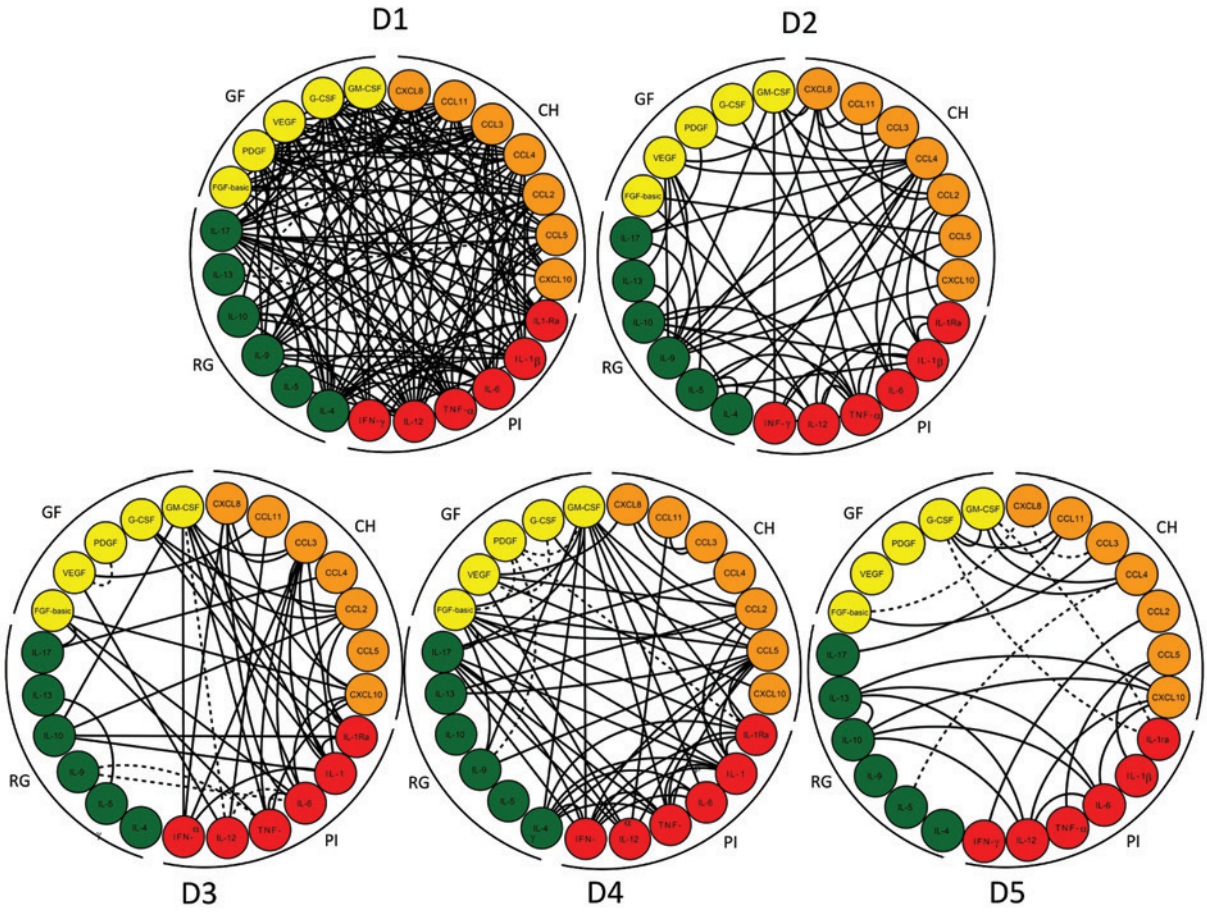

Fig. 6: biomarker networks along a timeline during early stages of Zika virus (ZIKV) infection in adults. Integrative systems biology analysis of attributes was conducted using the Cytoscape software platform to build a circular nodal network layout for each time point following ZIKV infection, from day 1 (D1) up to day 5 (D5), based on Spearman's correlation matrices. Significance was considered at $p < .05$. The timeline of networks is displayed as circular layouts to characterize the interaction along the early time points. Coloured nodes are employed to identify chemokines (CH - orange), pro-inflammatory cytokines (PI - red), regulatory cytokines (RG - green), and growth factors (GF - yellow). Connecting edges underscore the association between attributes, classified as positive (solid line) or negative (dashed line).

come infected, producing a second wave of viral replication that reaches the blood and causes secondary viremia. The equine infection by African horse sickness virus, another arbovirus of the *Orbivirus* genus, *Reoviridae* family, also shows two viremia peaks. The first peak is observed after viral multiplication in lymph nodes, whereas the second peak is observed after viral replication in spleen, lungs and endothelial cells (Mellor and Hamblin 2004).

Interestingly, bimodal viremia has been found in patients after low dose live attenuated 17DD yellow fever vaccine administration (Campi-Azevedo et al. 2014). As compared to the standard dosage vaccine, the low dose live attenuated vaccine is hypothesized to elicit a less robust immune response that does not clear the initial viremia, leading to a second peak of viremia a few days later. Although bimodal viremia, including in flavivirus infections, was observed in the aforementioned studies, our results should be interpreted with caution, as we did not evaluate patients longitudinally. Thus, future studies on this topic are recommended.

In this manuscript, we report high levels of pro-inflammatory mediators during the acute phase of ZIKV infection. Paradoxically, although the inflammatory response leads to viral clearance, the high levels of circulating pro-inflammatory biomarkers may facilitate the transmission of viruses from the circulation to the central nervous system by increasing the permeability of the blood-brain barrier. This phenomenon has been reported for the West Nile virus (Wang et al. 2004), as well as another neurovirulent flavivirus, and may partially explain ZIKV neuroinvasiveness.

Remarkably, CXCL10 expression was increased more than 200-fold in ZIKV-infected subjects as compared to controls. This CXCL10 overexpression has been linked to the IFN-γ signalling pathway induced by ZIKV NS5 protein. According to Chaudhary et al. (2017), NS5 promotes IFN-γ gene activation through the degradation of STAT2 and subsequent induction of STAT1-STAT1 homodimerization. Augmented serum levels of CXCL10 have been found during severe clinical

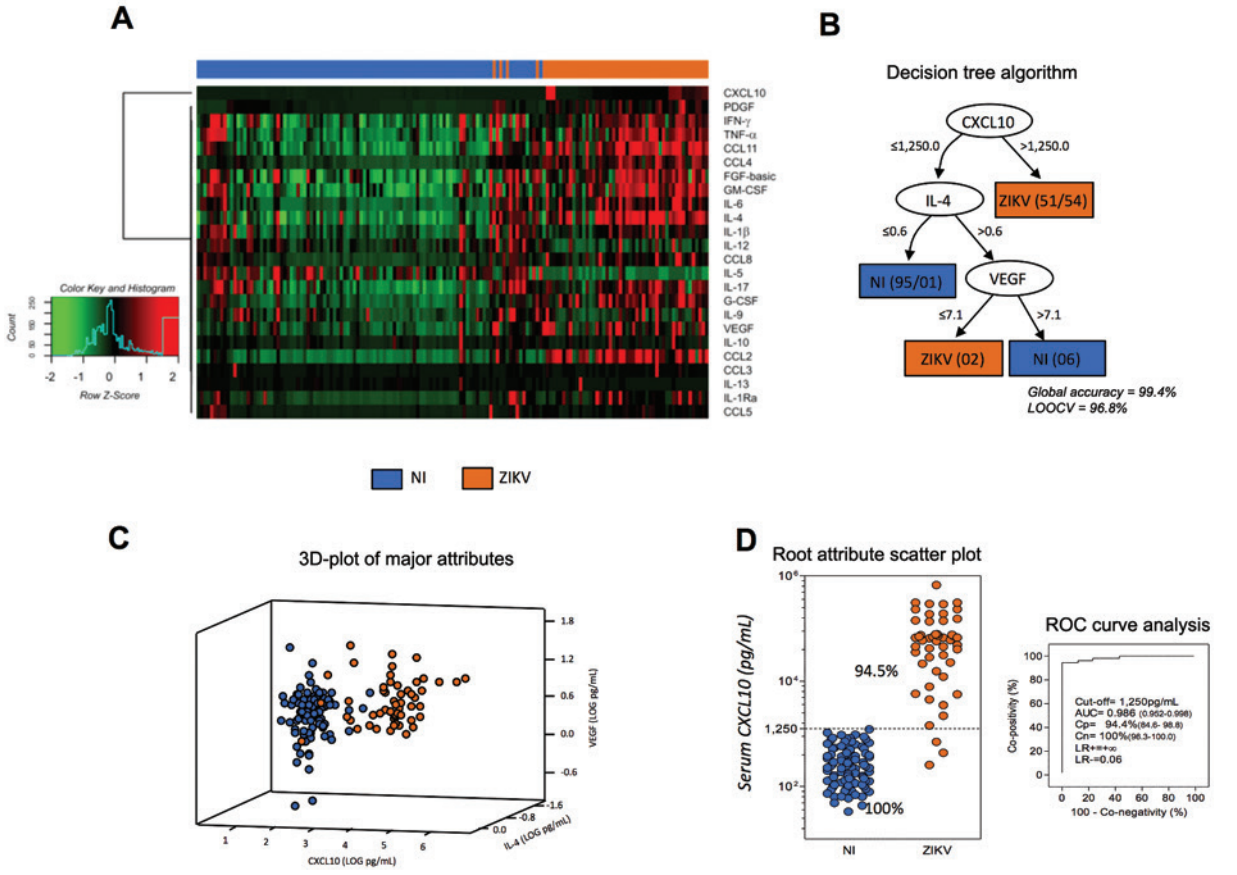

Fig. 7: high-dimensional data analysis during early stages of Zika virus (ZIKV) infection in adults. Machine-learning high-dimensional data approaches were applied to further explore and identify feasible criteria applicable for the clinical follow-up of ZIKV infection. (A) Heatmap panels were built to verify the ability of attributes to segregate ZIKV (orange) and non-infected (NI) (blue) groups as they present low (green) or high (red) levels of serum biomarkers. (B) Decision tree algorithms were generated to define root and branch attributes to segregate patients (ZIKV = orange) from NI controls (NI = blue). Global accuracy and leave-one-out cross-validation (LOOCV) values are provided in the figure. (C) The root/branch attributes selected by the decision tree algorithm were compiled into a 3D-plot to verify their cluster strengths. (D) The performance of the selected root attribute to discriminate ZIKV (orange) from NI (blue) was evaluated by scatterplot distribution and validated by receiver operating characteristic indices (AUC: area under the curve; Cp: co-positivity; Cn: co-negativity; LR+/LR-: positive/negative likelihood ratio).

manifestations of dengue and yellow fever (Melchjorsen et al. 2003). Surprisingly, CXCL10 has also been shown to play an important role in CD-8+ T-cell recruitment as part of an anti-flaviviral response to West Nile virus in the central nervous system (Klein et al. 2005). Furthermore, CXCL10 has been previously identified as a biomarker of severity in several diseases including those caused by bacteria such as *Mycobacterium tuberculosis* and *Legionella pneumophila*, as well as protozoans like *Trypanosoma brucei*, *Leishmania major*, *Plasmodium vivax* or *Plasmodium falciparum* (Liu et al. 2011). Other studies showed that the overexpression of CXCL10 leads to apoptosis in foetal neurons (Liu et al. 2011). CXCL10 has also been strongly implicated in Guillain-Barré syndrome pathogenesis (Chiang and Ubogu 2013). Thus, we hypothesize that the high levels of CXCL10 in ZIKV patients may contribute to neuronal damage affecting the developing foetal brain and potentially targeting peripheral nerves in Guillain-Barré syndrome as well. Consistent with this hypothesis, Kam et al. (2017) specifically identified higher levels of CXCL10 in ZIKV-infected patients with neurological complications compared to those without and higher levels of CXCL10 in ZIKV-infected pregnant women carrying babies with foetal growth associated malformations.

High levels of CXCL10 have been previously described in acute and convalescent phases, with more prominent expression in the latter (Tappe et al. 2016). Unfortunately, although our data strongly suggest that CXCL10 is a biomarker of acute ZIKV infection, we were unable to perform a longitudinal analysis to verify its kinetics in order to further confirm whether the concentrations of this chemokine would be down or up-regulated across different stages of the disease. In addition, CXCL10 elevation is also observed in pre-eclampsia and hypertension in pregnancy, which can result in a range of foetal injuries including intrauterine growth retardation and neurological damage induced by hypoxia (Gotsch et al. 2007). Thus, it is reasonable to suggest that ZIKV-induced inflammation may increase the frequency of foetal injuries.

CXCL10 may also be an important therapeutic target (Liu et al. 2011). For example, CXCL10 neutralization by specific antibodies or genetic deletion in CXCL10-/-mice protected against cerebral malaria infection and inflammation (Nie et al. 2009). Passive transfer of anti-CXCL10 antibodies reduced inflammatory leukocyte recruitment across the blood-brain barrier. Furthermore, statin medications commonly used for cholesterol control have been shown to decrease CXCL10 and to be effective in CXCL10-mediated Crohn's disease (Grip and Janciauskiene 2009).

In this work, we also describe the relationship between the timing of viremia and cytokine elevations. We assessed the acute phase biomarkers and viral titres at different time points (until day 5). Augmented levels of CCL4, CCL2, CCL5, CXCL5, CXCL10, IL-6, IL-4, PDGF, and G-CSF immunomodulators were observed at all time points. The peaks of viremia, at Day 2 and Day 4, were accompanied by increased TNF-α levels. IL-10 elevation appeared to be directly related to the lowest virus titres (Day 3 and Day 5), while the highest levels of IL-12 were found at Day 5. These findings allow us to deduce that the acute phase of ZIKV is characterized mainly by an innate immune system inflammatory response, with overlap of the inflammatory biomarkers and viremia peaks, while the anti-inflammatory response coincides with viremia decay. Altogether, this study identifies unique characteristics of the acute inflammatory and multifactorial immune response induced by ZIKV and identifies CXCL10 as a potential biomarker of acute infection and, perhaps, a predictor of severity. Nevertheless, further longitudinal studies that measure the host immunopathological response at several time points are required to better characterize the immunological factors involved in Zika disease. The altered concentrations of serum biomarkers observed in this study may bring new insights to the ZIKV immunopathology puzzle.

ACKNOWLEDGEMENTS

To the Programa de Desenvolvimento Tecnológico em Insumos para a Saúde - PDTIS-FIOCRUZ, for use of the flow cytometry (CPqRR) and Real-Time PCR (ILMD) facilities.

AUTHORS' CONTRIBUTION

FGN and RR conceived and designed the study; GAVS, VAN, DCSM, MSS, LFA, JHAS, TAPA, MCCM, TGRM, and HVSE were responsible for the acquisition and quality of the clinical and laboratory data; FGN, VAN and DCSM performed the molecular diagnosis, whereas GAVS, ATC, OAMF, LRVA, ACCA and JGCR performed the serum biomarker measurements; FGN, GSP, AYC, MSG, LRA, ATC and OAMF completed the data mining and statistical analysis; FGN, GSP, AYC, ACCA, JGCR, LRVA, ATC and OAMF wrote the first version of the paper. All authors were involved in the interpretation of the data and participated in the final writing of the manuscript. The authors declare that the funders had no role in the study design, data collection and analysis, decision to publish, or preparation of the manuscript.

REFERENCES

Campi-Azevedo AC, Estevam PA, Coelho-dos-Reis JG, Peruhype-Magalhães V, Villela-Rezende G, Quaresma PF, et al. Subdoses of 17DD yellow fever vaccine elicit equivalent virological/immunological kinetics timeline. BMC Infect Dis. 2014; 14: 391.

Chaudhary V, Yuen KS, Chan JF, Chan CP, Wang PH, Cai JP, et al. Selective activation of type II interferon signaling by Zika virus NS5 protein. J Virol. 2017; 91(14): pii:e00163-17.

Chiang S, Ubogu EE. The role of chemokines in Guillain-Barré syndrome. Muscle Nerve. 2013; 48(3): 320-30.

de Oliveira WK, Cortez-Escalante J, de Oliveira WTGH, do Carmo GMI, Henriques CMP, Coelho GE, et al. Increase in reported prevalence of microcephaly in infants born to women living in areas with confirmed Zika virus transmission during the first trimester of pregnancy - Brazil, 2015. MMWR Morb Mortal Wkly Rep. 2016; 65(9): 242-7.

Edwards MR, Strong K, Cameron A, Walton RP, Jackson DJ, Johnston SL. Viral infections in allergy and immunology: how allergic inflammation influences viral infections and illness. J Allergy Clin Immunol. 2017; 140(4): 909-20.

Fenner F. The pathogenesis of the acute exanthems; an interpretation based on experimental investigations with mousepox (infectious ectromelia of mice). Lancet. 1948; 2(6537): 915-20.

Figueiredo RMP, Naveca FG, Bastos MS, Melo MDN, Viana SS, Mourão MPG, et al. Dengue virus type 4, Manaus, Brazil. Emerging Infect Dis. 2008; 14(4): 667-9.

Galliez RM, Spitz M, Rafful PP, Cagy M, Escosteguy C, Germano CSB, et al. Zika virus causing encephalomyelitis associated with immunoactivation. Open Forum Infect Dis. 2016; 3(4): ofw203.

Gotsch F, Romero R, Friel L, Kusanovic JP, Espinoza J, Erez O, et al. CXCL10/IP-10: a missing link between inflammation and anti-angiogenesis in preeclampsia? J Matern Fetal Neonatal Med. 2007; 20(11): 777-92.

Grip O, Janciauskiene S. Atorvastatin reduces plasma levels of chemokine (CXCL10) in patients with Crohn's disease. PLoS One. 2009; 4(5): e5263.

Gurukumar KR, Priyadarshini D, Patil JA, Bhagat A, Singh A, Shah PS, et al. Development of real time PCR for detection and quantitation of dengue viruses. Virol J. 2009; 6: 10.

Hamel R, Dejarnac O, Wichit S, Ekchariyawat P, Neyret A, Luplertlop N, et al. Biology of Zika virus infection in human skin cells. J Virol. 2015; 89(17): 8880-96.

Kam Y-W, Leite JA, Lum F-M, Tan JJL, Lee B, Judice CC, et al. Specific biomarkers associated with neurological complications and congenital central nervous system abnormalities from Zika virus-infected patients in Brazil. J Infect Dis. 2017; 216(2): 172-81.

Klein RS, Lin E, Zhang B, Luster AD, Tollett J, Samuel MA, et al. Neuronal CXCL10 directs CD8+ T-cell recruitment and control of West Nile virus encephalitis. J Virol. 2005; 79(17): 11457-66.

Klein SL. Sex influences immune responses to viruses, and efficacy of prophylaxis and treatments for viral diseases. Bioessays. 2012; 34(12): 1050-9.

Lanciotti RS, Kosoy OL, Laven JJ, Panella AJ, Velez JO, Lambert AJ, et al. Chikungunya virus in US travelers returning from India, 2006. Emerging Infect Dis. 2007; 13(5): 764-7.

Lanciotti RS, Kosoy OL, Laven JJ, Velez JO, Lambert AJ, Johnson AJ, et al. Genetic and serologic properties of Zika virus associ-

ated with an epidemic, Yap state, Micronesia, 2007. Emerging Infect Dis. 2008; 14(8): 1232-9.

Liu M, Guo S, Hibbert JM, Jain V, Singh N, Wilson NO, et al. CXCL10/IP-10 in infectious diseases pathogenesis and potential therapeutic implications. Cytokine Growth Factor Rev. 2011; 22(3): 121-30.

Luiza-Silva M, Campi-Azevedo AC, Batista MA, Martins MA, Avelar RS, Lemos DS, et al. Cytokine signatures of innate and adaptive immunity in 17DD yellow fever vaccinated children and its association with the level of neutralizing antibody. J Infect Dis. 2011; 204(6): 873-83.

Melchjorsen J, Sørensen LN, Paludan SR. Expression and function of chemokines during viral infections: from molecular mechanisms to in vivo function. J Leukoc Biol. 2003; 74(3): 331-43.

Mellor PS, Hamblin C. African horse sickness. Vet Res. 2004; 35(4): 445-66.

Naveca FG, do Nascimento VA, de Souza VC, Nunes BTD, Rodrigues DSG, Vasconcelos PFC. Multiplexed reverse transcription real-time polymerase chain reaction for simultaneous detection of Mayaro, Oropouche, and Oropouche-like viruses. Mem Inst Oswaldo Cruz. 2017; 112(7): 510-3.

Nie CQ, Bernard NJ, Norman MU, Amante FH, Lundie RJ, Crabb BS, et al. IP-10-mediated T cell homing promotes cerebral inflammation over splenic immunity to malaria infection. PLoS Pathog. 2009; 5(4): e1000369.

Oehler E, Watrin L, Larre P, Leparc-Goffart I, Lastere S, Valour F, et al. Zika virus infection complicated by Guillain-Barre syndrome - case report, French Polynesia, December 2013. Euro Surveill. 2014; 19(9): pii:20720.

Ornelas AMM, Pezzuto P, Silveira PP, Melo FO, Ferreira TA, Oliveira-Szejnfeld PS, et al. Immune activation in amniotic fluid from Zika virus-associated microcephaly. Ann Neurol. 2017; 81(1): 152-6.

Sathupan P, Khongphattanayothin A, Srisai J, Srikaew K, Poovorawan Y. The role of vascular endothelial growth factor leading to vascular leakage in children with dengue virus infection. Ann Trop Paediatr. 2007; 27(3): 179-84.

Tappe D, Pérez-Girón JV, Zammarchi L, Rissland J, Ferreira DF, Jaenisch T, et al. Cytokine kinetics of Zika virus-infected patients from acute to reconvalescent phase. Med Microbiol Immunol. 2016; 205(3): 269-73.

ter Meulen J, Sakho M, Koulemou K, Magassouba N, Bah A, Preiser W, et al. Activation of the cytokine network and unfavorable outcome in patients with yellow fever. J Infect Dis. 2004; 190(10): 1821-7.

Wang T, Town T, Alexopoulou L, Anderson JF, Fikrig E, Flavell RA. Toll-like receptor 3 mediates West Nile virus entry into the brain causing lethal encephalitis. Nat Med. 2004; 10(12): 1366-73.

Zlotnik A, Yoshie O. The chemokine superfamily revisited. Immunity. 2012; 36(5): 705-16.

ANEXO 3

Title: Molecular detection of Zika virus in serum, urine, and saliva from acute-phase patients: effects of differential RNA shedding and RT-PCR sensitivity

Author's names: Ligia Fernandes Abdalla[1,2*]; Fernando Abad-Franch[3*]; João Hugo Abdalla[4,5]; Valdinete Alves Nascimento[6,7]; Felipe Gomes Naveca[1,5,6]

Institutional affiliations:

1 Programa de Pós-Graduação em Imunologia Básica e Aplicada, Universidade Federal do Amazonas, Manaus, Amazonas, Brazil

2 Universidade Estadual do Amazonas, Manaus, Amazonas, Brazil

4 Universidade Federal do Amazonas, Manaus, Amazonas, Brazil

5 Hospital Adventista de Manaus, Manaus, Amazonas, Brazil

6 Instituto Leônidas e Maria Diane – Fiocruz Amazônia, Manaus, Amazonas, Brazil

*These authors contributed equally to this work.

Corresponding author:

Dr. Felipe Gomes Naveca

Rua Teresina, 476 - Adrianópolis, Manaus - AM, 69057-070.

Tel: +55 (92) 3621-2323

E-mail: felipe.naveca@fiocruz.br

Abstracts

Sponsorships

Funding: FGN is funded by Conselho Nacional de Desenvolvimento Científico e Tecnológico (http://www.cnpq.br, grant 440856/2016-7) and Coordenação de Aperfeiçoamento de Pessoal de Nível Superior (http://www.capes.gov.br, grants 88881.130825/2016-00 and 88887.130823/2016-00). OAMF is funded by the Conselho Nacional de Desenvolvimento Científico e Tecnológico (http://www.cnpq.br, grant 440682/2016-9); Coordenação de Aperfeiçoamento de Pessoal de Nível Superior (http://www.capes.gov.br, grants 88881.130829/2016-01) and Financiadora de Estudos e Projetos (http://www.finep.gov.br, grant TED264/16). The funders had no role in study design, data collection and analysis, decision to publish or preparation of the manuscript.

Introduction

Zika fever is an emerging disease caused by a mosquito-borne flavivirus (Petersen et al, 2016). Zika virus (ZIKV) recently caused a massive outbreak Brazil and is now widespread across the Americas (Zanluca et al, 2015; WHO, 2017). The Brazilian epidemic revealed that the usually mild, self-limited infection with ZIKV can lead to severe neurologic disorders including microcephaly and Guillain-Barré syndrome (Leal, 2016; Krauer et al, 2017). ZIKV is primarily spread by *Aedes* mosquitoes but can also be transmitted sexually, from mother to offspring, and through other routes (Grischott et al, 2016; Petersen et al, 2016; Leal, 2016). In humans, ZIKV shedding varies over time and across bodily fluids including blood, semen, urine, and saliva, and this variation can affect both

transmission dynamics and infection diagnosis (Petersen et al, 2016, Lustig et al, 2016; Froeschl et al, 2017; Prisant et al, 2016; Nicastri et al, 2016;(Musso et al. 2014; Rozé et al, 2016; Sun et al, 2016; Kodati et al, 2017).

ZIKV diagnosis is not straightforward. Most patients are asymptomatic – and symptoms, when present, are similar to those caused by dengue or chikungunya. Serological tests can detect anti-ZIKV antibodies, but cross-reactivity complicates the interpretation of results in areas where other arboviruses are endemic. Molecular detection of ZIKV RNA through real time reverse-transcriptase PCR (RT-PCR) is the method of choice for ZIKV diagnosis. Even with highly accurate RT-PCR, however, the process of ZIKV RNA detection is not without difficulties. First, detection depends upon the sample containing viral RNA at a concentration above the assay's (usually very small) detection limit. Second, factors like RNA integrity and sequence variability, PCR inhibition, or sample contamination may all result in incorrect RT-PCR results (Petersen et al, 2016; Charrel et al, 2016; Corman et al, 2016; Waggoner & Pinsky, 2016).

More formally, the process of ZIKV detection depends upon a three-level hierarchy of probabilities – the probability that the patient is infected, the probability that a specimen drawn from an infected patient contains ZIKV RNA, and the probability that an RT-PCR assay detects ZIKV RNA in a sample when it is present. While this hierarchical structure is often implicit in diagnostic-test studies, a formal treatment of the ZIKV detection process across all three levels is currently lacking. Here, we use a hierarchical modeling approach to investigate the process of RT-PCR-based ZIKV detection in clinical samples. This allows us to formally disentangle the effects of differential viral shedding and differential test performance on ZIKV detection. We illustrate our approach with a study of serum,

urine, and saliva samples from 108 acute-phase patients repeatedly tested with two RT-PCR assays. Apart from clarifying the relative importance of viral shedding and test sensitivity in ZIKV molecular detection, our findings suggest that noninvasive saliva sampling could play an important role in the diagnosis of acute Zika fever.

Materials and methods

Study Population

From December 2015 to April 2016 were recruited 108 subjects with clinical suspicion of ZIKV infection – defined by diagnosis of maculopapular rash with pruritus, with or without fever up to 38.5°C, and at least one of the following: conjunctivitis, arthralgia, or joint swelling. Seventy-four patients sought care at the Hospital Adventista de Manaus (HAM), a ZIKV surveillance sentinel hospital in Manaus, Amazonas state, Brazil. Serum samples (stored at −80°C) from 34 additional subjects who sought care at different hospitals in Manaus were made available by the Central Public Health Laboratory of Amazonas state health department. Of all 108 patients, the mean age was 35.63 years (ranging from 18 to 70 years) and 74 (79.92%) were females. All samples were taken one to seven days (median 3.0) after symptom onset.

Ethics

All the procedures performed were according to the Ethics Committee of the State University of Amazonas (CAAE: 56745116.6.0000.5016) and with the Declaration of Helsinki of 1975, revised in 1983.

Sample collection and processing

Standard operating procedures (SOPs) were used for the collection, processing and manipulation of serum and urine samples, while the saliva samples followed a methodology previously described by the author (Abdalla et al, 2010; Schmidt et al, 2017). After collection, the samples were sent to Instituto Leônidas e Maria Deane - Fiocruz Amazônia and kept at -80ºC until molecular testing.

Molecular testing

Viral RNA from serum, saliva and urine was extracted with QIAmp® Viral RNA Mini Kit (QIAGEN Inc., Germany) using 140 µL of each specimen, eluted in 60µL of AVE buffer, following the manufacturer's instructions.

All the samples were test by two differents RT-qPCR assays (Applied Biosystems, US): One was previously described by Lanciotti (2008) - Env gene - and the other was designed by our group based on coding sequences of the non-structural protein 5 (NS5) of Zika virus (Asian genotype) available on may 2016. This target at positions 9,171 to 9,297 of the tentative RefSeq (KX369547) for Zika Asian genotype was amplified and detected with the forward primer ZIKA_FNF 5’ – TGTTGAAGGGCTGGGATTAC; reverse primer ZIKA_FNR 5’ –

CTCCAGATCAAACCTGCTGAT and the probe ZIKA_FNP 5' (FAM) – TGAGTCGCA / ZEN / TACCAGGAGGAAGGA – 3' (Iowa Black FQ). All primers and probes were ordered from the same supplier (IDT DNA Technologies, Coralville, IA).

Samples were still tested by RT-qPCR for Chikungunya virus (CHIKV) (Lanciotti et al. 2007), DENV (Gurukumar et al. 2009), Mayaro virus (MAYV) (Naveca et al. 2017) and Oropouche virus (OROV) infection (Naveca et al. 2017). Samples positive for another arbovirus were excluded.

Sample inclusion criteria also required the internal control (spiked MS2 bacteriophage) to display a Ct value between 30-32. The viremia was indirectly estimated by RT-qPCR and reported as 1/Ct*100.

Rationale

We aimed at understanding what factors affect ZIKV RNA detection through RT-PCR in acute-phase patients. As previously stated, we used two RT-PCR assays (Env and NS5) and applied them multiple times to serum, urine and saliva samples from individual patients. We noted that the *non*-detection of ZIKV RNA in a given RT-PCR assay run on a given specimen can be due to:

(a) Absence of the target molecule from the specimen; this can reflect two distinct processes – either (i) the patient was not infected or (ii) the specimen did not contain ZIKV RNA, in spite of patient infection, because at the time of sampling there was no viral shedding in the bodily fluid sampled by that specimen; or

(b) Unsuccessful RT-PCR, in spite of ZIKV RNA presence in the specimen – i.e., a false-negative result. (We note that an RT-PCR run may also yield a negative result if the concentration of the target molecule in the sample is below the assay's detection threshold; the Env assay we used can detect about 2–5 viral particles per ml according to the literature (Corman et al, 2016; Lanciotti et al. 2008).

We thus hypothesized that, conditional on a patient being infected, the detection of ZIKV RNA can primarily depend on (i) differential ZIKV RNA shedding across bodily fluids and over time (the 'shedding effect hypothesis') or (ii) variation in the sensitivity of different RT-PCR assays or tests (the 'false-negative effect hypothesis') **(Table 1)**. Here, we define *shedding* as the probability that a specimen from an infected patient contains ZIKV RNA, and *sensitivity* as the per-RT-PCR assay probability of detecting ZIKV RNA in a specimen that comes from an infected patient *and* contains ZIKV RNA (or, strictly speaking, contains at least ~2–5 viral particles per ml) (Waggoner & Pinsky, 2016; Lanciotti et al, 2008).

Table 1. Main hypotheses about Zika virus RNA detection in acute-phase clinical samples: description and examples of predicted model ranking

Hypothesis	Description (including some specific variants)	Model ranking
'Shedding effect'	Detection primarily depends on shedding variation rather than on RT-PCR sensitivity variation	$\theta(fluid),p(.) > \theta(.),p(test/target/fluid)$
	No variation in shedding across bodily fluids, with shedding probability ≈ 1.0	$\theta(1.0) > \theta(./fluid)$
	No variation in shedding across bodily fluids, but shedding probability < 1.0	$\theta(.) > \theta(fluid/1.0)$
	Shedding varies across bodily fluids	$\theta(fluid) > \theta(./1.0)$
'False-negative effect'	Detection primarily depends on RT-PCR sensitivity variation rather than on shedding variation	$\theta(.),p(test/target/fluid) > \theta(fluid),p(.)$
	Sensitivity is constant across tests	$p(.) > p(test)$
	Sensitivity varies across tests	$p(test) > p(.)$
	Sensitivity varies primarily across RT-PCR targets	$p(target) > p(test) > p(.)$
	Sensitivity varies primarily across bodily fluids	$p(fluid) > p(test) > p(.)$

'Model ranking' refers to relative model performance, as measured by sample size-corrected Akaike's information criterion (AICc); better-performing models rank higher, as indicated by '>'

θ, Zika virus RNA shedding probability; *p*, per-RT-PCR assay Zika virus RNA detection probability
θ and *p* can be constant (coded '(.)'), vary as a function of covariates (in *italics*, and as defined in Table 3), or be fixed (with 'θ(1.0)' meaning that shedding probability is fixed at 1.0); slashes ('/') denote models including any of the effects inside the brackets – e.g., 'θ(./*fluid*)' refers to either 'θ(.)' (constant-θ model) or 'θ(*fluid*)' (in which θ can vary across bodily fluids)

Modeling

To explicitly account for detection-process uncertainties, we used the multilevel occupancy models developed by JD Nichols and colleagues (Nichols et al, 2009). Originally designed to study wildlife biology when organisms are detected imperfectly, occupancy models have found wide application in infectious disease ecology (MacKenzie & Bailey, 2004; McClintock et al, 2010; Lachish et al, 2012; Abad-Franch et al, 2014; Elmore et al, 2016; Leal, 2016). Our models consider a three-level hierarchy of (i) patients, who are infected with probability Ψ; (ii) different specimens (bodily fluid samples) taken from each patient, which contain ZIKV RNA, given patient infection, with shedding probability θ; and (iii) RT-PCR assays, which detect ZIKV, given the patient is infected and the specimen contains ZIKV RNA, with detection probability *p* **(Table 2, Fig 1)** (Nichols et al, 2009). The models use the results of repeated RT-PCR assays run on specimens from each patient to simultaneously derive maximum-likelihood estimates of Ψ, θ, and *p*. (Nichols et al, 2009). Each assay can yield detection (Ct ≤ 40.0, coded '1') or non-detection (Ct > 40.0, coded '0') of the target RNA, and the set of replicate assays carried out on specimens from a patient yields a detection history for that patient **(Fig 1)** (Nichols et al, 2009; McClintock et al, 2010). The probabilities of infection (Ψ), shedding (θ), and detection (*p*) may vary as a function of covariates describing, e.g., patient or assay traits, with effects

evaluated using the logit link function in a generalized linear modeling framework (McClintock et al, 2010; MacKenzie & Bailey, 2004). Covariate names are highlighted in *italics* the first time they appear in the next paragraph.

Table 2. Key parameters involved in the process of Zika virus RNA detection by RT-PCR: a multilevel perspective

Parameter	Definition (*interpretation*)	Level
Ψ	Probability of Zika virus RNA presence (*infection*)	Patient
θ	Probability of Zika virus RNA presence in a sample, given patient infection (*shedding*)	Bodily fluid sample
p	Probability of detecting Zika virus RNA through RT-PCR, given infection and shedding (*sensitivity*)	RT-PCR assay (reaction)

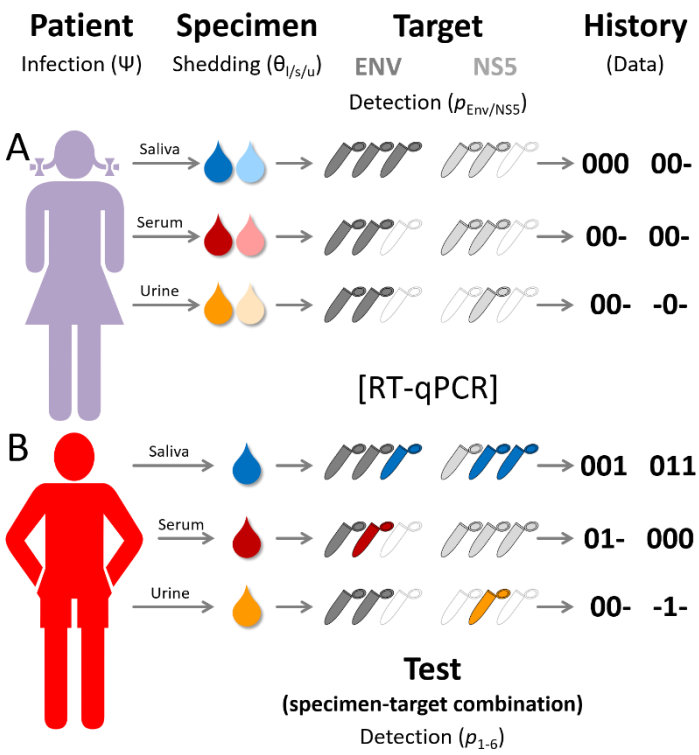

Figure 1. Models consider a three-level hierarchy of patients, who are infected with probability Ψ; different specimens (bodily fluid samples) taken from each patient, which contain ZIKV RNA, given patient infection, with shedding probability θ; and RT-PCR assays, which detect ZIKV, given the patient is infected and the specimen contains ZIKV RNA, with detection probability p in two RT-PCR assays (Env and NS5). Each assay can yield detection (Ct ≤ 40.0, coded '1') or non-detection (Ct > 40.0, coded '0') of the target RNA, and the set of replicate assays carried out on specimens from a patient yields a detection history for that patient

Given our focal interest on investigating the detection process, we held Ψ constant in all models. To evaluate the 'shedding effect hypothesis', we estimated a separate θ intercept for each bodily *fluid* – serum, urine, and saliva. After exploratory analyses **(Text. S1)**, we modeled shedding in serum and urine (but not saliva) as a function of *days* since symptom onset. Patient *gender* and *age* were tested for common effects on θ in all three bodily fluids **(Table 3)**. We also ran alternative shedding models including (i) same intercept across bodily fluids (which, if supported by the data, would suggest no differences in shedding); (ii) a common effect of days across bodily fluids (which, if supported, would suggest that shedding in all fluids varies equally through time); and (iii) θ fixed at 1.0 (to assess support for the hypothesis that, if a patient is infected, ZIKV RNA will be present in all her bodily fluids with probability 1.0 – so that any detection failure would be due to the 'false-negative effect'). To further assess the 'false-negative effect hypothesis', we modeled *p* as a function of *test* (specimen/RT-PCR target combination) while considering potential confounders (days, gender, and age). We also assessed more parsimonious alternatives, namely that sensitivity may depend primarily on (i) RT-PCR *target* (Env *vs*. NS5), irrespective of bodily fluid, or (ii) bodily fluid, irrespective of RT-PCR target **(Table 3)**.

Table 3. Factors investigated in multilevel occupancy models assessing the process of Zika virus RNA detection through RT-PCR

Factor	Definition	Can affect	
		Shedding (θ)[a]	Sensitivity (*p*)[b]
Fluid	Bodily fluid (serum, urine or saliva)	**Likely**	Uncertain
Target	RT-PCR molecular target (Env or NS5)	No	Likely
Test	Fluid-target combination (six levels)	No	**Likely**
Days	Days since symptom onset	Uncertain[c]	Uncertain
Gender	Male or female	Uncertain	Unlikely
Age	Age in years	Uncertain	Unlikely

[a] Probability that a sample contains Zika RNA, given the patient is infected; [b] Probability of detecting Zika RNA in a sample, given the patient is infected and the sample contains Zika RNA; [c] Uncertain given

the short (1–7d) span of the *days* covariate in our acute-phase group of patients. *A priori* focal expectations are highlighted in **bold** typeface

Our models assume that (i) patient infection status does not change during sampling (which simultaneous sampling ensured), (ii) there are no false-positive results (which we believe is reasonable given the high specificity of RT-PCR (Charrel et al, 2016; Rozé et al, 2016; Waggoner & Pinsky, 2016; Lanciotti et al, 2008) and because none of the negative-control samples we ran in each experiment yielded a positive result), and (iii) patients are independent with respect to infection status (which may not be the case in some instances but does not affect RNA detection). This modeling framework accommodates missing test data and, importantly, takes into account the lack of independence among detections induced by repeated specimen testing (Nichols et al, 2009; MacKenzie & Bailey, 2004). We fit the models via maximum likelihood and evaluated relative model performance using the finite sample-size version of Akaike's information criterion (AICc) and related metrics (Burnham & Anderson, 2002). These analyses were done in PRESENCE v. 11.8 (Hines, 2006).

With our approach, inference is first based on relative model performance **(Table 1)** (Burnham & Anderson, 2002). For example, we may compare two candidate models representing, respectively, the 'shedding effect' and the 'false-negative effect' hypotheses. Model 1 states that shedding θ can vary among bodily fluids but RT-PCR sensitivity *p* is constant: $M_{\theta(fluid)} = \Psi(.),\theta(fluid),p(.)$. Model 2 states that θ is constant across bodily fluids but *p* can vary among RT-PCR tests: $M_{p(test)} = \Psi(.),\theta(.),p(test)$. Suppose we fit both models and find that $M_{\theta(fluid)}$ has an AICc score 4.0 units smaller than that of $M_{p(test)}$. Conditional on this two-model set, we would interpret this as evidence that the shedding effect is more relevant to detecting ZIKV with RT-PCR than the false-negative effect. The

second inferential step entails examination of the values of regression coefficients and of Ψ, θ, and *p* estimates (and their SEs). To account for model selection uncertainty, we calculated model-averaged coefficients and parameters with unconditional SEs (Burnham & Anderson, 2002). For simplicity, we present predictions derived from the top-ranking model in the figures below. This model included all covariates with measurable effects on shedding and sensitivity (and only those covariates), and its intercept and slope estimates were virtually identical to model-averaged estimates (**Table 4**). Further details on the modeling strategy are provided in **Text S1** and **Table S1.**

Table 4. Model-averaged estimates with unconditional 95% confidence interval limits and model weights

Component	Term (scale)	Category	Estimate	CI-low	CI-up	Weight
Infection (Ψ)	Intercept (probability)		0.9353	0.8525	0.9731	1*
Shedding in serum (θ_s)	Intercept (probability)		0.9510	0.7201	0.9932	**1**
	Days (OR)		0.5872	0.3829	0.9007	**0.8990**
	Gender (OR)	Female	Ref.			0.0274
		Male	0.5706	0.1867	1.7436	
	Age (OR)		1.0062	0.9621	1.0524	0.0385
Shedding in urine (θ_u)	Intercept (probability)		0.0816	0.0117	0.4008	**1**
	Days (OR)		1.6700	1.0668	2.6142	**0.8990**
	Gender (OR)	Female	Ref.			0.0274
		Male	0.5641	0.1658	1.9189	
	Age (OR)		0.9992	0.9506	1.0501	0.0385
Shedding in saliva (θ_l)	Intercept (probability)		0.9177	0.7155	0.9802	**1**
	Days (OR)**		1	-	-	NA
	Gender (OR)	Female	Ref.			0.0274
		Male	0.4570	0.0434	4.8075	
	Age (OR)		1.0933	0.9439	1.2663	0.0385
Shedding (common slopes)	Days (OR)		1.0321	0.7877	1.3524	0.0151
	Gender (OR)	Female	Ref.			
		Male	0.6325	0.2951	1.3556	0.0239
	Age (OR)		1.0123	0.9790	1.0468	0.0179
Sensitivity (*p*)	Intercept (probability)		0.7851	0.6296	0.8871	1*
	Target (OR)	NS5	Ref.			
		Env	4.0576	2.5742	6.3958	**0.9784**
	Test (OR)	Urine-NS5	Ref.			0.0215
		Serum-Env	2.9070	0.9168	9.2172	

		Serum-NS5	0.7300	0.2464	2.1623	
		Saliva-Env	3.9840	1.1876	13.3651	
		Saliva-NS5	0.7216	0.2434	2.1397	
		Urine-Env	1.5242	0.4198	5.5345	
	Days (OR)		0.7978	0.6747	0.9432	**0.9482**
	Gender (OR)	Female	Ref.			
		Male	0.7328	0.4491	1.1958	0.3270
	Age (OR)		0.9998	0.9802	1.0197	0.1916

CI-low and CI-up, lower and upper limits of the unconditional 95% confidence interval
Weight, sum of Akaike weights over models containing each term
OR, odds ratio
*Included in all models by construction
**Fixed at 1.00

Results

756 RT-PCR assays were ran (378 targeting the Env gene and 378 targeting the NS5 gene) on 372 serum, 148 urine, and 236 saliva specimens from patients with suspected acute-phase ZIKV infection; the results are summarized in **Table 5**.

Table 5. Diagnostic RT-PCR assays run during the study: results by specimen (serum, urine, saliva) and RT-PCR target (Env, NS5)

RT-PCR assays	Serum		Urine		Saliva		Target/total	
	Env	NS5	Env	NS5	Env	NS5	Env	NS5
Run	186	186	74	74	118	118	378	378
Positive	120	87	17	15	85	57	222	159
% positive	64.5	46.8	23.0	20.3	72.0	48.3	58.7	42.1
Total run (positive)	372 (207)		148 (32)		236 (142)		756 (381)	
% positive (95% CI)	55.6 (50.6–60.6)		21.6 (15.8–28.9)		60.2 (53.8–66.2)		50.4 (46.8–54.0)	

Env, envelope gene; NS5, non-structural protein 5 gene
95% CI, score 95% confidence interval limits

Table 6 shows individual-patient ZIKV RNA testing and detection histories. Overall, 99 out of 108 patients (91.7%) tested ZIKV-positive in at least one RT-PCR run.

Table 6. Patterns of Zika virus RNA detection in acute-phase clinical samples: number of RT-PCR assays run and positive in different specimen-RT-PCR target combinations

Serum-Env		Serum-NS5		Urine-Env		Urine-NS5		Saliva-Env		Saliva-NS5		No. patients
Run	+	Run	+	Run	+	Run	+	Run	+	Run	+	
3	3	3	3	1	0	1	0	3	3	3	3	2
3	3	3	3	1	0	1	0	3	3	3	2	1
3	3	3	3	1	0	1	0	3	0	3	0	2
3	3	3	0	1	0	1	0	3	3	3	3	2
3	3	3	0	1	0	1	0	3	3	3	0	1
3	2	3	2	1	0	1	1	3	1	3	0	1
3	2	3	2	1	0	1	0	3	2	3	0	1
3	2	3	1	1	0	1	0	3	3	3	3	1
3	2	3	1	1	0	1	0	3	3	3	0	1
3	1	3	0	1	0	1	0	3	3	3	3	1
3	0	3	0	1	1	1	1	3	1	3	0	1
3	0	3	0	1	0	1	0	3	3	3	3	2
3	0	3	0	1	0	1	0	3	3	3	0	1
3	0	3	0	1	0	1	0	3	2	3	0	1
3	0	3	0	1	0	1	0	3	1	3	0	1
3	0	3	0	1	0	1	0	3	0	3	0	3
1	1	1	1	1	1	1	1	1	1	1	1	2
1	1	1	1	1	1	1	0	1	1	1	1	2
1	1	1	1	1	0	1	1	1	1	1	0	1
1	1	1	1	1	0	1	0	1	1	1	1	8
1	1	1	1	1	0	1	0	1	1	1	0	1
1	1	1	1	1	0	1	0	1	0	1	0	2
1	1	1	0	1	1	1	1	1	1	1	1	3
1	1	1	0	1	1	1	1	1	1	1	0	1
1	1	1	0	1	1	1	0	1	1	1	0	1
1	1	1	0	1	0	1	0	1	1	1	1	6
1	1	1	0	1	0	1	0	1	1	1	0	1
1	0	1	0	1	1	1	1	1	1	1	1	2
1	0	1	0	1	1	1	1	1	1	1	0	1
1	0	1	0	1	1	1	1	1	0	1	1	1
1	0	1	0	1	1	1	0	1	1	1	1	1
1	0	1	0	1	1	1	0	1	1	1	0	1
1	0	1	0	1	1	1	0	1	0	1	0	1
1	0	1	0	1	0	1	1	1	1	1	1	1
1	0	1	0	1	0	1	1	1	1	1	0	1
1	0	1	0	1	0	1	0	1	1	1	1	5
1	0	1	0	1	0	1	0	1	1	1	0	4
1	0	1	0	1	0	1	0	1	0	1	0	6
2	2	2	2	0	-	0	-	0	-	0	-	22
2	2	2	1	0	-	0	-	0	-	0	-	2
2	2	2	0	0	-	0	-	0	-	0	-	3
2	1	2	1	0	-	0	-	0	-	0	-	2
2	1	2	0	0	-	0	-	0	-	0	-	3
2	0	2	1	0	-	0	-	0	-	0	-	2

Env, envelope gene; NS5, non-structural protein 5 gene

Run, number of RT-PCR assays run; +, number of assays in which Zika virus RNA was detected

Note that only serum samples were available for 34 patients (last six rows of the Table, with dashes indicating 'test not run'); hierarchical occupancy models accommodate such missing observations, which simply do not contribute to the likelihood (see refs. 40,46)

When we analyzed patient gender and age by exploratory analyzes, we suggested that neither patient nor RT-PCR assay positivity were correlated with these covariates.

Out of 74 patients tested with more than a single sample type, five were found positive in serum only, one in urine only, 14 in saliva only, 25 in serum and saliva but not in urine, nine in urine and saliva but not in serum, and 11 in all three fluids; none was found positive in serum and urine **(Fig 2)**.

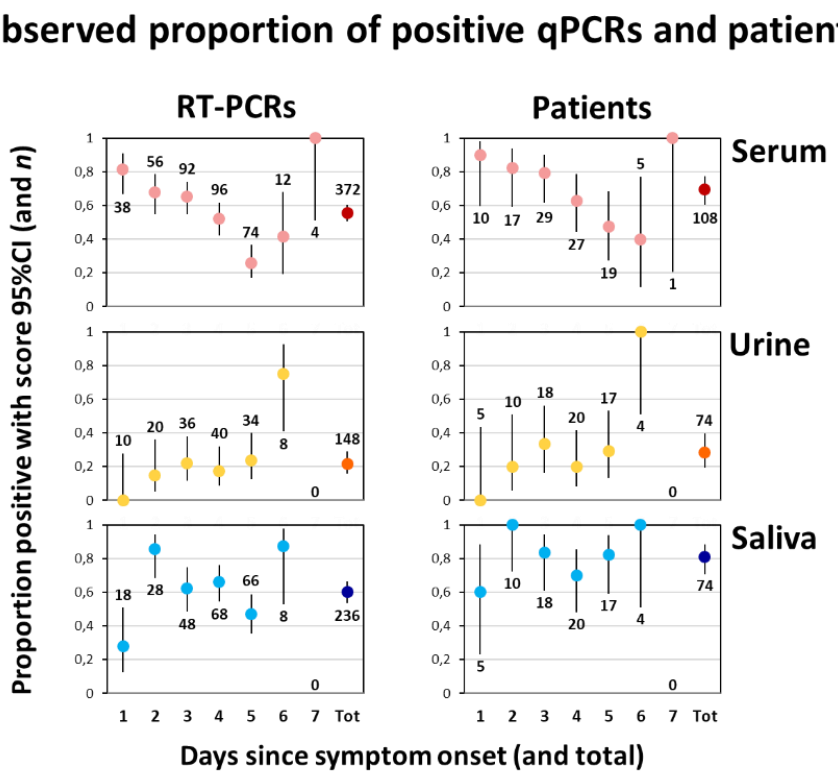

Figure 2. Proportion of positive qPCRs and patients with score 95%CI (and n)

316 Regarding the *Sensitivity (p)* which is defined by the probability of detecting
317 Zika virus RNA in a specimen from an infected patient using two different RT-
318 qPCR assays (Env and NS5 gene), we checked that the samples tested by RT-
319 qPCR assays described by Lanciotti (2008) - gene Env - were more efficient to
320 detecting Zika virus RNA independent at the time of sampling or bodily fluid
321 sampled **(Fig 3).** We also observed a higher viral load (i.e. a global lower Ct) in
322 saliva when compared to serum and urine.

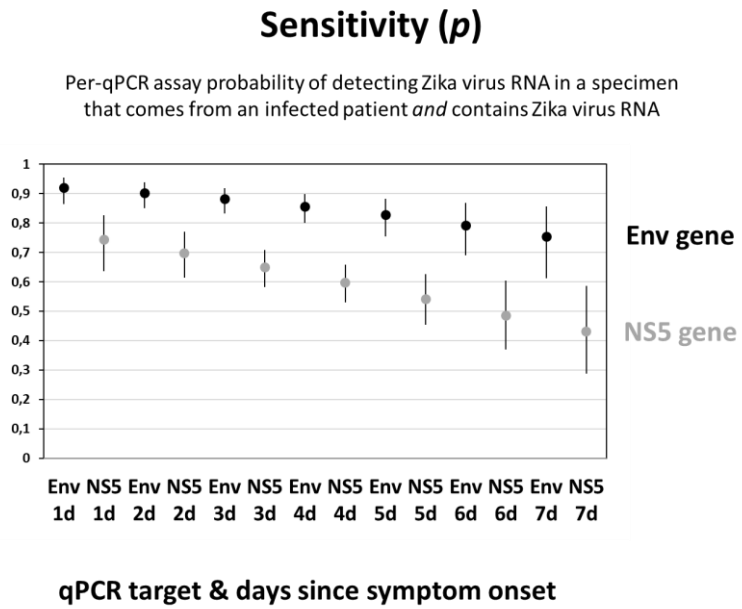

323

324 **Figure 3.** Probability of detecting Zika virus RNA in a specimen that comes from an
325 infected patient using two differents RT-qPCR assays.

326

327 Besides that, we found some evidence suggesting that patient and RT-
328 PCR positivity varied with days since symptom onset for serum (decreasing
329 trend) and urine (increasing trend), but not for saliva samples **(Fig 4).**

330

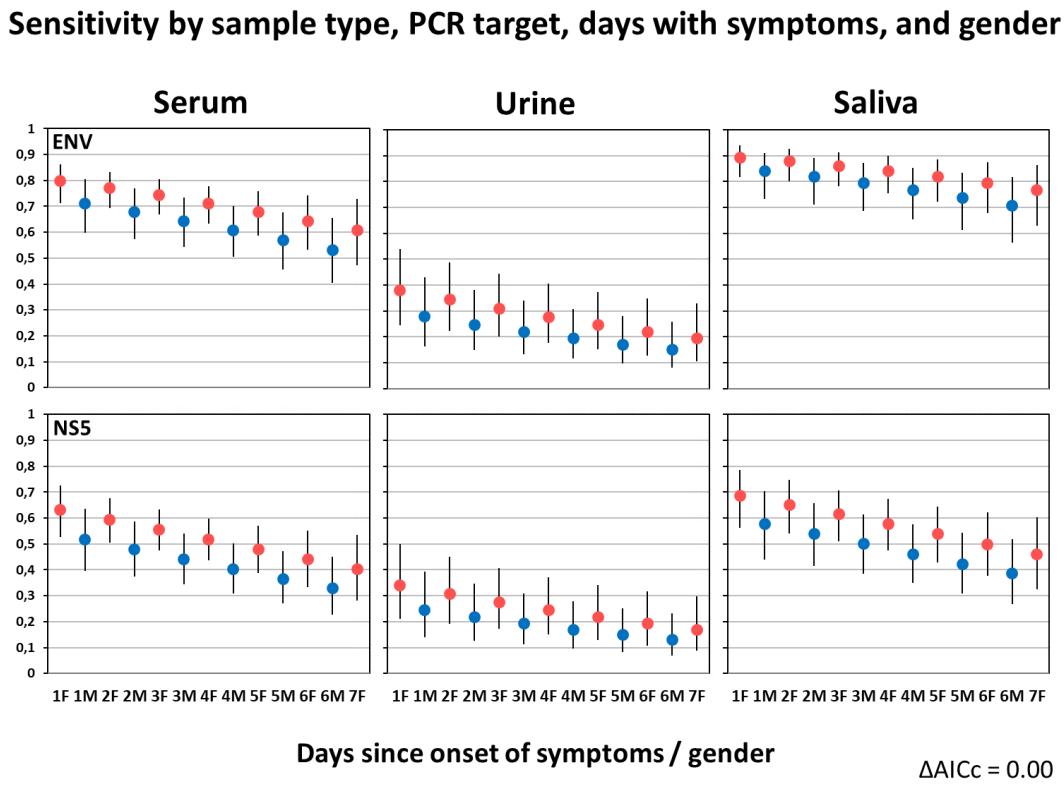

Figure 4. Sensitivity by sample type, PCR target, days with symptoms and gender.

Figure 5 shows the *shedding* results that it is defined by the probability that a specimen from an infected patient contains ZIKV RNA. The results suggest that the *shedding* is higher in saliva.

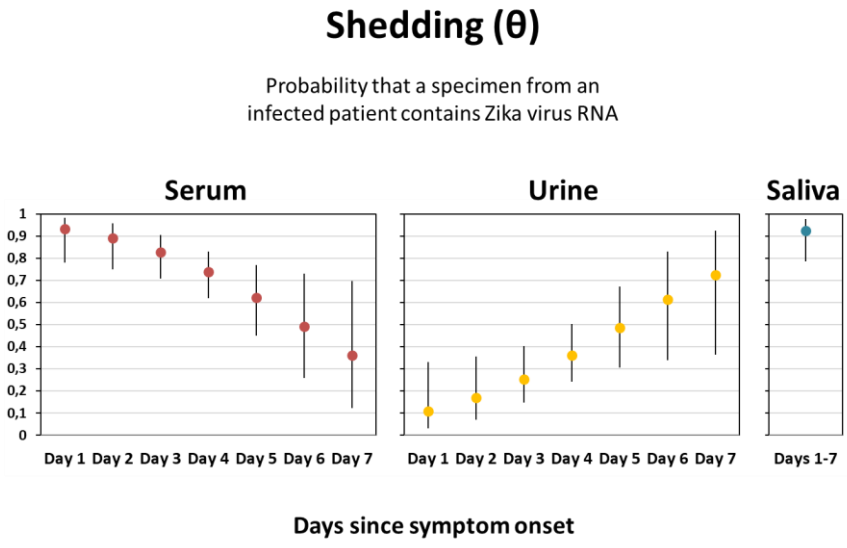

Figure 5 - Results of the *shedding* (probability that a specimen from an infected patient contains ZIKV RNA).

The probability (p) of detection in an infected patient is represented in **Figure 6** where we can also observe that the detection in the saliva is greater when compared to other fluids and the probability also increases when we use gene Env.

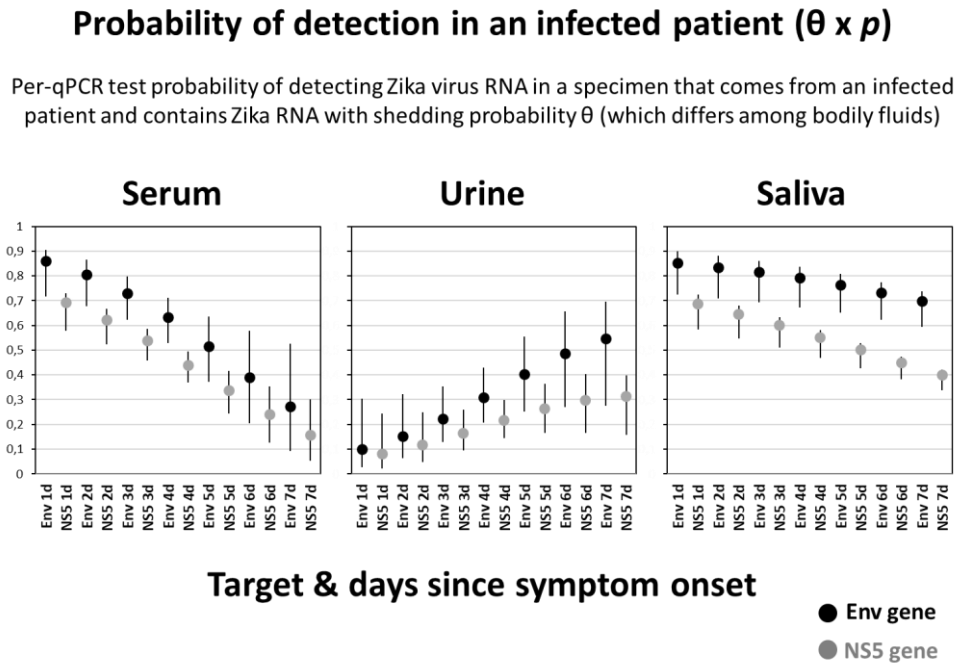

Figure 6 - Per-qPCR test probability of detecting Zika virus RNA in a specimen that comes from an infected patient and contains Zika RNA with shedding probability θ (which differs among bodily fluids)

In **Figure 7** we used our three-level hierarchy models considering Ψ (infected patients probability), θ (shedding probability) and *p* (detection probability).

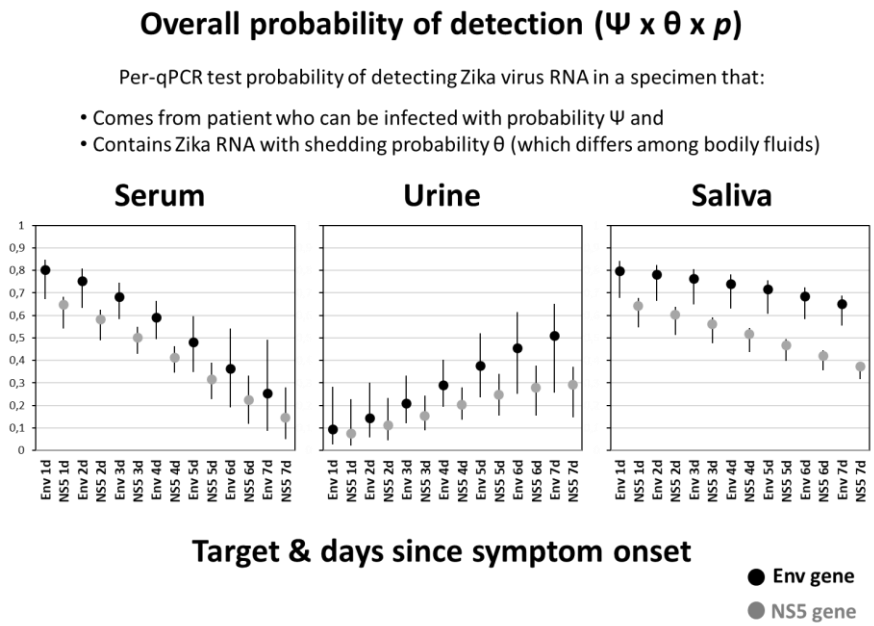

356

357 **Figure 7 -** Per-qPCR test probability of detecting Zika virus RNA in a specimen that comes from
358 patient who can be infected with probability Ψ and contains Zika RNA with shedding probability
359 θ (which differs among bodily fluids).

360

361 Ten models in the set of 50 candidate models were <6.0 AICc units from
362 M_{top} (**Table 7** and **S1 Figure**). Three of them had extra covariates on *p*: *gender*
363 or on θ (*gender*, with $\beta_{\theta(male)} = -0.535 \pm 0.308$ SE; or *age*, with $\beta_{\theta(age)} = 0.012 \pm$
364 0.017 SE). Since none of these estimates was distinguishable from zero at the
365 95% level, and since the deviance of these three models was <2.0 units smaller
366 than that of M_{top} (**S1 Figure**), we regarded these parameters as uninformative. In
367 what follows, hence, we emphasise the results from the M_{top} model (Arnold 2010;
368 Burnham & Anderson 2002).

369

370

Discussion

According to World Health Organization (WHO), currently, there is no standardization of NAT-based assays for the detection of ZIKV RNA (Baylis et al, 2016). Therefore, the purpose of the current study was to evaluate three different biological specimens (serum, urine and saliva) collected at the same day, from the same patients, to check the probability of detecting ZIKV RNA in the specimens, during the acute phase of the illness.

The most interesting finding of the present study is that the detection of ZIKV RNA in saliva was much more sensitive than observed in urine or serum, regardless the RT-qPCR protocol used or the statistical model evaluated. The idea of using saliva as a specimen for diagnostic methods was reported in the 1970s (Dawes, 1974). Dawes (1974) suggested that this approach could be relevant and feasible because of the ease of collecting and the richness of biological compounds present in this specimen. Once saliva has a straightforward and non-invasive collection; easiest storage and low-cost handling when compared to blood collection, it has aroused a particular interest for its use in laboratory diagnostics of several diseases.

The possibility to detect systemic pathologies in saliva samples has been demonstrated for several diseases, including non-infectious illness like cancer (Kaur et al, 2018), metabolic syndrome (Dezayee & Al-Nimer, 2016), diabetes (Gupta et al, 2017), cardiovascular diseases (Abdul Rehman et al, 2017), as well as infectious diseases like tuberculosis (Namuganga et al, 2017), leprosy (Abdalla et al, 2010), HIV (Rakesh et al, 2016) and viral hepatitis (Portilho et al, 2018). Besides, there are scientific reports of the detection of flavivirus infection

through the collection and testing of saliva for dengue (Andries et al, 2015), chikungunya virus (Musso et al, 2016) and Zika (Musso et al, 2015).

Musso et al (2015) recommend to collect both blood and saliva samples to increase the sensitivity of molecular detection of ZIKV and urine sample can be associated at the late stages of the disease. Our findings emphasize these results. However, note that we obtained a patient who was in the acute phase of the disease and showed only positive urine sample showing that the simultaneous collection of several fluids increases the sensitivity. But, when comparing fluids, we can say that saliva is the one with the greatest sensitivity and can be used as the first choice of collection. Supported by these results, recent studies have been using saliva as the fluid of choice for the development of new rapid and reliable diagnostic techniques for ZIKV detection (Song et al, 2016; Sabalza et al, 2018)

Bingham et al (2016) found a different result when evaluating serum, saliva and urine samples for ZIKV RNA detection and suggested that urine may be the preferred type of sample to identify the acute Zika virus disease. This report also demonstrated that saliva specimens can also yield a higher rate of RNA detection than serum even during the first 5 days and the detection rate in saliva also approaches the detection rate in urine. However, no cases were identified through saliva testing alone. in a recent study on the dynamics of Zika virus in body fluids in a non-endemic area did not detect positive results in patients' saliva even when they were positive in other fluids (Sánchez-Montalvá et al, 2018). Particular variables of each experiment might explain this disparity, including distinguished efficiencies in the performance of viral RNA extraction, or RT-qPCR amplification in different protocols. Hence, further research on the current topic

420 are recommended and should be encouraged to improve Zika virus laboratory
421 diagnosis.

422 The results of the present study evaluate the previous results of other
423 studies (Musso et al, 2015; Bingham et al, 2016), where there were contradictions
424 in the results found. However, our model of viral exclusion contributes to support
425 the discovery of Musso et al (2015), which also observed a greater sensitivity of
426 detection for ZIKV RNA in saliva. Ours results suggest that the collection of saliva
427 alone should be considered for the diagnosis of the Zika vírus in the acute phase
428 of the disease.

429 Once Zika infection may be unapparent or present mild symptoms, it is not
430 unexpected that some patients may not precisely determinate the date of the
431 initial symptoms. Thus, including distinct approaches (i.e. including different
432 specimens, with different shedding kinetics for testing) may be of particular
433 interest to confirm Zika infection, notably for patients at higher risk, such as
434 pregnant women, who cares closer monitoring due to fetuses' risk.

435 There has been growing interest in the use of saliva as a means of
436 diagnosing diseases and this interest increases as we observe the reliability,
437 sensitivity and specificity of the results obtained with this fluid. In this work, we
438 collect saliva after stimulating its production. We believe that this approach may
439 contribute to a greater leakage of viral particles, thus allowing greater sensitivity
440 in comparison to oral swabs, but this hypothesis should be clarified.

441 Another important point is about the use of two different RT-qPCR assays
442 (Env and NS5 gene). As shown in the results, the gene Env protocol was shown
443 to be more sensitive independent of the time of collection or the type of sample
444 analysed. However, we had five patients positive only in the gene NS5 protocol,

being four samples of serum and one of saliva. These results, leads us to believe that the sensitivity of detecting Zika virus RNA is greater when we use more than one RT-qPCR assay.

It was beyond the scope of this study to understanding what factors affect ZIKV RNA detection through RT-PCR in acute-phase patients. For that, we hypothesized that the detection of ZIKV RNA depended on shedding effect hypothesis or the false-negative effect hypothesis. The findings of this study strongly suggest that the adoption of saliva testing improves the sensitivity the molecular diagnosis of Zika, increasing the number of laboratory confirmed cases. Regarding the use of different RT-qPCR tests, it can be stated that sensitivity increases when we use more than one protocol.

BIBLIOGRAFIA

Abad-Franch F, Valença-Barbosa C, Sarquis O, Lima MM 2014. All That Glisters Is Not Gold: Sampling-Process Uncertainty in Disease-Vector Surveys with False- Negative and False-Positive Detections.

Abdalla LF, Hugo J, Santos A, Souza C, Collado C, Graça M Da, Cunha S, Gomes Naveca F 2010. Mycobacterium leprae in the periodontium, saliva and skin smears of leprosy patients. *Rev. odonto ciênc. Rev. odonto ciênc* 2525.

Abdul Rehman S, Khurshid Z, Hussain Niazi F, Naseem M, Waddani H Al, Sahibzada H, Sannam Khan R 2017. Role of Salivary Biomarkers in Detection of Cardiovascular Diseases (CVD). *Proteomes* 5: 21.

Andries AC, Duong V, Ly S, Cappelle J, Kim KS, Lorn Try P, Ros S, Ong S, Huy R, Horwood P, Flamand M, Sakuntabhai A, Tarantola A, Buchy P

2015. Value of Routine Dengue Diagnostic Tests in Urine and Saliva Specimens. *PLoS Negl. Trop. Dis.* 9.

Arnold TW 2010. Uninformative Parameters and Model Selection Using Akaike's Information Criterion. *Source J. Wildl. Manag.* 74: 1175–1178.

Baylis SA, Hanschmann K-MO, Schnierle BS, Trösemeier J-H, Blümel J 2016. Collaborative Study to Evaluate a Candidate World rganization International Standard for Zika Virus for Nucleic Acid Amplification Technique (NAT)-Based AssaysHealth O. *WHO*.

Bingham AM, Cone M, Mock V, Heberlein-Larson L, Stanek D, Blackmore C, Likos A 2016. Comparison of Test Results for Zika Virus RNA in Urine, Serum, and Saliva Specimens from Persons with Travel-Associated Zika Virus Disease — Florida, 2016. *MMWR. Morb. Mortal. Wkly. Rep.* 65: 475–478.

Burnham KP, Anderson DR 2002. *Model Selection and Multimodel Inference: A Practical Information-Theoretic Approach (2nd ed)*.

Charrel RN, Leparc-Goffart I, Pas S, Lamballerie X de, Koopmans M, Reusken C 2016. Background review for diagnostic test development for Zika virus infection. *Bull. World Health Organ.* 94: 574–584D.

Corman VM, Rasche A, Baronti C, Aldabbagh S, Cadar D, Reusken CBEM, Pas SD, Goorhuis A, Schinkel J, Molenkamp R, Kuemmerer BM, Bleicker T, Brünink S, Eschbach-Bludau M, Eis-Hübinger AM, Koopmans MP, Schmidt-Chanasit J, Grobusch MP, Lamballerie X de, Drosten C, Drexler JF 2016. Clinical comparison, standardization and optimization of Zika virus molecular detection. *Bull. World Health Organ.*

Dawes C 1974. The effects of flow rate and duration of stimulation on the

concentrations of protein and the main electrolytes in human submandibular saliva. *Arch. Oral Biol.* 19: 887–895.

Dezayee ZMI, Al-Nimer MSM 2016. Saliva C-reactive protein as a biomarker of metabolic syndrome in diabetic patients. *Indian J. Dent. Res.* 27: 388–391.

Elmore SA, Huyvaert KP, Bailey LL, Iqbal A, Su C, Dixon BR, Alisauskas RT, Gajadhar AA, Jenkins EJ 2016. Multi-scale occupancy approach to estimate Toxoplasma gondii prevalence and detection probability in tissues: an application and guide for field sampling. *Int. J. Parasitol.* 46: 563–570.

Felipe Schmidt R, por E, Bianchini Fernandes S, por Rubrica Data Cristine Ferreira A, Scarduelli Luciano K 2017. Sistema Único de Saúde Estado de Santa Catarina Secretaria de Estado da Saúde Superintendência de Vigilância em Saúde Laboratório Central de Saúde Pública Página 1/74 MANUAL MANUAL DE ORIENTAÇÃO PARA COLETA, ACONDICIONAMENTO E TRANSPORTE DE AMOSTRAS BIOLÓGICAS.

Froeschl G, Huber K, Sonnenburg F von, Nothdurft HD, Bretzel G, Hoelscher M, Zoeller L, Trottmann M, Pan-Montojo F, Dobler G, Woelfel S 2017. Long-term kinetics of Zika virus RNA and antibodies in body fluids of a vasectomized traveller returning from Martinique: A case report. *BMC Infect. Dis.* 17: 1–9.

Grischott F, Puhan M, Hatz C, Schlagenhauf P 2016. Non-vector-borne transmission of Zika virus: A systematic review. *Travel Med. Infect. Dis.* 14: 313–330.

Gupta S, Nayak MT, Sunitha JD, Dawar G, Sinha N, Rallan NS 2017. Correlation of salivary glucose level with blood glucose level in diabetes

mellitus. *J. Oral Maxillofac. Pathol.* 21: 334–339.

Kaur J, Jacobs R, Huang Y, Salvo N, Politis C 2018. Salivary biomarkers for oral cancer and pre-cancer screening: a review. *Clin. Oral Investig.* 22: 633–640.

Kodati S, Palmore TN, Spellman FA, Cunningham MEd D, Weistrop BB, Nida Sen H 2017. Bilateral posterior uveitis associated with Zika virus infection. *www.thelancet.com* 389.

Krauer F, Riesen M, Reveiz L, Oladapo OT, Martínez-Vega R, Porgo T V., Haefliger A, Broutet NJ, Low N 2017. Zika Virus Infection as a Cause of Congenital Brain Abnormalities and Guillain–Barré Syndrome: Systematic Review. *PLoS Med.* 14: 1–27.

Lachish S, Gopalaswamy AM, Knowles SCL, Sheldon BC 2012. Site-occupancy modelling as a novel framework for assessing test sensitivity and estimating wildlife disease prevalence from imperfect diagnostic tests. *Methods Ecol. Evol.* 3: 339–348.

Lanciotti RS, Kosoy OL, Laven JJ, Velez JO, Lambert AJ, Johnson AJ, Stanfield SM, Duffy MR 2008. Genetic and serologic properties of Zika virus associated with an epidemic, Yap State, Micronesia, 2007. *Emerg. Infect. Dis.* 14: 1232–1239.

Leal WS 2016. Zika mosquito vectors: the jury is still out. *F1000Research* 5: 2546.

Lustig Y, Mendelson E, Paran N, Melamed S, Schwartz E 2016. Detection of Zika virus RNA in whole blood of imported Zika virus disease cases up to 2 months after symptom onset, Israel, December 2015 to April 2016. *Eurosurveillance* 21: 1–4.

MacKenzie DI, Bailey LL 2004. Assessing the fit of site-occupancy models. *J. Agric. Biol. Environ. Stat.* 9: 300–318.

McClintock BT, Nichols JD, Bailey LL, MacKenzie DI, Kendall WL, Franklin AB 2010. Seeking a second opinion: uncertainty in disease ecology. *Ecol. Lett.* 13: 659–674.

Musso D, Nhan T, Robin E, Roche C, Bierlaire D, Zisou K, Shan Yan A, Cao-Lormeau VM, Broult J 2014. Potential for Zika virus transmission through blood transfusion demonstrated during an outbreak in French Polynesia, November 2013 to February 2014. *Eurosurveillance* 19.

Musso D, Roche C, Nhan TX, Robin E, Teissier A, Cao-Lormeau VM 2015. Detection of Zika virus in saliva. *J. Clin. Virol.* 68: 53–55.

Musso D, Teissier A, Rouault E, Teururai S, Pina JJ De, Nhan TX 2016. Detection of chikungunya virus in saliva and urine. *Virol. J.* 13.

Namuganga AR, Chegou NN, Mubiri P, Walzl G, Mayanja-Kizza H 2017. Suitability of saliva for Tuberculosis diagnosis: Comparing with serum. *BMC Infect. Dis.* 17.

Nicastri E, Castilletti C, Balestra P, Galgani S, Ippolito G 2016. Zika Virus Infection in the Central Nervous System and Female Genital Tract. *Emerg Infect Dis* 22: 2228–2230.

Nichols JD, Thomas L, Conn PB 2009. *Modeling Demographic Processes In Marked Populations*.

Petersen LR, Jamieson DJ, Powers AM, Honein MA 2016. Zika Virus. *N. Engl. J. Med.* 374: 1552–1563.

Portilho MM, Cancella Nabuco L, Villela-Nogueira CA, Brandão-Mello CE, Pilotto JH, Flores GL, Lewis-Ximenez LL, Lampe E, Melo Villar L 2018.

570 Detection of occult hepatitis B in serum and oral fluid samples. *Mem Inst*
571 *Oswaldo Cruz Rio Janeiro* 113: 62–65.
572 Prisant N, Bujan L, Benichou H, Hayot PH, Pavili L, Lurel S, Herrmann C, Janky
573 E, Joguet G 2016. Zika virus in the female genital tract. *Lancet Infect. Dis.*
574 16: 1000–1001.
575 Rakesh N, Shetty S, Sujatha S, Sharma S, Saxena A 2016. Assessment of the
576 Accuracy of Whole Blood/Serum Rapid Point-of-Care HIV Three Dot Test
577 for Oral Fluid Specimens. *Curr. HIV Res.* 14: 354–359.
578 Rozé B, Najioullah F, Signate A, Apetse K, Brouste Y, Gourgoudou S, Fagour
579 L, Abel S, Hochedez P, Cesaire R, Cabié A 2016. Zika virus detection in
580 cerebrospinal fluid from two patients with encephalopathy, Martinique,
581 February 2016. *Euro Surveill. Bull. Eur. sur les Mal. Transm. = Eur.*
582 *Commun. Dis. Bull.* 21: 1–4.
583 Sabalza M, Yasmin R, Barber CA, Castro T, Malamud D, Kim BJ, Zhu H,
584 Montagna RA, Abrams WR 2018. Detection of Zika virus using reverse-
585 transcription LAMP coupled with reverse dot blot analysis in saliva. *PLoS*
586 *One* 13: e0192398.
587 Sánchez-Montalvá A, Pou D, Sulleiro E, Salvador F, Bocanegra C, Treviño B,
588 Rando A, Serre N, Pumarola T, Almirante B, Molina I 2018. Zika virus
589 dynamics in body fluids and risk of sexual transmission in a non-endemic
590 area. *Trop. Med. Int. Heal.* 23: 92–100.
591 Song J, Mauk MG, Hackett BA, Cherry S, Bau HH, Liu C 2016. Instrument-Free
592 Point-of-Care Molecular Detection of Zika Virus. *Anal. Chem.* 88: 7289–
593 7294.
594 Sun J, Wu D, Zhong H, Guan D, Zhang H, Tan Q, Ke C 2016. Presence of Zika

595 virus in conjunctival fluid. *JAMA Ophthalmol.* 134: 1330–1332.
596 Waggoner JJ, Pinsky BA 2016. Zika virus: Diagnostics for an emerging
597 pandemic threat. *J. Clin. Microbiol.* 54: 860–867.
598 WHO 2017. Who Situation Report - Zika Virus. 2007: 1–6.
599 Zanluca C, Campos Andrade De Melo V, Luiza A, Mosimann P, Viana GI,
600 Santos D, Duarte CN, Luz K 2015. First report of autochthonous
601 transmission of Zika virus in Brazil. *Mem Inst Oswaldo Cruz Rio Janeiro*
602 110: 569–572.
603

Table S1. Key parameters involved in the process of Zika virus RNA detection by RT-PCR: a multilevel perspective

Parameter	Definition (*interpretation*)	Level
Ψ	Probability of Zika virus RNA presence (*infection*)	Patient
θ	Probability of Zika virus RNA presence in a sample, given patient infection (*shedding*)	Bodily fluid sample
p	Probability of detecting Zika virus RNA through RT-PCR, given infection and shedding (*sensitivity*)	RT-PCR assay (reaction)

Text. S1. Exploratory Analyses - Details on the modeling strategy

To avoid fitting hundreds of models, we heuristically began by fitting the 'null' models

$\Psi(.), \theta(.), p(.)$

$\Psi(.), \theta_{serum}(.), \theta_{urine}(.), \theta_{saliva}(.), p(.)$

Second, we fitted the model representing our focal hypothesis of fluid-specific shedding and test-specific sensitivity:

$\Psi(.), \theta_{serum}(.), \theta_{urine}(.), \theta_{saliva}(.), p(test)$

and alternative confounder structures on p

$\Psi(.), \theta_{serum}(.), \theta_{urine}(.), \theta_{saliva}(.), p(test + days)$

$\Psi(.), \theta_{serum}(.), \theta_{urine}(.), \theta_{saliva}(.), p(test + gender)$

$\Psi(.), \theta_{serum}(.), \theta_{urine}(.), \theta_{saliva}(.), p(test + age)$

$\Psi(.), \theta_{serum}(.), \theta_{urine}(.), \theta_{saliva}(.), p(test + days + gender)$

$\Psi(.), \theta_{serum}(.), \theta_{urine}(.), \theta_{saliva}(.), p(test + days + age)$

$\Psi(.), \theta_{serum}(.), \theta_{urine}(.), \theta_{saliva}(.), p(test + gender + age)$

$\Psi(.), \theta_{serum}(.), \theta_{urine}(.), \theta_{saliva}(.), p(test + days + gender + age)$

Third, we tested alternatives on *p* including confounders

$\Psi(.), \theta_{serum}(.), \theta_{urine}(.), \theta_{saliva}(.), p(target)$

$\Psi(.), \theta_{serum}(.), \theta_{urine}(.), \theta_{saliva}(.), p(target + days)$

$\Psi(.), \theta_{serum}(.), \theta_{urine}(.), \theta_{saliva}(.), p(target + gender)$

$\Psi(.), \theta_{serum}(.), \theta_{urine}(.), \theta_{saliva}(.), p(target + age)$

$\Psi(.), \theta_{serum}(.), \theta_{urine}(.), \theta_{saliva}(.), p(target + days + gender)$

$\Psi(.), \theta_{serum}(.), \theta_{urine}(.), \theta_{saliva}(.), p(target + days + age)$

$\Psi(.), \theta_{serum}(.), \theta_{urine}(.), \theta_{saliva}(.), p(target + gender + age)$

$\Psi(.), \theta_{serum}(.), \theta_{urine}(.), \theta_{saliva}(.), p(target + days + gender + age)$

$\Psi(.), \theta_{serum}(.), \theta_{urine}(.), \theta_{saliva}(.), p(fluid)$

$\Psi(.), \theta_{serum}(.), \theta_{urine}(.), \theta_{saliva}(.), p(fluid + days)$

$\Psi(.), \theta_{serum}(.), \theta_{urine}(.), \theta_{saliva}(.), p(fluid + gender)$

$\Psi(.), \theta_{serum}(.), \theta_{urine}(.), \theta_{saliva}(.), p(fluid + age)$

$\Psi(.), \theta_{serum}(.), \theta_{urine}(.), \theta_{saliva}(.), p(fluid + days + gender)$

$\Psi(.), \theta_{serum}(.), \theta_{urine}(.), \theta_{saliva}(.), p(fluid + days + age)$

$\Psi(.), \theta_{serum}(.), \theta_{urine}(.), \theta_{saliva}(.), p(fluid + gender + age)$

$\Psi(.), \theta_{serum}(.), \theta_{urine}(.), \theta_{saliva}(.), p(fluid + days + gender + age)$

This procedure identified this model as the best-performing (lowest-AICc: 785.36):

$\Psi(.), \theta_{serum}(.), \theta_{urine}(.), \theta_{saliva}(.), p(target + days)$

We then used this model to test alternatives on θ:

$\Psi(.), \theta_{common}(.), p(target + days)$ [common intercept]

$\Psi(.), [\theta_{serum}(.), \theta_{urine}(.), \theta_{saliva}(.)] + [days], p(target + days)$ [common slope]

$\Psi(.)$, $[\theta_{serum}(.), \theta_{urine}(.), \theta_{saliva}(.)] + [gender]$, $p(target + days)$ [common slope]

$\Psi(.)$, $[\theta_{serum}(.), \theta_{urine}(.), \theta_{saliva}(.)] + [age]$, $p(target + days)$ [common slope]

$\Psi(.)$, $[\theta_{serum}(.), \theta_{urine}(.), \theta_{saliva}(.)] + [days + gender]$, $p(target + days)$ [common slopes]

$\Psi(.)$, $[\theta_{serum}(.), \theta_{urine}(.), \theta_{saliva}(.)] + [days + age]$, $p(target + days)$ [common slopes]

$\Psi(.)$, $[\theta_{serum}(.), \theta_{urine}(.), \theta_{saliva}(.)] + [gender + age]$, $p(target + days)$ [common slopes]

$\Psi(.)$, $[\theta_{serum}(.), \theta_{urine}(.), \theta_{saliva}(.)] + [days + gender + age]$, $p(target + days)$ [common slopes]

$\Psi(.)$, $\theta_{serum}(days)$, $\theta_{urine}(days)$, $\theta_{saliva}(.)$, $p(target + days)$ [fluid-specific intercepts and slopes]

$\Psi(.)$, $\theta_{serum}(gender)$, $\theta_{urine}(gender)$, $\theta_{saliva}(gender)$, $p(target + days)$ [fluid-specific intercepts and slopes]

$\Psi(.)$, $\theta_{serum}(age)$, $\theta_{urine}(age)$, $\theta_{saliva}(age)$, $p(target + days)$ [fluid-specific intercepts and slopes]

$\Psi(.)$, $\theta_{serum}(days + gender)$, $\theta_{urine}(days + gender)$, $\theta_{saliva}(gender)$, $p(target + days)$ [fluid-specific intercepts and slopes]

$\Psi(.)$, $\theta_{serum}(days + age)$, $\theta_{urine}(days + age)$, $\theta_{saliva}(age)$, $p(target + days)$ [fluid-specific intercepts and slopes]

$\Psi(.)$, $\theta_{serum}(gender + age)$, $\theta_{urine}(gender + age)$, $\theta_{saliva}(gender + age)$, $p(target + days)$ [fluid-specific intercepts and slopes]

$\Psi(.)$, $\theta_{serum}(days + gender + age)$, $\theta_{urine}(days + gender + age)$, $\theta_{saliva}(gender + age)$, $p(target + days)$ [fluid-specific intercepts and slopes]

We then identified the best-performing model (AICc = 779.61) in the model set above, which was

$\Psi(.)$, $\theta_{serum}(days)$, $\theta_{urine}(days)$, $\theta_{saliva}(.)$, $p(target + days)$

and tested alternative *p* structures on this model:

$\Psi(.)$, $\theta_{serum}(days)$, $\theta_{urine}(days)$, $\theta_{saliva}(.)$, $p(target + days + gender)$

$\Psi(.)$, $\theta_{serum}(days)$, $\theta_{urine}(days)$, $\theta_{saliva}(.)$, $p(target + days + age)$

$\Psi(.)$, $\theta_{serum}(days)$, $\theta_{urine}(days)$, $\theta_{saliva}(.)$, $p(target + days + gender + age)$

including more parsimonious models:

$\Psi(.)$, $\theta_{serum}(days)$, $\theta_{urine}(days)$, $\theta_{saliva}(.)$, $p(target)$

$\Psi(.)$, $\theta_{serum}(days)$, $\theta_{urine}(days)$, $\theta_{saliva}(.)$, $p(days)$

and alternatives on *p* with either fluid or test

$\Psi(.)$, $\theta_{serum}(days)$, $\theta_{urine}(days)$, $\theta_{saliva}(.)$, $p(fluid)$

$\Psi(.)$, $\theta_{serum}(days)$, $\theta_{urine}(days)$, $\theta_{saliva}(.)$, $p(fluid + days)$

$\Psi(.)$, $\theta_{serum}(days)$, $\theta_{urine}(days)$, $\theta_{saliva}(.)$, $p(fluid + gender)$

$\Psi(.)$, $\theta_{serum}(days)$, $\theta_{urine}(days)$, $\theta_{saliva}(.)$, $p(fluid + age)$

$\Psi(.)$, $\theta_{serum}(days)$, $\theta_{urine}(days)$, $\theta_{saliva}(.)$, $p(fluid + days + gender)$

$\Psi(.)$, $\theta_{serum}(days)$, $\theta_{urine}(days)$, $\theta_{saliva}(.)$, $p(fluid + days + age)$

$\Psi(.)$, $\theta_{serum}(days)$, $\theta_{urine}(days)$, $\theta_{saliva}(.)$, $p(fluid + gender + age)$

$\Psi(.)$, $\theta_{serum}(days)$, $\theta_{urine}(days)$, $\theta_{saliva}(.)$, $p(fluid + days + gender + age)$

$\Psi(.)$, $\theta_{serum}(days)$, $\theta_{urine}(days)$, $\theta_{saliva}(.)$, $p(test)$

$\Psi(.)$, $\theta_{serum}(days)$, $\theta_{urine}(days)$, $\theta_{saliva}(.)$, $p(test + days)$

$\Psi(.)$, $\theta_{serum}(days)$, $\theta_{urine}(days)$, $\theta_{saliva}(.)$, $p(test + gender)$

$\Psi(.)$, $\theta_{serum}(days)$, $\theta_{urine}(days)$, $\theta_{saliva}(.)$, $p(test + age)$

$\Psi(.)$, $\theta_{serum}(days)$, $\theta_{urine}(days)$, $\theta_{saliva}(.)$, $p(test + days + gender)$

$\Psi(.)$, $\theta_{serum}(days)$, $\theta_{urine}(days)$, $\theta_{saliva}(.)$, $p(test + days + age)$

$\Psi(.)$, $\theta_{serum}(days)$, $\theta_{urine}(days)$, $\theta_{saliva}(.)$, $p(test + gender + age)$

$\Psi(.)$, $\theta_{serum}(days)$, $\theta_{urine}(days)$, $\theta_{saliva}(.)$, $p(test + days + gender + age)$

The final, whole model-set comparison selected

$\Psi(.)$, $\theta_{serum}(days)$, $\theta_{urine}(days)$, $\theta_{saliva}(.)$, $p(target + days)$

as the best-performing model.

We also tested a few model with fixed parameter values, namely

$\Psi(.)$, $\theta = 1.0$, $p(.)$

$\Psi(.)$, $\theta = 1.0$, $p(target + days)$

$\Psi(.)$, $\theta_{serum}(days)$, $\theta_{urine}(days)$, $\theta_{saliva}(.)$, $p = 1.0$

for a total of 65 models in the full model set...

Table S2. Patterns of Zika virus RNA detection in acute-phase clinical samples: number of RT-qPCR assays run and positive in different specimen-RT-qPCR target combinations

Serum-ENV		Serum-NS5		Urine-ENV		Urine-NS5		Saliva-ENV		Saliva-NS5		No. patients
Run	+	Run	+	Run	+	Run	+	Run	+	Run	+	
3	3	3	3	1	0	1	0	3	3	3	3	2
3	3	3	3	1	0	1	0	3	3	3	2	1
3	3	3	3	1	0	1	0	3	0	3	0	2
3	3	3	0	1	0	1	0	3	3	3	3	2
3	3	3	0	1	0	1	0	3	3	3	0	1
3	2	3	2	1	0	1	1	3	1	3	0	1
3	2	3	2	1	0	1	0	3	2	3	0	1
3	2	3	1	1	0	1	0	3	3	3	3	1
3	2	3	1	1	0	1	0	3	3	3	0	1
3	1	3	0	1	0	1	0	3	3	3	3	1
3	0	3	0	1	1	1	1	3	1	3	0	1
3	0	3	0	1	0	1	0	3	3	3	3	2
3	0	3	0	1	0	1	0	3	3	3	0	1
3	0	3	0	1	0	1	0	3	2	3	0	1

3	0	3	0	1	0	1	0	3	1	3	0	1
3	0	3	0	1	0	1	0	3	0	3	0	3
1	1	1	1	1	1	1	1	1	1	1	1	2
1	1	1	1	1	1	1	0	1	1	1	1	2
1	1	1	1	1	0	1	1	1	1	1	0	1
1	1	1	1	1	0	1	0	1	1	1	1	8
1	1	1	1	1	0	1	0	1	1	1	0	1
1	1	1	1	1	0	1	0	1	0	1	0	2
1	1	1	0	1	1	1	1	1	1	1	1	3
1	1	1	0	1	1	1	1	1	1	1	0	1
1	1	1	0	1	1	1	0	1	1	1	0	1
1	1	1	0	1	0	1	0	1	1	1	1	6
1	1	1	0	1	0	1	0	1	1	1	0	1
1	0	1	0	1	1	1	1	1	1	1	1	2
1	0	1	0	1	1	1	1	1	1	1	0	1
1	0	1	0	1	1	1	1	1	0	1	1	1
1	0	1	0	1	1	1	0	1	1	1	1	1
1	0	1	0	1	1	1	0	1	1	1	0	1
1	0	1	0	1	1	1	0	1	0	1	0	1
1	0	1	0	1	0	1	1	1	1	1	1	1
1	0	1	0	1	0	1	1	1	1	1	0	1
1	0	1	0	1	0	1	0	1	1	1	1	5
1	0	1	0	1	0	1	0	1	1	1	0	4
1	0	1	0	1	0	1	0	1	0	1	0	6
2	2	2	2	0	-	0	-	0	-	0	-	22
2	2	2	1	0	-	0	-	0	-	0	-	2
2	2	2	0	0	-	0	-	0	-	0	-	3
2	1	2	1	0	-	0	-	0	-	0	-	2
2	1	2	0	0	-	0	-	0	-	0	-	3
2	0	2	1	0	-	0	-	0	-	0	-	2

ENV, envelope gene; NS5, non-structural protein 5 gene
Run, number of RT-PCR assays run; +, number of assays in which Zika virus RNA was detected
Note that only serum samples were available for 34 patients (last six rows of the Table, with dashes indicating 'test not run'); hierarchical occupancy models accommodate such missing observations, which simply do not contribute to the likelihood (see refs. 40,46)

Table S3. Constructing the likelihood: two examples of Zika RNA detection histories with their associated probabilities and a short interpretation of each history and term

Detection history* / Term	Interpretation
Pr(000 000 00- 0-- 000 000)	No detection; just two urine-Env and one urine-NS5 tests run
$(1-\Psi)$ +	No infection or
$\Psi(1-\theta_s)(1-\theta_u)(1-\theta_l)$ +	Infection but no RNA shedding or
$\Psi\theta_s(1-p_1)^3(1-p_2)^3(1-\theta_u)(1-\theta_l)$ +	Infection and shedding in serum (but RNA not detected) and no shedding in urine or saliva or
$\Psi\theta_u(1-p_1)^2(1-p_2)(1-\theta_s)(1-\theta_l)$ +	Infection and shedding in urine (but RNA not detected) and no shedding in serum or saliva or
$\Psi\theta_l(1-p_1)^3(1-p_2)^3(1-\theta_s)(1-\theta_u)$ +	Infection and shedding in saliva (but RNA not detected) and no shedding in serum or urine or
$\Psi\theta_s\theta_u\theta_l(1-p_1)^8(1-p_2)^7$	Infection and shedding in all specimens but RNA not detected
Pr(000 000 0-- 0-- 101 000)	Only two detections, both by saliva-Env; just one urine-Env and one urine-NS5 tests run
Ψ ×	Infection and

$[\theta_s(1-p_1)^3(1-p_2)^3 + (1-\theta_s)] \times$	Shedding in serum (but RNA not detected) or no shedding in serum and
$[\theta_u(1-p_1)(1-p_2) + (1-\theta_u)] \times$	Shedding in urine (but RNA not detected) or no shedding in urine and
$[\theta_l(1-p_1)^3(1-p_2)^3]$	Shedding in serum (but RNA not detected)

730 *Of the form 'Pr(aaa bbb ccc ddd eee fff)', with Pr = probability; a = serum-Env; b = serum-NS5; c =
731 urine-Env; d = urineNS5; e = saliva-Env; f = saliva-NS5; '0s' indicate non-detections, '1s' indicate
732 detections, and dashes ('-') indicate that the test was not run
733

734 **Figure S1.** Parameter estimates from the top-ranking model ("top") and from averaging over the
735 whole model set ("avg")

736

737

ANEXO 4

DESENVOLVIMENTO DE MODELO DE REGRESSÃO LOGÍSTICA MÚLTIPLA PARA APOIO AO DIAGNÓSTICO DIFERENCIAL DAS INFECÇÕES SINTOMÁTICAS PELO VÍRUS ZIKA E DENGUE

A circulação concomitante de diferentes arbovírus em território brasileiro demanda novos procedimentos destinados ao diagnóstico diferencial das arboviroses no contexto da vigilância em saúde. Este trabalho teve como objetivo desenvolver um modelo de classificação para apoio ao diagnóstico diferencial da infecção sintomática pelos vírus Zika (ZIKV) e dengue (DENV). Foram utilizados os registros de casos de zika (203) e dengue (288) atendidos no serviço de infectologia de um hospital privado de Manaus, AM, no período de 2014 a 2017. Para confirmação diagnóstica foram considerados resultados positivos para RT-qPCR (ZIKV) e NS1 (DENV). Os casos foram submetidos a um protocolo de investigação clínica e laboratorial. Razões de chances (*odds ratios* – OR) de diagnóstico de zika em relação à dengue, baseadas na presença de sinais e sintomas (exantema maculopapular, febre, prurido, artralgia, edema articular, cefaleia, conjuntivite, mialgia, linfadenopatia, diarreia, náuseas e vômitos) foram estimadas por meio de modelo de regressão logística múltipla. Para a entrada e retenção (*stepwise backward*) das variáveis explicativas no modelo considerou-se a significância estatística da associação de ZIKV com a presença de sinais e sintomas nos níveis de 20% e 5%, respectivamente. A significância estatística foi determinada pelo teste de *Wald* e a qualidade do ajuste do modelo final pela análise de medidas de *deviance*, utilizando-se o programa Stata 12. As idades médias dos casos de zika e dengue corresponderam a 37,4 (±11,4) e 33,6 (±12,4) anos, e as proporções do sexo feminino a 66,0% e 50,4%, respectivamente. Cerca de 66% dos casos de dengue foram diagnosticados em 2014/15 e 100% dos casos de zika em 2016. Em relação à dengue, as chances de diagnóstico de zika foram mais elevadas na presença de conjuntivite (OR=63,8; IC95%: 15,0-270,7), exantema maculopapular (OR=24,7; 6,8-89,5), prurido (OR=12,4; 4,2-37,0) e linfadenopatia (OR=8,0; 1,3-51,1). Quando presentes as quatro manifestações simultaneamente, a probabilidade estimada para o correto diagnóstico de zika foi 0,999. O modelo de regressão logística mostrou-se útil para a classificação de casos de zika em relação à dengue, com base na avaliação clínica realizada por infectologistas. Análises adicionais, baseadas em avaliações clínicas realizadas por profissionais da atenção básica são necessárias antes da decisão sobre o uso de tais modelos em apoio à classificação de casos de arboviroses na vigilância em saúde.

Palavras chave: Vírus Zika, Vigilância Epidemiológica, Infecções por Arbovirus, Diagnóstico Diferencial, Classificação.

Autores:
Ligia Fernandes Abdalla [1,2], João Hugo Abdalla Santos [3,4],Erick Martins e Souza[3], Caroline de Oliveira Pacheco[5], Erick Alan Alaña Wandersleben[5], Valdinete Alves Nascimento[6,7],Dana Cristina da Silva Monteiro [1], Tatiana Amaral Pires de Almeida [8], Matilde del Carmen ContrerasMejía[8], Vanderson de Souza Sampaio [9,10], Antonio José Leal Costa [11], Felipe Gomes Naveca[1,6,7,8]

1 Programa de Pós-Graduação em Imunologia Básica e Aplicada, Universidade Federal doAmazonas, Manaus, Amazonas, Brasil.

2 Universidade do Estado do Amazonas, Manaus, Amazonas,Brasil

3 Universidade Federal do Amazonas, Manaus, Amazonas, Brasil.

4 Hospital Adventista deManaus, Manaus, Amazonas, Brasil.

5 Universidad Adventista del Plata, San Martin, Entre Rios, Argentina.

6 Laboratório de Ecologia de Doenças Transmissíveis naAmazônia, Instituto Leônidas e Maria Diane - Fiocruz Amazônia, Manaus, Amazonas, Brasil.

7 Programa de Pós-Graduação em Biologia Celular e Molecular, Instituto Oswaldo Cruz, Fiocruz, Rio de Janeiro,Brasil.

8 Fundação Oswaldo Cruz-Fiocruz, Instituto Leônidas e Maria Deane, Programa de Pós-Graduação em Biologia da Interação Patógeno- Hospedeiro, Manaus, AM, Brasil

9 Fundação de Vigilância em Saúde do Amazonas, Manaus, AM, Brasil

10 Universidade do Estado do Amazonas, Programa de Pós Graduação Medicina Tropical, Manaus, AM, Brasil

11 Universidade Federal do Rio de Janeiro, Instituto de Estudos em Saúde Coletiva, Programa de Pós Graduação em Saúde Coletiva, Rio de Janeiro, RJ, Brasil

Financiamento: CNPq, Capes, MS-DECIT, FAPEAM.

APÊNDICES

APÊNDICE A - FICHA CLÍNICA

NOTIFICAÇÃO DE CASOS SUSPEITOS DE ZIKA VÍRUS

DEFINIÇÃO DE CASO:

Pacientes que apresentem febre ou ausência de febre, medida ou referida, até 38,5 C e exantema maculo-papular pruriginoso com início em até 48h após os primeiros sintomas, acompanhado de pelo menos **UM** dos seguintes sinais e sintomas:

- ✓ Hiperemia conjutival se secreção ou prurido **OU** Artralgia **OU** Edema periarticular de membros.

INFORMAÇÕES DO SERVIÇO DE SAÚDE

Unidade sentinela:_____

Nome:_____

Data de nascimento:___/___/____ Idade:____ Sexo: Masculino( ) Feminino ( )

Gestante: Sim ( ) Não ( ) Não se aplica ( )

Caso sim: 1º trimestre( ) 2º trimestre( ) 3º trimestre( ) Ignorado( )

Munícipio de residência:_____

Endereço:_____Nº_____Bairro:_____ Complemento:_____

Ponto de Referência_____ Telefone:_____

CARACTERÍSTICAS CLÍNICAS (Seguir a legenda:1-sim/2-não/3-ignorado)

Data de início de sintomas:___/____/_____

Data de início do exantema:____/_____/_____

Febre: ( ) Se febre, data de início da febre:____/____/_____ Temperatura (Cº):_____

Prurido: ( ) Se prurido, data de início de início:___/_____/_____

Dor em articulação: ( ) Edema em articulação: ( ) Dor de cabeça: ( ) Conjuntivite :( )

Mialgia: ( ) Linfadenopatia: ( ) Diarreia: ( ) Náusea: ( ) Vômito: ( )

EXAMES INESPECÍFICOS

Prova do laço: Positiva ( ) Negativa ( ) Não realizada: ( )

Outros sinais e sintomas_____

Plaquetas:_____x$10^3$$mm^3$	Hematócrito:_____	Leucócitos:_____x$10^3$$mm^3$
Linfócitos:____	Hemoblobina(g/dL):	Neutrófilos:_____%
Eosinófilos:_____%	TGP:	TGO:

Outros resultados:_____

EXAMES ESPECÍFICOS PARA DENGUE

Dengue: Reagente ( ) Não Reagente ( ) Ignorado ( )

Dengue Imunoglubulina: IgM ( ) IgG ( )

Se realizado dengue, data de coleta da amostra: ____/_____/_____

EXAMES ESPECÍFICOS PARA CHIKUNGUNYA

Chikungunya: Reagente ( ) Não reagente ( ) Ignorado ( )

EXAMES ESPECÍFICOS PARA RUBÉOLA

Rubéola: Reagente ( ) Não reagente ( ) Ignorado ( )

Rubéola imunoglobulina: IgM ( ) IgG ( )

Se realizado rubéola, data de coleta da amostra:___/____/____

EXAMES ESPECÍFICOS PARA SARAMPO

Sarampo: Reagente ( ) Não reagente ( ) Ignorado ( )

Sarampo imnuglobulina: IgM ( ) IgG ( )

Se realizado sarampo, data de coleta da amostra:___/____/_____

EXAMES ESPECÍFICOS PARA PARVOVÍRUS

Parvovírus B19: Reagente ( ) Não reagente ( ) Ignorado ( )

Parvovírus B19 imunoglobulina: IgM ( ) IgG ( )

Se realizado parvovírus, data de coleta da amostra:___/____/____

Outros exames específicos:_____

DATA:____/_____/_____

Investigador:_____

Função:_____

APÊNDICE B – Protocolo de extrações do RNA

1. OBJETIVO:

Este POP fixa condições, padroniza, define e estabelece regras que devem ser aplicadas na extração de RNA Viral de amostras de Plasma/Soro (Kit QIAamp Viral RNA Mini Kit Qiagen).

2. CAMPO DE APLICAÇÃO:

Este método aplica-se aos procedimentos de extração de RNA de plasma/soro no Laboratório de Virologia.

3. CONDIÇÕES DE BIOSSEGURANÇA:

Todos os ensaios devem ser realizados utilizando luvas de procedimento; bata com mangas longas; calçados que proteja o pedartículo; acompanhado/excecutado por profissional treinado.

4. SIGLAS:

POP Procedimento operacional padrão
DNA Ácido Desoxirribonucleico
RNA Ácido Ribonucleico
UV Ultra Violeta
PCR Reação em Cadeia da Polimerase

5. RESPONSABILIDADES:

Execução das operações é da responsabilidade do pesquisador do laboratório e, na ausência deste, do responsável treinado indicado pelo pesquisador .

6. PROCEDIMENTO:

Verificar os seguintes itens antes do inicio do procedimento de extração:

A) Coloque as amostras para atingirem a temperatura ambiente (15-25ºC);
B) Coloque o tampão AVE para atingir a temperatura ambiente (15-25ºC) para ser usado na eluição;
C) Verifique se os tampões AW1 e AW2 foram adicionados de Etanol;
EXTRAÇÃO DE RNA QIAamp Viral RNA Mini Kit

Adicione o RNA carreador reconstituído em tampão AVE ao tampão AVL

Procedimento:

Observação 1: Ao trabalhar com amostras biológicas, preparar um descarte com hipoclorito de sódio (2%).
Observação 2: Fazer identificação dos tubos à lápis.
Observação 3: Cuidado!!! Não descartar ponteiras e tubos contendo tampão AVL no Hipoclorito de sódio.

1. Colocar 5 µL de MS2 na diluição 10-4 em todos os microtubos que serão utilizados na extração (utilizar microtubos de 1,5mL ou 2mL)
2. Adicionar 560µL de Tampão AVL + 5,6 µL de RNA carreador no microtubo contendo MS2;
3. Adicionar 140µL de plasma/soro ao tubo anterior e misture por vortex 15s;
4. Incubar a temperatura ambiente (15-25ºC) durante 10 min;
5. Centrifugar brevemente para remover gotas da tampa (20 segundos);
6. Adicionar 560µL de Etanol (96-100%) a amostra e misture por vórtex 15s. Centrifugar brevemente (20 segundos) para remover gotas da tampa;
7. Transfira 630µL da solução do passo anterior para uma coluna do kit. Feche a tampa e centrifugue a 6.000g (8.600 RPM) 1 min e 15 segundos. Coloque a coluna em um tubo coletor novo e descarte o utilizado com o filtrado;
8. Abra a coluna com cuidado e repita o passo anterior.
9. Coloque a coluna em um novo tubo coletor, adicione 500µL de tampão AW1, centrifugue 6000g (8.600 RPM) durante 1 min e 15 segundos, descarte o líquido e o tubo coletor;
10. Coloque a coluna em um novo tubo coletor e adicione 500µL de tampão AW2, centrifugue 16.000g (14.000 RPM) durante 3 min, descarte o líquido;
11. Coloque a coluna no mesmo tubo coletor e centrifugue a 16.000g (14.000 RPM) por 1 minuto. Descarte o líquido e o tubo coletor;

Observação 4: Centrifugar sem a tampa interna e dos tubos abertas para secar todo álcool das amostras.

12. Coloque a coluna em um tubo de 1,5ml e pipete 60µL do tampão AVE (temperatura ambiente), feche a tampa e incube temperatura ambiente 1 min. Centrifugue 6000g (8.600 RPM) durante 2 min.
13. Estocar de -20ºC à -80ºC até 1 ano.

Observação 5: Armazenar os tampões AWI E AW2 na geladeira após o uso.
Observação 6: Atenção!!!O Tampão AVE contém azida sódica que interfere na quantificação por espectrofotômetro 260/280nm.

Esse POP foi elaborado por VALDINETE ALVES DO NASCIMENTO, colaboradora do projeto.

APÊNDICE C – Protocolos de Reação em Cadeia da Polimerase da Transcriptase Reversa em Tempo Real (RT-qPCR)

PCR em Tempo Real (qPCR) TaqManFastvirus

100nM de sonda e 300nM de cada iniciador

Reagentes ZIKV NS5	**1X**	
TaqMan Virus	2,5 µL	
Sonda ZIKV [10µm]	0,1 µL	
Primer mix ZIKV [5µm]	0,6 µL	
H_2O	4,3 µL	
RNA	2,5 µL	

Reagentes ZIKV-MS2	**1X**		
TaqMan Virus	2,5 µL		
Sonda ZIKV [10µm] FAM	0,1 µL		
Primer mix ZIKV [5µm]	0,6 µL		
Sonda MS2 [10µm] ATTO	0,1 µL		
Primer mix MS2 [5µm]	0,6 µL		
H_2O	3,6 µL		
RNA	2,5 µL		

7,5 µL de mix + 2,5 µL de RNA

Layout da placa

	1	2	3	4	5	6	7	8	9	10	11	12
A												
B												
C												
D												
E												
F												
G												
H												

Esse POP foi elaborado por VALDINETE ALVES DO NASCIMENTO, colaboradora do projeto.